

Visualization of integrin molecules by fluorescence imaging and techniques

CHEN CAI¹; HAO SUN²; LIANG HU³; ZHICHAO FAN^{1,*}

¹ Department of Immunology, School of Medicine, UConn Health, Farmington, 06030, USA

² Department of Medicine, University of California, San Diego, La Jolla, 92093, USA

³ Cardiovascular Institute of Zhengzhou University, Department of Cardiology, The First Affiliated Hospital of Zhengzhou University, Zhengzhou, 450051, China

Key words: Integrins, Fluorescence imaging, Fluorescence labeling, Live-cell imaging, Super-resolution imaging, Intravital imaging, FRET

Abstract: Integrin molecules are transmembrane $\alpha\beta$ heterodimers involved in cell adhesion, trafficking, and signaling. Upon activation, integrins undergo dynamic conformational changes that regulate their affinity to ligands. The physiological functions and activation mechanisms of integrins have been heavily discussed in previous studies and reviews, but the fluorescence imaging techniques –which are powerful tools for biological studies– have not. Here we review the fluorescence labeling methods, imaging techniques, as well as Förster resonance energy transfer assays used to study integrin expression, localization, activation, and functions.

Introduction

Integrins are a family of adhesion receptors that are abundantly expressed in all cell types of metazoans except for erythrocytes. Their integral roles in mediating cell–cell and cell–extracellular matrix (ECM) interactions make integrins indispensable for the existence of multicellular organisms. Interactions between integrins and their ligands trigger profound changes of the cytoskeleton and signaling apparatus during biological processes, such as adhesion (Evans *et al.*, 2019; Fan *et al.*, 2019; Fan *et al.*, 2016; Stubb *et al.*, 2019; Sun *et al.*, 2020a; Valencia-Gallardo *et al.*, 2019), migration (Bernadskaya *et al.*, 2019; Martens *et al.*, 2020; Sun *et al.*, 2014), proliferation (Clark *et al.*, 2020; Erusappan *et al.*, 2019), differentiation (Martins Cavaco *et al.*, 2018; Schumacher *et al.*, 2020; Xie *et al.*, 2019), inflammation (Arnaout, 2016; Sun *et al.*, 2020b), tumor invasion (Bui *et al.*, 2019; Haeger *et al.*, 2020), and metastasis (Fuentes *et al.*, 2020; Howe *et al.*, 2020; Osmani *et al.*, 2019). Fine-tuned integrin signaling is crucial for cellular homeostasis, and abnormal integrin activities give rise to many pathological conditions, including autoimmune diseases, cardiovascular diseases, and cancer. Extensive efforts have been made to discover and develop molecules targeting integrins as potential means of therapy (Ley *et al.*, 2016). Several integrin-targeting antibodies and synthetic

compounds are approved for treating inflammatory diseases or are under investigation in clinical trials. Fluorescent imaging techniques provide a powerful tool for better understanding integrin structures and conformational changes (by Förster resonance energy transfer, conformational reporting antibody, and super-resolution imaging), and integrin-ligand interactions to develop more effective therapies for a vast array of diseases.

Structure of integrins

Integrins are heterodimers consisting of noncovalently associated α (120–180 kDa) and β (90–110 kDa) subunits (Hynes, 1992). In the vertebrates, 18 α subunits and 8 β subunits form 24 $\alpha\beta$ pairs (Barczyk *et al.*, 2010; Hynes, 2002) (Fig. 1). Integrin families are separated into four major categories: those with specificity for intercellular adhesion molecules and inflammatory ligands (leukocyte integrins, $\alpha4$, αE , αL , αM , αX , and αD), Arg-Gly-Asp (RGD) motifs (αIIb , αV , $\alpha5$, and $\alpha8$), collagens ($\alpha1$, $\alpha2$, $\alpha10$, and $\alpha11$), and laminins ($\alpha3$, $\alpha6$, and $\alpha7$) (Campbell and Humphries, 2011; Humphries *et al.*, 2006; Tolomelli *et al.*, 2017). Both α and β subunits are type I transmembrane glycoproteins containing a relatively large extracellular domain (ectodomain), a single transmembrane domain, and a short cytoplasmic tail (Arnaout, 2016; Campbell and Humphries, 2011; Fan and Ley, 2015; Luo *et al.*, 2007).

The ectodomain is an asymmetric structure with a “head” carrying two “legs” (~16 nm long). The head

*Address correspondence to: Zhichao Fan, zfan@uchc.edu
Received: 18 September 2020; Accepted: 22 November 2020



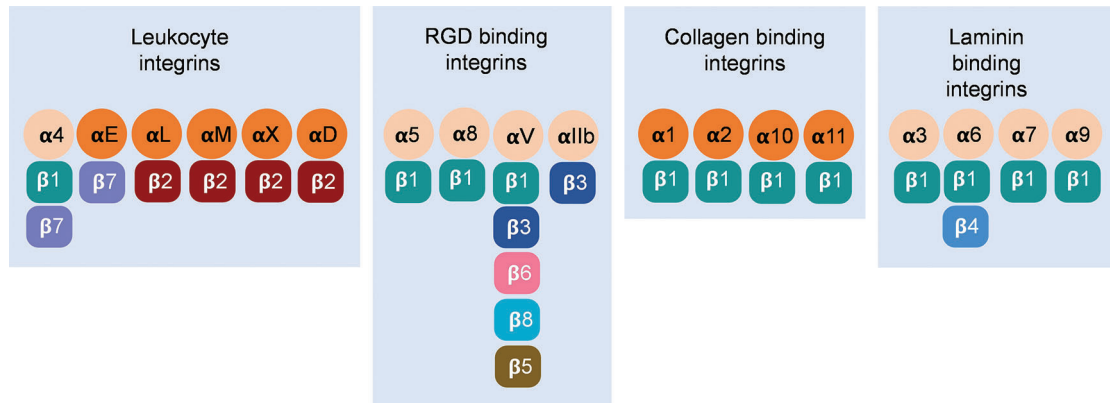


FIGURE 1. Twenty-four $\alpha\beta$ pairs of vertebrate integrins constituted by 18 α subunits and 8 β subunits have been classified into four separate groups.

Dark and light oranges represent α subunits with or without the $\alpha A/\alpha I$ domain. Different β subunits were colored differently. RGD is the abbreviation of Arg-Gly-Asp peptides.

consists of a predicted seven-bladed β -propeller domain (~60 amino acids each) of an α subunit (Xiao *et al.*, 2004; Xiong *et al.*, 2001) (nine of eighteen α subunits also contain an additional ~200 amino acids $\alpha A/\alpha I$ domain) (Larson *et al.*, 1989) and a ~250 amino acid $\beta A/\beta I$ -like domain inserted in a hybrid domain of β subunit. The $\alpha A/\alpha I$ domain and $\beta A/\beta I$ -like domain are homologous to small ligand-binding von Willebrand Factor type A (vWFA) domain (Arnaout, 2002; Arnaout *et al.*, 2007). The $\beta A/\beta I$ -like domain contains two additional segments: one forms the interface with the β -propeller, and the other is a specificity-determining loop (SDL) mediating the ligand-binding (Luo *et al.*, 2007). As structures of $\alpha V\beta 3$ and $\alpha IIb\beta 3$ showed, the α subunit leg domain is composed of an immunoglobulin-like “thigh” domain, a genu loop, and two similar β -sandwich domains named calf-1 and calf-2. The β subunit leg is formed by a plexin-semaphorin-integrin (PSI) domain, a hybrid domain (Bork *et al.*, 1999), four tandem epidermal growth factor (EGF)-like domains, and a β -tail domain (β TD) (Bode *et al.*, 1988; Janowski *et al.*, 2001). The knee of the α subunit (α genu) lies at the junction between the thigh and calf-1 domains, and the knee of the β -subunit (β genu) is within the PSI and EGF1-2 region (Takagi and Springer, 2002). In integrins containing an $\alpha A/\alpha I$ domain, ligand binding is mediated by this domain. As for integrins lacking the $\alpha A/\alpha I$ domain, binding sites of ligands localize in the interface between β subunit β -I domain and α subunit β -propeller domain. Transmembrane domains of both α and β subunits are single α -helices. NMR studies of $\alpha IIb\beta 3$ show that the transmembrane domain of $\beta 3$ is longer than αIIb and tilted with a ~25° angle to ensure the formation of inner and outer membrane clasp (IMC and OMC), which are important for proper integrin activity (Ginsberg, 2014; Kim *et al.*, 2011; Lau *et al.*, 2009; Sun *et al.*, 2018).

Conformations of integrins

Many techniques have been applied to distinguish two major models of conformational changes influencing integrin affinity, namely “switchblade” (Luo *et al.*, 2007) and “deadbolt” (Arnaout *et al.*, 2005). Although height change is a conspicuous readout, no consistent conclusions have been drawn owing to the plasticity of integrin structure. Most

studies of ectodomains favor the switchblade model: extension (E^+) of the integrin is the prerequisite for rearrangement of the ligand-binding site, leading to high affinity (H^+). Three major conformations with different ligand binding affinities provide evidence for this model: inactive bent ectodomain with low-affinity headpiece (E^-H^-), primed extended ectodomain with low-affinity headpiece (E^+H^-) with low affinity, and fully activated extended ectodomain with high-affinity headpiece (E^+H^+) (Chen *et al.*, 2010; Springer and Dustin, 2012; Takagi *et al.*, 2002). However, crystallography results showed that the conformations of bent ectodomain with open headpiece (E^-H^+) found in $\alpha V\beta 3$ and $\alpha X\beta 2$ (Sen *et al.*, 2013) had the capacity to bind its ligand. In primary human neutrophils, the “switchblade” transition (E^-H^- to E^+H^- to E^+H^+) was observed. And an alternative transition from E^-H^- to E^-H^+ to E^+H^+ was also observed (Fan *et al.*, 2016). E^-H^+ $\beta 2$ integrins bind intercellular adhesion molecules (ICAMs) in cis (Fan *et al.*, 2016) and form a face-to-face orientation (Fan *et al.*, 2019), inhibiting leukocyte adhesion and aggregation (Fan *et al.*, 2016). E^-H^+ $\alpha M\beta 2$ integrins were shown binding Fc γ RIIA in cis to limit antibody-mediated neutrophil recruitment (Saggu *et al.*, 2018). These findings suggest an alternative allosteric pathway other than the “switchblade” model.

Integrin labeling in fluorescence imaging

Monoclonal antibodies

Immunofluorescent staining is the most commonly used method for integrin labeling, and antibody selection is extremely important for studying integrins. Monoclonal antibodies targeting different epitopes of specific integrin α and β subunits have been developed (Tab. 1). Some of these have been discussed in a previous review (Byron *et al.*, 2009). Briefly, most of these clones target human integrins and can be classified into three categories: Blocking/inhibitory, non-blocking/non-functional, and stimulatory/activation specific. Blocking antibodies can be used in integrin loss-of-function assays, such as adhesion and phagocytosis, or testing integrin expression when there is no ligand binding, such as flow cytometry. Non-blocking antibodies do not interfere with the biological functions of

TABLE 1

Human integrin-targeting monoclonal antibodies

Integrin	Epitope (Domain)	Clone name	Integrin	Epitope (Domain)	Clone name
Blocking/inhibitory					
$\alpha 1$	$\alpha A/\alpha I$	FB12 (Fabbri <i>et al.</i> , 1996)	$\beta 1$	$\beta A/\beta I$ -like	4B4 (Takada and Puzon, 1993) mAb13 (Takada and Puzon, 1993)
$\alpha 2$	$\alpha A/\alpha I$	12F1 (Kamata <i>et al.</i> , 1994) Gi9 (Tuckwell <i>et al.</i> , 2000) JA218 (Tuckwell <i>et al.</i> , 2000) P1E6 (Kamata <i>et al.</i> , 1994)		Hybrid	AIIB2 (Takada and Puzon, 1993) P4C10 (Takada and Puzon, 1993) JB1A (Ni and Wilkins, 1998)
$\alpha 3$	β -propeller	ASC-6 (Zhang <i>et al.</i> , 1999) P1B5 (Zhang <i>et al.</i> , 1999)	$\beta 2$	$\beta A/\beta I$ -like	CLB LFA-1/1 (Zang <i>et al.</i> , 2000) MHM23 (Hildreth <i>et al.</i> , 1983) TS1/18 (Lu <i>et al.</i> , 2001a) IB4 (Wright <i>et al.</i> , 1983) L130 (Zang <i>et al.</i> , 2000)
	Not known	IA3 (Turner <i>et al.</i> , 2006)			
$\alpha 4$	β -propeller	HP2/1 (Kamata <i>et al.</i> , 1995) P4C2 (Kamata <i>et al.</i> , 1995) PS/2 (Kamata <i>et al.</i> , 1995)		Hybrid	7E4 (Tng <i>et al.</i> , 2004)
	Not known	9F10 (Lei <i>et al.</i> , 2016) L25 (Chandele <i>et al.</i> , 2016) P1H4 (Stampolidis <i>et al.</i> , 2015) A4-PUJ1 (Martin <i>et al.</i> , 2015)	$\beta 3$	$\beta A/\beta I$ -like Not known	7E3 (Artoni <i>et al.</i> , 2004) SZ-21 (Sheng <i>et al.</i> , 2003)
			$\beta 4$	Not known	ASC-8 (Egles <i>et al.</i> , 2010)
			$\beta 5$	Not known	ALULA (Su <i>et al.</i> , 2007)
$\alpha 5$	β -propeller	JBS5 (Burrows <i>et al.</i> , 1999) mAb16 (Burrows <i>et al.</i> , 1999) P1D6 (Burrows <i>et al.</i> , 1999)	$\beta 6$	Not known	6.3G6 (Weinreb <i>et al.</i> , 2004)
	Not known	NKI-SAM-1 (Orecchia <i>et al.</i> , 2003)	$\beta 7$	$\beta A/\beta I$ -like	FIB504 (Andrew <i>et al.</i> , 1994) FIB27 (Andrew <i>et al.</i> , 1994) FIB30 (Andrew <i>et al.</i> , 1994)
$\alpha 6$	Not known	GoH3 (Lee <i>et al.</i> , 1992)	$\beta 8$	Not known	37E1 (Mu <i>et al.</i> , 2002)
$\alpha 7$	Not known	6A11 (Zhao <i>et al.</i> , 2004)	αIIb	β -propeller	10E5 (Nishimichi <i>et al.</i> , 2015) 2G12 (Kamata <i>et al.</i> , 1996)
$\alpha 8$	β -propeller	YZ3 (Nishimichi <i>et al.</i> , 2015)			
$\alpha 9$	Not known	Y9A2 (Staniszewska <i>et al.</i> , 2008)	$\alpha V\beta 3$	β -propeller	23C6 (Kamata <i>et al.</i> , 2013)
			$\alpha V\beta 5$	Not known	P1F6 (Singh <i>et al.</i> , 2007) P3G2 (Hendey <i>et al.</i> , 1996)
αV	β -propeller	17E6 (Kamata <i>et al.</i> , 2013) L230 (Nishimichi <i>et al.</i> , 2015)	$\alpha V\beta 6$	Not known	10D5 (Weinreb <i>et al.</i> , 2004) 6.3G9 (Weinreb <i>et al.</i> , 2004)
	Not known	NKI-M9 (Grzeszkiewicz <i>et al.</i> , 2001)			
αE	$\alpha A/\alpha I$	$\alpha E7$ -1 (Russell <i>et al.</i> , 1994) $\alpha E7$ -2 (Russell <i>et al.</i> , 1994)	$\alpha L\beta 2$	$\alpha A/\alpha I$, β -propeller, and $\beta A/\beta I$ -like	YTA-1 (Zang <i>et al.</i> , 2000)
	Not known	Ber-ACT8 (Kruschwitz <i>et al.</i> , 1991)			

(Continued)

Table 1 (continued).

Integrin	Epitope (Domain)	Clone name	Integrin	Epitope (Domain)	Clone name
α L	α A/ α I	TS1/22 (Lu <i>et al.</i> , 2004) HI111 (Ma <i>et al.</i> , 2002) CBR LFA-1/1 (Ma <i>et al.</i> , 2002)	α M	α A/ α I	2LPM19c (Osicka <i>et al.</i> , 2015) MAN-1 (Eisenhardt <i>et al.</i> , 2007) anti-M7 (Wolf <i>et al.</i> , 2018) ICRF44 (Osicka <i>et al.</i> , 2015)
	Not known	mAb38 (Lomakina and Waugh, 2004)			Thigh M1/70 (Osicka <i>et al.</i> , 2015)
α X	α A/ α I	3.9 (Hogg <i>et al.</i> , 1986)	α D	α A/ α I	217I (Van Der Vieren <i>et al.</i> , 1999)
	Not known	496K (Sadhu <i>et al.</i> , 2008) Bu15 (Sadhu <i>et al.</i> , 2008)			240I (Van Der Vieren <i>et al.</i> , 1999)
Non-blocking/non-functional					
α 1	Not known	TS2/7 (Woods <i>et al.</i> , 1994)	α 5	Calf-1 to 2 β -propeller	mAb11 (Askari <i>et al.</i> , 2010) VC5 (Askari <i>et al.</i> , 2010)
α 2	Not known	16B4 (Tuckwell <i>et al.</i> , 2000)	α 6	Not known	J1B5 (Damsky <i>et al.</i> , 1994)
		31H4 (Tuckwell <i>et al.</i> , 1995)			
α 3	Not known	A3-X8 (Weitzman <i>et al.</i> , 1993)	α 7	Not known	3C12 (Mielenz <i>et al.</i> , 2001)
α 4	Not known	44H6 (Bridges <i>et al.</i> , 2005)	α 9	Not known	A9A1 (Vlahakis <i>et al.</i> , 2005)
		8F2 (Newham <i>et al.</i> , 1998)			
α IIb	Not known	PL98DF6 (Puzon-Mclaughlin <i>et al.</i> , 2000)	α V	Not known	LM142 (Mathias <i>et al.</i> , 1998)
					α D
α L	β -propeller	TS2/4 (Zang <i>et al.</i> , 2000)	β 1	I-EGF	K20 (Askari <i>et al.</i> , 2010)
	Not known	YTH81.5 (Stanley <i>et al.</i> , 2008)			
α M	β -propeller	CBRM1/20 (Oxvig and Springer, 1998)	β 2	Not known	CBR LFA-1/7 (Lu <i>et al.</i> , 2001a)
	Thigh	OKM1 (Osicka <i>et al.</i> , 2015) CyaA (Osicka <i>et al.</i> , 2015)			
α X	Not known	CBR-p150/2E1 (Shang and Issekutz, 1998)	β 4	Not known	ASC-3 (Egles <i>et al.</i> , 2010)
			β 5	Not known	11D1 (Ricono <i>et al.</i> , 2009)
Stimulatory or activation-specific					
α 2	Not known	JBS2 (Ho <i>et al.</i> , 1997)	β 2	β A/ β I-like	mAb24 (Lu <i>et al.</i> , 2001a) 327C (Beals <i>et al.</i> , 2001)
α 4	β -propeller	HP1/3 (Kamata <i>et al.</i> , 1995)	Hybrid	EGF-like 2	MEM-148 (Tang <i>et al.</i> , 2005)
α 5	Calf-1 & 2	SNAKA51 (Clark <i>et al.</i> , 2005)			EGF-like 3
			α IIb	β -propeller	PT25-2 (Puzon-Mclaughlin <i>et al.</i> , 2000)
α L	Calf-1	MBC370.2 (Chen <i>et al.</i> , 2019)	β 3	Hybrid	AP3 (Peterson <i>et al.</i> , 2003)
	Calf-2	PMI-1 (Loftus <i>et al.</i> , 1987)			PSI
α L	α A/ α I	2E8 (Carreno <i>et al.</i> , 2010) MEM83 (Gronholm <i>et al.</i> , 2016)	β 7	β A/ β I-like and hybrid	LIBS6 (Frelinger <i>et al.</i> , 1991) LIBS2 (Du <i>et al.</i> , 1993)
	Genu	NKI-L16 (Keizer <i>et al.</i> , 1988)			10F8 (Tidswell <i>et al.</i> , 1997) 2B8 (Tidswell <i>et al.</i> , 1997)
α M	α A/ α I	CBRM1/5 (Oxvig <i>et al.</i> , 1999)			2G3 (Tidswell <i>et al.</i> , 1997)
	Thigh	VIM12 (Osicka <i>et al.</i> , 2015)			

Table 1 (continued).

Integrin	Epitope (Domain)	Clone name	Integrin	Epitope (Domain)	Clone name		
α X β 1	Not known β A/ β I-like	496B (Sadhu <i>et al.</i> , 2008)	α Ib β 3	β -propeller and β A/ β I-like	PAC-1 (Kamata <i>et al.</i> , 1996)		
		12G10 (Mould <i>et al.</i> , 1995)			α V β 3	β -propeller and β A/ β I-like	WOW-1 (Pampori <i>et al.</i> , 1999)
		8A2 (Takada and Puzon, 1993)	LM609 (Kamata <i>et al.</i> , 2013)				
		TS2/16 (Takada and Puzon, 1993)	α V β 6	β -propeller and β A/ β I-like			6.8G6 (Weinreb <i>et al.</i> , 2004)
		A1A5 (Takada and Puzon, 1993)			Hybrid	15/7 (Mould <i>et al.</i> , 2003)	HUTS-4 (Luque <i>et al.</i> , 1996)
	HUTS-7 (Luque <i>et al.</i> , 1996)	α 4 β 7	β -propeller and β A/ β I-like	J19 (Qi <i>et al.</i> , 2012)			
	HUTS-21 (Luque <i>et al.</i> , 1996)			β 1			
	8E3 (Mould <i>et al.</i> , 2005)	PSI	N29 (Mould <i>et al.</i> , 2005)				

integrins. Thus, they are useful in live-cell fluorescence imaging to monitor the expression, localization, and clustering of integrins when interacting with ligands (Ezraty *et al.*, 2009; Garmy-Susini *et al.*, 2013; Huang *et al.*, 2009; Jamerson *et al.*, 2012; Shao *et al.*, 2019; Tchaicha *et al.*, 2011; Xiao *et al.*, 2019). Among integrin antibodies, a unique kind of integrin antibody recognizes epitopes only expressed when integrins are activated or inactivated. Some of them further stabilize certain conformation(s) by steric effect resulting in enhancement or attenuation of ligand binding. Immunofluorescent imaging using antibodies with different effects on integrin activation can help illuminate novel biological functions.

Integrin antibodies that recognize activated epitopes have been applied to understanding β 2 integrins-leukocyte-specific integrins that are critical for leukocyte recruitment and functions. Monoclonal antibody KIM127 (Robinson *et al.*, 1992) recognizes the cysteine-rich repeat residues in the stalk region of integrin β 2 subunits (Lu *et al.*, 2001a). Monoclonal antibody mAb24 (Dransfield and Hogg, 1989) recognizes Glu173 and Glu175 within the CPNKEKEC sequence (residues 169–176) of the β 2 I domain (Kamata *et al.*, 2002; Lu *et al.*, 2001b). These epitopes are shielded by the stalk region, and the α A/ α I domain or the β -propeller of integrin α subunit are exposed and recognized by KIM127 and mAb24 upon integrin activation. KIM127 binding indicates integrin extension (E^+), and mAb24 binding indicates rearrangement in the ligand-binding site leading to high-affinity (H^+) (Kuwano *et al.*, 2010; Lefort *et al.*, 2012; Sorio *et al.*, 2016). Owing to noninterference with each other (Fan *et al.*, 2016), KIM127 and mAb24 were used to label different conformational states of β 2 integrin on live human neutrophils (Fan *et al.*, 2019; Fan *et al.*, 2016; Sun *et al.*, 2020a; Wen *et al.*, 2020b), which enables to distinguish E^+H^- , E^-H^+ , and E^+H^+ β 2 integrins in live cells and. These studies demonstrated that other than the canonical switchblade model (E^-H^- to E^+H^- to E^+H^+), an alternative integrin activation pathway (E^-H^- to E^-H^+ to E^+H^+) exists on primary human neutrophils. Monoclonal antibody 327C has

been mapped to the upstream C-terminal region between amino acids 23 and 411 of the β 2 integrin and also reports β 2 integrin H^+ (Zhang *et al.*, 2008). 327C has been used to monitor β 2 integrin activation during neutrophil migration (Green *et al.*, 2006) and T cell spreading (Feigelson *et al.*, 2010) using epifluorescence imaging, and neutrophil-platelet interaction using confocal microscopy (Evangelista *et al.*, 2007).

Antibodies for activated integrins have also been used to study β 1 integrins, which are expressed on various cells, such as leukocytes (Rullo *et al.*, 2012; Werr *et al.*, 1998), endothelial cells (Xanthis *et al.*, 2019), epithelial cells (Spiess *et al.*, 2018), and fibroblasts (Samarelli *et al.*, 2020), and they are critical for several cell functions, such as adhesion and migration. Monoclonal antibody 9EG7 binds to the upper portion of the lower β -leg, which is approximately within the I-EGF2 domain, and reports β 1 integrin extension (Lenter *et al.*, 1993; Su *et al.*, 2016) similar to KIM127 binding in β 2 integrin. Antibody 12G10 binds to the β I domain of high-affinity β 1 integrin (Su *et al.*, 2016), which is similar to mAb24 binding in β 2 integrin. Using 9EG7, 12G10, and a pan- β 1 integrin antibody AIIB2, distinct nanoclusters of active and inactive β 1 integrins have been identified in focal adhesions (FAs) (Spiess *et al.*, 2018). Antibody TS2/16 binds an epitope similar to what 12G10 binds, where it activates and appears to stabilize an H^+ β I domain conformation without requiring extension or hybrid domain swing-out (Van De Wiel-Van Kemenade *et al.*, 1992). Antibodies HUTS-4, HUTS-7, and HUTS-21 recognize overlapping epitopes located in the hybrid domains of the β 1 subunit. Their expressions parallel the ligand-binding activity of β 1 integrins induced by various extracellular and intracellular stimuli (Luque *et al.*, 1996; Su *et al.*, 2016).

Antibodies recognizing and binding to the inactive conformation or that inhibit function are also used for integrin labeling. mAb13 recognizes an epitope within the β I domain of β 1 integrin and is dramatically attenuated in the ligand-occupied form of α 5 β 1. The binding of mAb13 to ligand-occupied α 5 β 1 induces a conformational change in the integrin, resulting in the displacement of the ligand

(Mould *et al.*, 1996). Antibody SG/19 has been reported to inhibit the function of the $\beta 1$ integrin on the cell surface. SG/19 recognizes the wild-type $\beta 1$ subunit that exists in a conformational equilibrium between the high and low-affinity states but binds poorly to a mutant $\beta 1$ integrin that is locked in a high-affinity state. SG/19 binds Thr82 located at the outer face of the boundary between the I-like and hybrid domains of the $\beta 1$ subunit. SG/19 attenuates the ligand-binding function by restricting the conformational shift to the high-affinity state involving the swing-out of the hybrid domain without directly interfering with ligand docking (Luo *et al.*, 2004). Monoclonal antibody SNAKA51 binds to the calf-1/calf-2 domains of the $\alpha 5$ subunit when the $\alpha 5\beta 1$ integrin is active (Su *et al.*, 2016). Alexa Fluor 488-conjugated SNAKA51 facilitates the detection of a conformation that promotes fibrillar adhesion formation. Gated stimulated emission depletion (g-STED) confocal microscopy analyses of PPFIA1 (protein tyrosine phosphatase receptor type F polypeptide interacting protein $\alpha 1$) and SNAKA51 activating $\alpha 5\beta 1$ integrin in endothelial cells indicates that PPFIA1 localizes close to both focal and fibrillar adhesions (Mana *et al.*, 2016).

$\beta 3$ integrins are also widely expressed, and antibodies have been developed to study their functions. Vitronectin receptor integrin $\alpha V\beta 3$ is expressed on leukocytes (Antonov *et al.*, 2011), endothelial cells (Liao *et al.*, 2017), and platelets (Bagi *et al.*, 2019), etc. Active and inactive conformations of $\alpha V\beta 3$ integrins can be detected by antibodies anti- $\alpha V\beta 3$ clone LM609 and clone CBL544, respectively (Drake *et al.*, 1995). WOW-1 is a ligand-mimic Fab fragment that reports $\alpha V\beta 3$ integrin activation (Pampori *et al.*, 1999). It has been used in detecting $\alpha V\beta 3$ integrin activation on endothelial cells during shear sensing (Tzima *et al.*, 2001) and migration (Lu *et al.*, 2006) using fluorescence imaging. $\alpha IIb\beta 3$ integrins are also known as glycoprotein IIb/IIIa and expressed on platelets (Adair *et al.*, 2020; Chen *et al.*, 2019; Ting *et al.*, 2019). Antibody MBC370.2 binds to the calf-1 domain of the αIIb chain and reports the E⁺ of $\alpha IIb\beta 3$ integrins (Zhang *et al.*, 2013). PAC-1 is a ligand-mimic antibody and binds to both the β -propeller and $\beta A/\beta I$ -like domains of H⁺ $\alpha IIb\beta 3$ integrins (Kashiwagi *et al.*, 1997). AP5 recognizes an epitope in the $\beta 3$ PSI domain and reports hybrid domain swing-out (Cheng *et al.*, 2013). By using these three antibodies, it has been demonstrated that biomechanical platelet aggregation is mediated by E⁺ but not H⁺ of $\alpha IIb\beta 3$ integrins (Chen *et al.*, 2019).

Integrin $\alpha 4\beta 7$ is a lymphocyte homing receptor that mediates both rolling and firm adhesion of lymphocytes on vascular endothelium, two of the critical steps in lymphocyte migration and tissue-specific homing (Berlin *et al.*, 1993; Iwata *et al.*, 2004). Integrin $\alpha 4\beta 7$ is the target of the most successful integrin drug vedolizumab, which is a human-derived blocking antibody and has recently proven useful in the treatment of inflammatory bowel diseases (Fedyk *et al.*, 2012; Ley *et al.*, 2016; Sands *et al.*, 2019; Zingone *et al.*, 2020). An activation-specific antibody J19 for integrin $\alpha 4\beta 7$ has been developed (Qi *et al.*, 2012). This antibody does not block the mucosal vascular addressin cell adhesion molecule 1 (MAdCAM-1) binding site. Its binding site has been mapped to Ser-331, Ala-332, and Ala-333 of the $\beta 7$ A/I-like domain and a seven-residue segment from 184 to 190 of the $\alpha 4$ β -propeller domain.

Fluorescent proteins

Since the molecular cloning of green fluorescent protein (GFP) from the jellyfish *Aequorea victoria* (Chalfie *et al.*, 1994; Prasher *et al.*, 1992; Ward *et al.*, 1980), a wide spectrum of fluorescent proteins have provided excellent opportunities to monitor integrin localization and dynamics in living cells and tissues.

To study the separation of integrin α and β “legs” during activation, the monomeric cyan fluorescent protein (mCFP) and monomeric yellow fluorescent protein (mYFP) were fused to the C-termini of the α and β cytoplasmic domains of $\alpha V\beta 3$, respectively (Kim *et al.*, 2003). The “leg” separation was demonstrated by the decrease of Förster resonance energy transfer (FRET) from mCFP to mYFP. A similar strategy has been applied to study $\alpha M\beta 2$ integrin activation as well (Lefort *et al.*, 2009). To extend this idea in studying integrin activation in mouse disease models, knock-in (KI) mice with αM -mYFP (Lim *et al.*, 2015), αL -mYFP (Capece *et al.*, 2017), or $\beta 2$ -mCFP (Hyun *et al.*, 2012) were generated, in which the fluorescent proteins were inserted into the C terminus of each integrin. Intravital imaging was then performed to visualize αM -mYFP⁺ leukocytes (Lim *et al.*, 2015) or $\beta 2$ -mCFP leukocytes (Hyun *et al.*, 2012) within inflamed or infected tissues. The αL -mYFP KI mice helped reveal an intracellular pool of integrin $\alpha L\beta 2$ involved in CD8⁺ T cell activation and differentiation (Capece *et al.*, 2017). In combined KI mice, activation of $\alpha L\beta 2$ and $\alpha M\beta 2$ was observed during neutrophil transendothelial migration by intravital microscopy (IVM) (Hyun *et al.*, 2019).

In another study, GFP was inserted into the $\beta 3$ - $\beta 4$ loop of blade 4 of the αL integrin β -propeller domain with no appreciable influence on integrin function and conformational regulation (Nordenfelt *et al.*, 2017). The orientation of GFP can be measured by emission anisotropy microscopy (Ghosh *et al.*, 2012; Nordenfelt *et al.*, 2017; Ojha *et al.*, 2020). Thus, they found that the direction of actin flow dictates integrin $\alpha L\beta 2$ orientation during leukocyte migration (Nordenfelt *et al.*, 2017). The role of $\alpha 5$ integrins in cell adhesion and migration was investigated by introducing the eukaryotic expression vectors pEGFP-N3, pECFP-N1, and pEYFP-N1 inserted with the integrin $\alpha 5$ cDNA and a 10-13 amino acid linker into CHO K1 and CHO B2 ($\alpha 5$ -deficient) cells (Laukaitis *et al.*, 2001). They found that $\alpha 5$ integrins stabilized cell adhesion and formed visible complexes after the arrival of α -actinin and paxillin. Integrin $\beta 4$ -YFP fusion proteins were introduced into HaCat cells as a marker of hemidesmosome protein complexes (HPCs). Meanwhile, CFP-tagged α -actinin was used as a marker of focal contacts (FCs). Tight co-regulation of HPCs and FCs was detected in keratinocytes undergoing migration during wound healing (Ozawa *et al.*, 2010). Wild type or mutated mouse integrin $\beta 3$ -EGFP fusion protein was used to investigate the mechanisms and dynamics of the clustering and incorporation of activated $\alpha V\beta 3$ integrins into FAs in living cells. Formation of the ternary complex consisting of activated integrins, immobilized ligands, talin, and PI(4,5)P₂ was found to contribute to integrin clustering (Cluzel *et al.*, 2005). Fluoppi is a technology providing an easy way to visualize protein-protein interactions (PPIs)

with a high signal-to-background ratio (Koyano *et al.*, 2014; Yamano *et al.*, 2015). It employs an oligomeric assembly helper tag (Ash-tag) and a tetrameric fluorescent protein tag (FP-tag) to create detectable fluorescent foci when there are interactions between two proteins fused to the tags. This technique has been used to prove the interaction of integrin $\beta 1$ and Procollagen-Lysine, 2-Oxoglutarate 5-Dioxygenase 2 (PLOD2) in cell migration (Ueki *et al.*, 2020).

In another study, an extracellular site of integrin $\beta 1$ was reported suitable for inserting different tags, including GFP and PH-sensitive pHluorin (Huet-Calderwood *et al.*, 2017). pHluorin is a GFP variant that displays a bimodal excitation spectrum with peaks at 395 and 475 nm and an emission maximum at 509 nm. Upon acidification, pHluorin excitation at 395 nm decreases with a corresponding increase in the excitation at 475 nm (Mahon, 2011). In this study, pHluorin tagged integrin $\beta 1$ was used to monitor the exocytosis of $\beta 1$ integrins in live cells. Since similar extracellular fluorescence protein insertion was performed in $\beta 2$ integrins (Bonasio *et al.*, 2007; Moore *et al.*, 2018; Nordenfelt *et al.*, 2017), it is feasible to use pHluorin in study $\beta 2$ integrin functions, such as degranulation and phagocytosis.

Other methods for fluorescently tagging integrins

HaloTag is a 34 kDa engineered, catalytically inactive derivative of a bacterial hydrolase. It can be fused to a protein of interest and covalently bound by synthetic HaloTag ligands with high specificity. A covalent bond can form rapidly under physiological conditions and is essentially irreversible. HaloTag allows adaptation of the targeted protein to different experimental requirements without altering the genetic construct (Los *et al.*, 2008; Los and Wood, 2007). For example, Atto655 was used to generate the HaloTag655 ligand, which is suitable for labeling live cells by expressing a $\beta 1$ -integrin-HaloTag fusion protein. The resulting living cells are suitable for STED microscopy, and intracellular distribution of the $\beta 1$ -integrin such as filopodia and endocytic vesicles were studied in unprecedented detail (Schroder *et al.*, 2009). Halo and SNAP tags were also inserted into the $\beta 1$ integrin extracellular domain in the study mentioned above (Huet-Calderwood *et al.*, 2017). Similar to HaloTag, SNAP (Keppler *et al.*, 2003) is also a self-labeling protein tag that can covalently bind to synthetic fluorescence dyes. Sequential fluorescence dye labeling of Halo-tagged integrin $\beta 1$ can distinguish surface and internal $\beta 1$ integrins in cells (Huet-Calderwood *et al.*, 2017).

Many integrins bind to ECM molecules through an RGD motif. RGD peptide was found to bind to resting integrins and induce integrin activation. Compared to linear peptides, suitable optimized cyclic RGD (cRGD) peptides interact with integrins in a more selective manner and with higher affinity (Weide *et al.*, 2007). Changing a three-dimensional structure or modifying the amino acid sequences flanking the RGD motif can enhance its ligand selectivity (Schaffner and Dard, 2003). Within this area, integrin $\alpha V\beta 3$ was studied most extensively for its role in tumor growth, progression, and angiogenesis. It was considered an interesting biological target for therapeutic cancer drugs and a diagnostic molecular imaging probe (Ye and Chen, 2011). Fluorescein isothiocyanate (FITC)-conjugated dimeric cRGD peptides

(FITC-RGD2, FITC-3P-RGD2, and FITC-GalactoRGD2) were used as fluorescent probes for *in vitro* assays of integrin $\alpha V\beta 3/\alpha V\beta 5$ expression in tumor tissues (Zheng *et al.*, 2014). Quantum dots (QDs) are fluorescent nanocrystals that absorb a wide-range spectrum (400–650 nm) of light and emit a narrow symmetric spectrum of bright fluorescence. These allow the QD signal to be clearly distinguished from the cellular autofluorescence background (Alivisatos *et al.*, 2005; Gao *et al.*, 2005; Michalet *et al.*, 2005; Pinaud *et al.*, 2006). cRGD peptides and a biotin-streptavidin linkage are used to specifically couple individual QDs to $\alpha V\beta 3$ integrins on living osteoblast cells. The positions of individual QDs were tracked with nanometer precision, and localized diffusive behavior was observed (Lieleg *et al.*, 2007). Near-infrared (650–900 nm) fluorescence imaging has provided an effective solution for improving the imaging depth along with sensitivity and specificity by minimizing the autofluorescence of some endogenous absorbers (Shah and Weissleder, 2005; Tung, 2004). Cyanine analogs, such as Cy5, Cy5.5, were used to label cyclic RGD analogs for *in vivo* optical imaging of integrin $\alpha V\beta 3$ positive tumors with high contrast in mice (Jin *et al.*, 2006; Wang *et al.*, 2004).

The C-terminal region of the fibrinogen γ subunit contains γC peptide uniquely binding to activated or primed $\alpha IIb\beta 3$ integrin at the interface between α and β subunits (Hantgan *et al.*, 2006; Springer *et al.*, 2008; Zhao *et al.*, 2016). Therefore, it may serve as the prototype for the design of a probe targeting activated $\alpha IIb\beta 3$ integrin. Gold nanoclusters are a newly developed class of fluorescent particles. The gold nanocluster Au_{18} conjugated with γC peptide peptides were used to detect $\alpha IIb\beta 3$ in HEL with an excitation wavelength of 514 nm and an emission wavelength of 650 nm (Zhao *et al.*, 2016). Due to the specific binding between the Leu-Asp-Val (LDV) peptide and integrin $\alpha 4\beta 1$, fluorophore-conjugated LDV is commonly used to monitor changes of $\alpha 4\beta 1$ integrin conformation or affinity in live cells (Chigaev *et al.*, 2001; Chigaev *et al.*, 2011b). LDV-FITC can be used as a FRET donor to reveal conformational changes of $\alpha 4\beta 1$ under different biological conditions (Chigaev *et al.*, 2003b; Chigaev *et al.*, 2004; Njus *et al.*, 2009).

Soluble ligands ICAM-1 (Lefort *et al.*, 2012; Margraf *et al.*, 2020), vascular cell adhesion protein 1 (VCAM-1) (Sun *et al.*, 2014), and MadCAM-1 (Sun *et al.*, 2018; Sun *et al.*, 2014) were used to detect the activation of $\beta 2$, $\beta 1$, and $\beta 7$ integrins. In the classic article imaging the immunological synapse (Grakoui *et al.*, 1999), Cy5-labeled ICAM-1 were anchored to the bilayer in a manner that allows their free diffusion in the supported bilayer to monitor the dynamic changes of integrin $\alpha L\beta 2$ activation and distribution during the formation of the immunological synapse. A similar approach became a canonical method to study integrins in immunological synapses (Kaizuka *et al.*, 2007; Kondo *et al.*, 2017; Somersalo *et al.*, 2004) and was also used to track active integrin $\alpha L\beta 2$ in leukocyte migration (Smith *et al.*, 2005).

Fluorophore-conjugated integrin allosteric antagonists and agonists are also widely used to label certain integrins. BIRT 377 and XVA-143 are integrin $\alpha L\beta 2$ -specific allosteric antagonists that belong to two distinct classes. The BIRT 377 binding site is located within the I domain of the αL integrin subunit. The XVA-143 site is located between the

α L β -propeller and the β 2 subunit I-like domain (Shimaoka and Springer, 2003). BIRT- and XVA-FITC were used to study conformational changes of integrin α L β 2 (Chigaev et al., 2015). A ligand-mimic small molecular probe has been developed to measure integrin α L β 2 activation (Chigaev et al., 2011a).

Imaging techniques

Live-cell imaging of integrins

Live-cell imaging has been abundantly used in biological studies, including some for integrins. This method has given rise to tremendous progress in documenting dynamic cellular processes, such as cell adhesion (Fan et al., 2016; Morikis et al., 2017; Morikis et al., 2020; Shao et al., 2020; Sun et al., 2020a; Sun et al., 2018; Wen et al., 2020b; Yago et al., 2015; Yago et al., 2018), migration (Kostelnik et al., 2019; Moore et al., 2018; Nordenfelt et al., 2017; Panicker et al., 2020; Ramadass et al., 2019; Tweedy et al., 2020; Zhou et al., 2020), cell-cell interactions (Hanna et al., 2019; Kretschmer et al., 2019; Lin et al., 2015a; Lin et al., 2015b; Omsland et al., 2018; Zucchetti et al., 2019), endocytosis/phagocytosis (Chu et al., 2020; Freeman et al., 2020; Levin-Konigsberg et al., 2019; Ostrowski et al., 2019; Walpole et al., 2020), exocytosis/degranulation (Cohen et al., 2015; Thiam et al., 2020), and cytoskeleton rearrangement (Balint et al., 2013; Ostrowski et al., 2019; Walpole et al., 2020), in real-time and down to the single molecular level (Balint et al., 2013; Katz et al., 2017; Katz et al., 2019; Moore et al., 2018; Mylvaganam et al., 2020). Fluorescent probes and proteins have been ubiquitously utilized in live-cell imaging, allowing observation of dynamics and function of cellular structures and macromolecules, such as integrins, over time and in-depth.

In epifluorescence microscopy, which is the most commonly used wide-field microscopy, all the emission light around the focal plane captured by the objective, which depends on its numerical aperture, is sent to the detector leading to high light-collecting efficiency. The use of the pinhole in confocal laser scanning microscopy (CLSM) decreases the background signal from out-of-focus light and increases the signal-to-background ratio. However, CLSM is limited by phototoxicity/photobleaching. This is mainly due to that most confocal microscopes have detectors with low quantum efficiency, such as photomultiplier tubes (PMT), in comparison to epifluorescence microscopes, such as charge-coupled device (CCD) or complementary metal-oxide-semiconductor (CMOS) cameras. Thus, to acquire images of similar brightness, CLSM needs higher power of the excitation light than epifluorescence microscopy. On the other hand, most CLSM setting has a limited imaging speed due to its scanner. For example, most CLSM has a laser dwell time of ≥ 1 μ s per pixel (Straub et al., 2020), which means that it will take more than 0.25 seconds to acquire a 512×512 image (≤ 4 frames per second). In comparison, most cameras in epifluorescence microscopes allow an imaging speed of ≥ 20 frames per second (1280×1024 pixels). The low speed of CLSM can be overcome by using a high-cost resonant scanner, which allows a speed of 30 fps for 512×512 images. Thus, if the specimen is a monolayer,

epifluorescence microscopy might be a good choice (Stephens and Allan, 2003; Waters, 2007).

Epifluorescence microscopy has been used to monitor β 2 integrin activation during leukocyte rolling on selectins (Kuwano et al., 2010). In the study developing the integrin α L-mYFP mice, an intracellular pool of α L integrins was discovered in CD8⁺ T cells using epifluorescence microscopy (Capece et al., 2017). In the study of the integrin α M-mYFP mice, epifluorescence images showed that α M integrins enriched in the lamellipodia during neutrophil migration (Lim et al., 2015). Epifluorescence-based live-cell fluorescence lifetime imaging microscopy (FLIM)-FRET has been used to demonstrate the cis interaction between sialylated Fc γ RIIA and the α I-domain of integrin α M β 2 (Saggu et al., 2018). In another study, epifluorescence imaging of platelet integrin α IIB β 3 showed that biomechanical platelet aggregation in disturbed flow is mediated by E⁺H⁻ α IIB β 3 integrins (Chen et al., 2019).

For thicker (e.g., 20–100 μ m) live-cell specimens, CLSM was used for imaging integrins (Fan et al., 2019; Lin et al., 2015a; Lock et al., 2018; Sahgal et al., 2019; Schymeinsky et al., 2009). For example, the distribution of integrin α L β 2 during immunological synapse formation was visualized using CLSM (Lin et al., 2015a). Imaging by CLSM, Integrin α V β 5 was found to form novel talin- and vinculin-negative reticular adhesion structures, which may be required for mediating attachment during mitosis (Lock et al., 2018). CLSM was also used to investigate the recycling of active β 1 integrins regulated by GGA2 and RAB13 (Sahgal et al., 2019). CLSM imaging of β 2 integrins illustrated the role of mAbp1 in regulating β 2 integrin-mediated phagocytosis and adhesion (Schymeinsky et al., 2009). CLSM helped to show the distribution of active β 2 integrins during lymphocyte migration, and roles of talin, ZAP-70, rap2, and SHARPIN during lymphocyte migration (Evans et al., 2011; Pouwels et al., 2013; Smith et al., 2005; Stanley et al., 2008; Stanley et al., 2012).

However, the slower imaging speed and higher phototoxicity limit its usage for live-cell imaging. There are some implementations that significantly increase imaging speed and reduce phototoxicity under the condition of CLSM. Such implementations include slit scanning and pinhole multiplexing methods, including spinning disk confocal microscopy (SDCM) (Graf et al., 2005; Maddox et al., 2003). In addition to the fundamental disk containing thousands of pinholes in a spiral, there is a second collector disk with a matching pattern of microlenses focusing excitation light with up to 70% efficiency onto the imaging pinholes. In combination with an electron-multiplying charge-coupled device (EMCCD) detector, SDCM turns to be an ideal solution for fast live-cell confocal imaging of thicker specimens (Wang et al., 2005). Using SDCM, it was found that ADP-ribosylation factor 6 directs the traffic of α 9 and β 1 integrins on dorsal root ganglion neurons (Eva et al., 2012). The dynamic changes of β 5 integrins were visualized by SDCM during mitosis, which suggested that a selective role for integrin β 5 in mitotic cell attachment (Lock et al., 2018). In another study, it was found that phosphatidylinositol 3,4,5-trisphosphate binder Rasa3 was translocated to integrin α IIB β 3 and involved in the integrin

outside-in signaling on platelets during α -thrombin stimulation (Battram *et al.*, 2017).

Another high-resolution live-cell imaging technique is total internal reflection fluorescence (TIRF) microscopy. In TIRF microscopy, a laser incident beam illuminating the boundary between two media of different refractive indices (usually the coverslip and the specimen) experiences total internal reflection. The totally internally reflected laser beam generates the evanescent wave, which excites fluorophores that are in the vicinity of the coverslip-specimen interface (~ 100 – 200 nm), resulting in a very high signal-to-background image with a ~ 100 nm optical section compared to ~ 700 nm of confocal or wide-field (Axelrod, 1981, 2001; Hocde *et al.*, 2009). The high signal-to-background is at the cost of penetration. TIRF can only reveal structures close to the coverslip surface, such as membrane proteins and FAs. As a family of membrane proteins, integrin molecules are highly suitable for analysis with TIRF microscopy. Almost all integrin molecules have been monitored by TIRF microscopy. By using TIRF, it has been shown that FA disassembly during cell migration requires endocytosis of $\beta 1$ integrins, which is regulated by clathrin (Chao and Kunz, 2009). TIRF imaging also showed that mechanical stimuli disassemble $\beta 1$ integrin clusters and enhance endocytosis of integrins expressed on human umbilical vein endothelial cells (HUVECs) (Kiyoshima *et al.*, 2011). H^+ $\beta 2$ integrins reported by monoclonal antibody 327C have been imaged by TIRF microscopy during neutrophil arrest and demonstrated that H^+ $\beta 2$ integrin-ICAM-1 binding initiates calcium influx (Dixit *et al.*, 2011), and kindlin-3 is responsible for $\beta 2$ integrin H^+ (Dixit *et al.*, 2012). H^+ $\beta 2$ integrins can also be reported by mAb24 (Dransfield and Hogg, 1989; Kamata *et al.*, 2002; Lu *et al.*, 2001b), as mentioned before. By using TIRF microscopy, the H^+ $\beta 2$ integrins were found polarized to the lead-edge during T cell migration (Hornung *et al.*, 2020). It has also been demonstrated that $\beta 2$ integrins form podosomes of dendritic cells imaged by TIRF microscopy (Gawden-Bone *et al.*, 2014). In another study, a Rap1-GTP-interacting adapter molecule (RIAM)/lamellipodin-talin-integrin ($\beta 3$) complex that guides cell migration was discovered by using TIRF microscopy (Lagarrigue *et al.*, 2015). The transport of $\beta 3$ to FA has been imaged by TIRF microscopy and was

found to be regulated by an AAK1L- and EHD3-dependent rapid-recycling pathway (Waxmonsky and Conner, 2013). The PDK1-mediated endocytosis of $\beta 3$ integrin during FA disassembly has also been monitored by TIRF microscopy (Di Blasio *et al.*, 2015).

As an update to TIRF microscopy, quantitative dynamic footprinting (qDF) microscopy was developed in 2010 (Sundd *et al.*, 2010), based on the calculation of the evanescent wave intensity and the fluorescence signals of the cell membrane. In the development of qDF microscopy, a two-step calibration procedure involved: (1) The distance of the closest approach of a stationary neutrophil with the coverslip was measured using variable angle TIRF microscopy and was designated Δ_0 (Suppl. Fig. 3 in Sundd *et al.* (2010)); and (2) The z -distance (Δ) of any region in the neutrophil footprint is calculated by fluorescence intensity using the following equation, $\Delta = \Delta_0 + \lambda/4\pi \times (n_1^2 \times \sin^2 \theta - n_2^2)^{-1/2} \times \ln (I_{Fmax}(\theta)/I_F(\theta))$. Fig. 2 described the Δ_0 and Δ (Two examples Δ_1 and Δ_2 are shown). In this equation, λ is the wavelength of the emission light, and n_1 and n_2 are the refractive indexes of the two medium types, such as glass coverslip and cell, respectively. qDF microscopy was used to reveal neutrophil rolling under high shear stress (Sundd *et al.*, 2010; Sundd and Ley, 2013) and was used in monitoring the dynamics of $\beta 2$ integrin activation during human neutrophil arrest (Fan *et al.*, 2019; Fan *et al.*, 2016). By combining qDF with conformational reporting antibodies KIM127 (Lu *et al.*, 2001a; Robinson *et al.*, 1992) and mAb24 (Dransfield and Hogg, 1989; Kamata *et al.*, 2002; Lu *et al.*, 2001b), the canonical switchblade model of $\beta 2$ integrin activation (Luo *et al.*, 2007) was confirmed (Fan *et al.*, 2016). Meanwhile, an unexpected E^-H^+ conformation of $\beta 2$ integrins was observed, which suggested an alternative pathway of $\beta 2$ integrin activation that E^-H^- integrins can acquire high-affinity first (E^-H^+) and then extended (E^+H^+). The E^-H^+ $\beta 2$ integrins can bind ICAM ligands expressed on the same neutrophil in cis and inhibit integrin activation and neutrophil adhesion (Fan *et al.*, 2016).

Super-resolution imaging of integrins

The spatial resolution of microscopic techniques is limited by Abbe's law, according to which the highest achievable lateral and axial resolution ($d_{x,y}$ and d_z), or diffraction limits, can be:

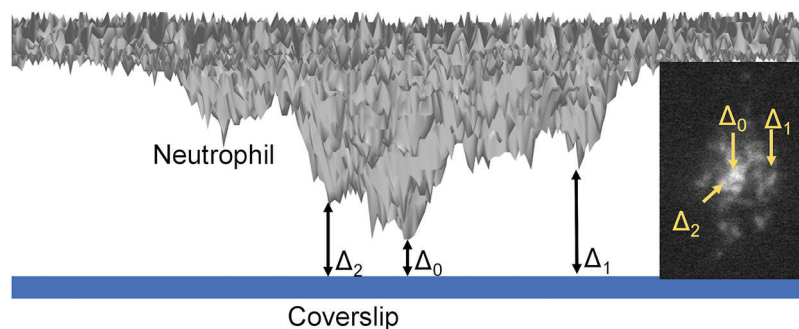


FIGURE 2. Schematics of qDF (quantitative dynamic footprinting) microscopy.

The side-view neutrophil footprint (~ 100 nm) converted from the TIRF (total internal reflection fluorescence) membrane fluorescence image (inset image) was shown (grey surface). The distance of the closest approach of the neutrophil with the coverslip is Δ_0 . This is the position with the brightness cell-membrane fluorescence signal (shown in the inset image). The z -distance (Δ) of other positions was calculated by their cell-membrane fluorescence signal. Two examples (Δ_1 and Δ_2) were shown.

$$d_{x,y} = \frac{\lambda}{2NA}$$

$$d_z = \frac{2\lambda}{NA^2}$$

in which λ is the wavelength of the excitation beam, and NA is the numerical aperture of the microscope objective. $NA = n \sin\alpha$, with n being the refractive index of the medium and α being the half-cone angle of the focused light produced by the objective (Abbe, 1881; Hon, 1882). For example, in a conventional microscope, when a specimen is excited by blue-green light whose wavelength is about 488–550 nm, and an oil immersion objective with $NA = 1.40$ is used, lateral and axial resolution can be ~ 200 nm and ~ 500 nm, respectively (Thompson et al., 2002). Abbe's law holds only true for wide-field microscopes.

Several super-resolution techniques circumvent the limits of diffraction and increase both lateral and axial resolution. One approach beyond the limit of diffraction is to sharpen the point-spread function of the microscope by spatially patterned excitation, including STED (Hell and Wichmann, 1994; Klar et al., 2000), reversible saturable optically linear fluorescence transitions (RESOLFT) (Hell, 2003, 2007, 2009; Hofmann et al., 2005), structured-illumination microscopy (SIM) (Gustafsson, 2000), and saturated structured-illumination microscopy (SSIM) (Gustafsson, 2005). Another is a pointillist approach that requires localization of individual fluorescent molecules (single-molecule localization microscopy, SMLM), such as stochastic optical reconstruction microscopy (STORM) (Rust et al., 2006), photoactivated localization microscopy (PALM) (Betzig et al., 2006), fluorescence photoactivation localization microscopy (fPALM) (Hess et al., 2006), points accumulation for imaging in nanoscale topography (PAINT) (Sharonov and Hochstrasser, 2006), ground-state depletion (GSD) microscopy (Folling et al., 2008). Expansion microscopy (ExM) expands the sample using a polymer system. Positions of labeled molecules were measured by using conventional microscopes. Based on the factor of expansion, the localization of these molecules in the unexpanded cells can be calculated back to achieve nanoscale resolution (Chen et al., 2015). Several super-

resolution microscopy techniques have been summarized before (Galbraith and Galbraith, 2011; Pujals et al., 2019; Wen et al., 2020a), but some will be described here in more detail (Tab. 2).

Super-resolution imaging techniques have been used to study integrin molecules in recent years. Interferometric photoactivation and localization microscopy (iPALM) was used to visualize the three-dimensional structure of FAs, which includes the integrin αV and paxillin-enriched integrin signaling layer, the talin and vinculin-enriched force transduction layer, and zyxin and vasodilator-stimulated phosphoprotein-enriched actin regulatory layer (Kanchanawong et al., 2010). SIM was used to illustrate the linear $\beta 1$ integrin distribution in FAs (Hu et al., 2015). Using a new super-resolution imaging technique with a similar principle to PALM, signal molecular tracking of $\beta 1$ and $\beta 3$ integrin molecules was performed, and they were found entering and exiting from FAs and repeatedly exhibiting temporary immobilizations (Tsunoyama et al., 2018). Using both STED and STORM microscopy, both active and inactive $\beta 1$ integrins were visualized in FAs and were found segregating into distinct nanoclusters (Spiess et al., 2018). STED was also used in testing the colocalization of active $\alpha 5\beta 1$ integrins and PPFIA1 to demonstrate the role of PPFIA1 in active $\alpha 5\beta 1$ integrin recycling. In another study, both active $\beta 1$ and $\beta 5$ integrins were found separately located in FAs (Stubb et al., 2019) by Airyscan confocal microscopy, a super-resolution technique with similar resolution compared to SIM (Huff, 2015). Airyscan confocal microscopy utilized a 32-channel gallium arsenide phosphide photomultiplier tube (GaAsP-PMT) area detector that collects a pinhole-plane image at every scan position. Each detector element functions as a single, very small pinhole. Knowledge about the beam path and the spatial distribution of each detector channel enables very light-efficient imaging with improved resolution and signal-to-noise ratio. αV and $\beta 5$ integrins in FAs were also imaged by iPALM in this study. Airyscan confocal microscopy was also used to identify the colocalization of GGA2, RAB13, and active $\beta 1$ -integrins to demonstrate the role of GGA2 and RAB13 in $\beta 1$ -integrin recycling (Sahgal et al., 2019), and image the localization of $\alpha 11$ and $\beta 1$ integrins on mammary gland stromal fibroblast spreading on collagen (Lerche et al., 2020). GSD microscopy was used to visualize the

TABLE 2

Claimed resolution of super-resolution microscopy used in integrin imaging

Name	lateral resolution	axial resolution
Structured-Illumination Microscopy	100 nm (Gustafsson et al., 2008)	250–350 nm (Gustafsson et al., 2008)
Airyscan Confocal Microscopy	120 nm (Huff et al., 2017)	350 nm (Huff et al., 2017)
Stimulated Emission Depletion Microscopy	45 nm (Neupane et al., 2014)	100 nm (Neupane et al., 2014)
Stochastic Optical Reconstruction Microscopy	20 nm (Rust et al., 2006)	50 nm (Huang et al., 2008)
Photoactivated Localization Microscopy	20 nm (Temprine et al., 2015)	50 nm (Temprine et al., 2015)
Interferometric Photoactivation and Localization Microscopy	20 nm (Shtengel et al., 2009)	10 nm (Shtengel et al., 2009)
Ground State Depletion Microscopy	20 nm (Dixon et al., 2017)	50 nm (Dixon et al., 2017)

LPS-induced colocalization of chloride intracellular channel protein 4 (CLIC4) and $\beta 1$ integrins, demonstrating the role of CLIC4 in cell adhesion and $\beta 1$ integrin trafficking (Argenzio *et al.*, 2014). By using iPALM, the extension of $\alpha L\beta 2$ integrins was monitored by the axial movement of the $\alpha L\beta 2$ headpiece towards the coating substrate during Jurkat T cell migration (Moore *et al.*, 2018). Using Fab fragments of mAb24 and KIM127, the distribution of $E^{-}H^{+}$, $E^{+}H^{-}$, and $E^{+}H^{+}$ $\beta 2$ integrins on neutrophil footprint during arrest was visualized by STORM (Fan *et al.*, 2019). Combined with molecular modeling, the SuperSTORM technique was developed (Fan *et al.*, 2020), and the orientation of $E^{-}H^{+}$, $E^{+}H^{-}$, and $E^{+}H^{+}$ $\beta 2$ integrins were indicated. This work enabled visualizing integrin molecules at the single molecular level and was the first to show the orientation of different conformation integrins. An unexpected face-to-face orientation of $E^{-}H^{+}$ $\beta 2$ integrins is held by cis interaction with ICAM dimers (Fan *et al.*, 2019). Airyscan confocal microscopy was used in imaging $\beta 2$ integrin activation on neutrophils interacting with HUVECs (Fan *et al.*, 2019). Our work (Fan *et al.*, 2019) and a previous one (Moore *et al.*, 2018) mentioned above were both focusing on the conformational changes of $\beta 2$ integrins. Using iPALM, Moore *et al.* (2018) were able to show the E^{+} of $\beta 2$ integrins by measuring the distance of $\beta 2$ integrin headpiece to the substrate. In our work, we measured not only the E^{+} but also the H^{+} of $\beta 2$ integrins. We can report all three active $\beta 2$ integrin conformations ($E^{-}H^{+}$, $E^{+}H^{-}$, and $E^{+}H^{+}$). The pitfall of our work is that we assessed fixed samples, and iPALM can assess live cells. STED was used to show the colocalization of integrin $\alpha L\beta 2$ and low-density lipoprotein receptor-related protein 1 (LRP1) on neutrophils during cytokine midkine-induced neutrophil recruitment. (Weckbach *et al.*, 2019). PALM was used to identify integrin $\beta 3$ nanoclusters within FAs (Deschout *et al.*, 2016; Deschout *et al.*, 2017) and discover the role of integrin $\beta 3$ nanoclusters in bridging thin matrix fibers and forming cell-matrix adhesions (Changede *et al.*, 2019).

Intravital imaging of integrins

Whereas cellular behavior is different between *in vitro* and *in vivo* settings, biological processes are the sum of individual cellular behaviors shaped by many environmental factors. Endless efforts have been made to image cells residing in live animals at microscopic resolution, giving rise to intravital microscopy (IVM), an ever-developing field. In its infancy, blood flow within microvessels and circulating leukocytes targeting to inflamed tissue have been seen through bright field transillumination (Kunkel *et al.*, 2000; Ley *et al.*, 1993; Pittet and Weissleder, 2011; Ramadass *et al.*, 2019). With the advent of fluorescence microscopy, genetically encoded fluorescent proteins (Cappenberg *et al.*, 2019; Deppermann *et al.*, 2020; Girbl *et al.*, 2018; Honda *et al.*, 2020; Hsu *et al.*, 2019; Lammermann *et al.*, 2013; Lefort *et al.*, 2012; Marcovecchio *et al.*, 2020; Matlung *et al.*, 2018; McArdle *et al.*, 2019; Owen-Woods *et al.*, 2020; Powell *et al.*, 2018; Schleicher *et al.*, 2000; Uderhardt *et al.*, 2019; Wen *et al.*, 2020b; Wolf *et al.*, 2018) and fluorescent dyes staining cells *ex vivo* before adoptive transfer or injected directly into the animal to enable visualization of endogenous structures are now available (Arokiasamy *et al.*, 2019; Bouso and Robey, 2004; Deppermann *et al.*, 2020; Girbl *et al.*, 2018;

Honda *et al.*, 2020; Marcovecchio *et al.*, 2020; Marki *et al.*, 2018; Owen-Woods *et al.*, 2020; Rapp *et al.*, 2019; Schoen *et al.*, 2019; Uderhardt *et al.*, 2019; Vats *et al.*, 2020; Wen *et al.*, 2020b; Wolf *et al.*, 2018). Detection of responses of individual cells within their natural environment over extended periods of time and space thus has become possible.

Epifluorescence microscopy can be used as IVM for studying integrins. One study showed that after 24 h of cecal ligation puncture, $\beta 1$ integrins were found in the neutrophil extracellular traps in the liver and helped to sequester circulating tumor cells (Najmeh *et al.*, 2017). In another study, RGD-Quantum Dot was used to report integrin activation on tumor vessel endothelium (Smith *et al.*, 2008). Confocal microscopes can also be used for IVM. Spinning disk confocal IVM was used to visualize $\beta 3$ integrins expressed on vascular endothelial cells, which tethers and interacts with *Borrelia burgdorferi* in circulation during infection (Kumar *et al.*, 2015). Integrin $\alpha 2$ has been used as a marker for platelet aggregates in the spinning disk confocal intravital imaging of hepatic ischemia-reperfusion injury (Van Golen *et al.*, 2015). Multiphoton laser scanning microscopy is another popular method for IVM. Its conception is based on the principle that a fluorophore can not only be excited by one high-energy photon but also two simultaneous low-energy near-infrared photons with longer wavelengths of around 700 to 1,000 nm (Göppert-Mayer, 2009; Kawakami *et al.*, 1999). Two-photon excitation needs a very high local photon density, which is reached at the focal plane. Thus, only fluorophores in the focal plane can be excited in two-photon microscopy. Fluorophores outside the focal plane are highly unlikely to be excited, making a high signal-to-background ratio. In confocal microscopy, fluorophores outside the focal plane will also be excited. In comparison, two-photon microscopy will have less photobleaching of fluorophores outside the focal plane, resulting in the lowest phototoxicity possible (Squirrell *et al.*, 1999; Svoboda and Block, 1994). Great improvement of penetration depths (200–300 μm or even 1000 μm) and longer recording periods can be achieved by this technology (Benninger and Piston, 2013; Hickman *et al.*, 2009; Kobat *et al.*, 2011; Theer *et al.*, 2003). Thus, multiphoton microscopy is a great choice of intravital imaging.

As mentioned before, integrin $\beta 2$ -mCFP mice were developed (Hyun *et al.*, 2012), and these mice helped discover a $\beta 2$ integrin-enriched uropod elongation during leukocyte extravasation using multiphoton IVM. Integrin αM -mYFP mice were developed (Lim *et al.*, 2015) as well. In this study, the migration of αM^{+} leukocytes in the cremaster or trachea during fMLP stimulation or influenza infection was imaged by multiphoton IVM, respectively. In the follow-up study using αM -mYFP/ $\beta 2$ -mCFP and αL -mYFP/ $\beta 2$ -mCFP mice (Hyun *et al.*, 2019), the activation of integrin $\alpha M\beta 2$ and $\alpha L\beta 2$ were reported by FRET *in vivo* for the first time using multiphoton IVM. It was found that $\alpha L\beta 2$ is more important than $\alpha M\beta 2$ in neutrophil transendothelial migration.

Förster Resonance Energy Transfer (FRET) of integrins

Since there are large conformational changes during integrin activation, techniques sensitive to distance changes like

FRET become useful tools in studying integrins. FRET used as a “molecular ruler” ushered in the quantification of intermolecular interactions (Johnson, 2005; Stryer and Haugland, 1967). The concept of FRET was originally proposed by Teodor Förster in 1948. FRET is a phenomenon of quantum mechanics involving two matched fluorophores when the emission spectrum of the donor fluorophore overlaps with the excitation spectrum of the acceptor fluorophore. When the two fluorophores are in close physical juxtaposition (≤ 10 nm), the excitation of the donor results in emitted photons, which are quenched by and transfer the energy to the acceptor, resulting in the emission of acceptor fluorescence (Huebsch and Mooney, 2007; Periasamy, 2001). The efficiency of energy transfer is inversely related to the 6th power of the inter-molecular distance:

$$E = \frac{1}{1 + (r/R_0)^6}$$

E is the efficiency, r is the intermolecular distance, and R_0 , known as Förster constant, is the value of r when this pair of donor and acceptor achieve 50% FRET efficiency. R_0 depends on the overlap integral of the donor emission spectrum with the acceptor absorption spectrum and their mutual molecular orientation as expressed by the following equation:

$$R_0 = \frac{9(\ln 10)}{128\pi^5 N_A} \cdot \frac{Q_D \kappa^2}{\eta^4} \cdot J$$

in which N_A is Avogadro's number; Q_D is the fluorescence quantum yield of the donor in the absence of acceptor; κ^2 is the dipole orientation factor; η is the refractive index of the medium; and J is the spectral overlap integral of the donor-acceptor pair (Wang and Chien, 2007). Therefore, the range over which FRET can be observed is very narrow; only intra- and inter-molecular distances within ~ 2 – 10 nm can be detected (Huebsch and Mooney, 2007; Periasamy, 2001). The FRET efficiency can be altered by any change of the orientation or distance between the two fluorophores (Tsien, 1998).

To obtain a FRET signal for studying the interaction of two proteins, they must be fluorescently labeled. One approach is to label the antibodies or antagonist/agonist binding to the two proteins with proper fluorophores. Fluorophore-conjugated antagonist/agonist can be synthesized, while labeling kits facilitating covalent binding (usually using amide bonds) of many different fluorescent molecules to antibodies are commercially available (Fan et al., 2019; Fan et al., 2016; Masi et al., 2010; Wen et al., 2020b). Another approach is introducing genes of two fluorescent proteins (FPs) to the donor/acceptor pair of proteins, respectively. Owing to their excellent extinction coefficients, quantum yield, and photostability, cyan fluorescence protein (CFP) and yellow fluorescence protein (YFP) are the most commonly used pair for FRET (Giepmans et al., 2006; Tsien, 1998). Green fluorescence protein (GFP) and red fluorescence protein (RFP) can also be utilized as a pair of fluorophores for FRET (Bajar et al., 2016; Lam et al., 2012). Genetic manipulation is conducted to gain recombinant fused genes, and the 1:1 ratio of donor/

adaptor protein to CFP/YFP greatly simplifies the calculations of FRET efficiency and the quantification of protein interactions. One drawback of fusion proteins is the possibility to exhibit altered biological function or molecular structure. Thus, careful characterization before FRET is recommended (Masi et al., 2010; McArdle et al., 2016).

Measurements of (1) signal intensity and (2) fluorescence lifetimes are two major ways to determine FRET efficiency. Regarding the signal intensity method, the comparable changes between the intensification of the acceptor's emission and synchronous decrease in donor's emission facilitate the detection of FRET by splitting the emission from the two fluorophores. The split lights are then filtered through a specific filter set and collected separately. The downsides of this method are: (1) The excitation light of acceptor may excite the donor owing to the possible overlap of their excitation spectrum, (2) The leak of donor emission to the detecting channel of the acceptor, and (3) The faster photobleaching of the donor compared with that of the acceptor (Masi et al., 2010). The fluorescence lifetime is an intrinsic property of fluorophores. It is the characteristic time that a fluorophore stays in the excited state before the emission of the fluorescence photon. Fluorescence lifetime imaging microscopy (FLIM) uses pulsed excitation lasers to acquire quantitative information through measurements of fluorescence lifetimes (Lakowicz et al., 1992; Le Marois and Suhling, 2017). Based on the fact that fluorescence lifetime decreases proportionally with the efficiency of FRET, FLIM-FRET serves as a precise way to determine FRET efficiency (Suhling et al., 2015). Although spectral overlap must always be taken into consideration in both methods, FLIM can rule out the influence of local fluorophore concentration or fluorescence intensity leading to the defects in signal intensity measurement (Lakowicz and Masters, 2008). There are additional strategies to measure FRET efficiency. “Donor de-quenching” (or “Acceptor photo-bleach”) method photo-bleaches the acceptor; thus, the increase of fluorescence in the “de-quenched” donor is proportional to FRET efficiency. FRET efficiency can be determined by measurement of donor fluorescence intensity before and after photobleaching of the acceptor. This method is an endpoint measurement making it incompatible with dynamic monitoring (Carman, 2012; Periasamy, 2001; Wang and Chien, 2007).

With the help of the improvement in microscopic techniques and labeling with fluorophores, great advantages have been made regarding integrin conformation and signaling. FRET can be used to identify the spatial movement of integrin cytoplasmic tails (Fig. 3A). In a classical study, leukocytes were stably transfected with FRET donor and acceptor pair mCFP and mYFP at the C-termini of the integrin α_L and β_2 subunits, respectively. In the resting state, high FRET efficiency was measured, indicating that the c-termini of the α_L and β_2 subunits were close to each other. Upon the triggering of the integrin inside-out signaling (chemokine SDF-1 and its receptor CXCR4) or outside-in signaling (ICAM-1 in the presence of Mn^{2+}), the FRET efficiency was significantly reduced, indicating a spatial separation of α_L and β_2 cytoplasmic tails. Bidirectional integrin signaling is accomplished by coupling extracellular conformational changes to the separation of the

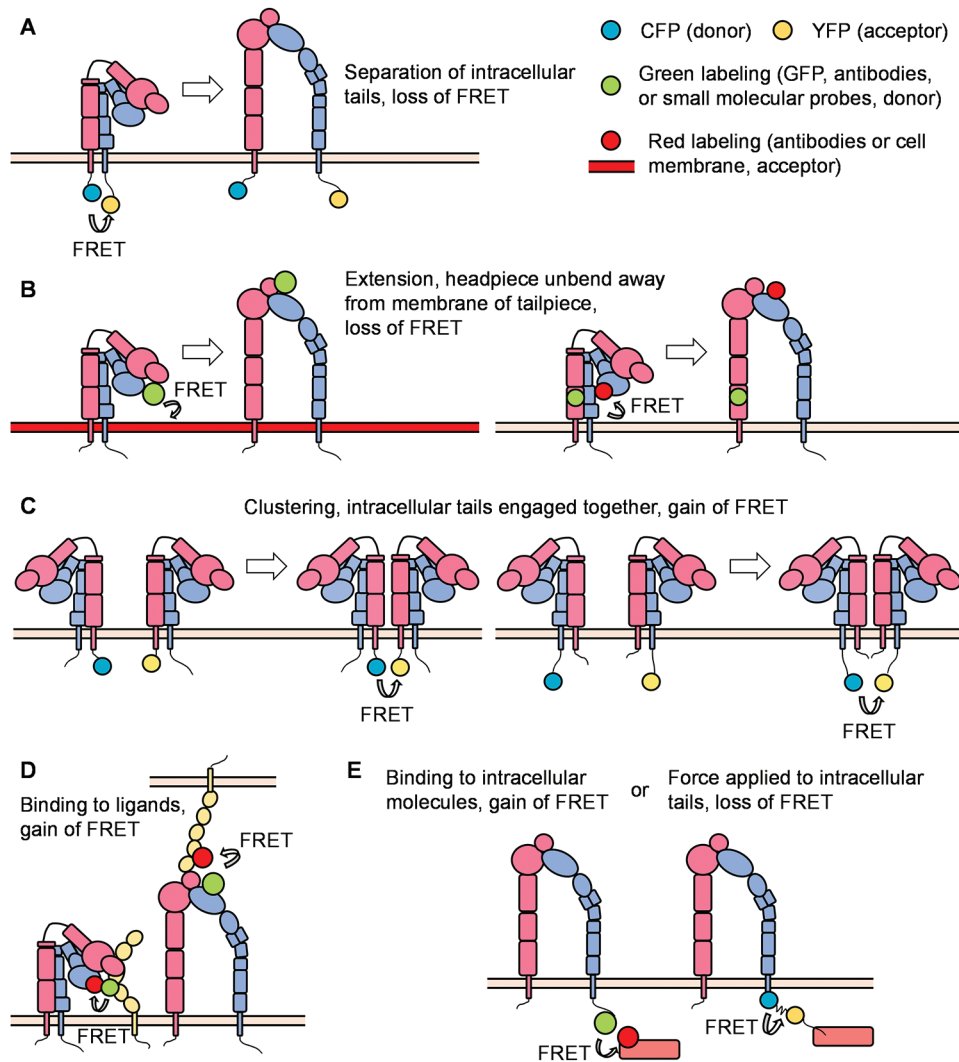


FIGURE 3. Principles of FRET (Förster resonance energy transfer) in integrin studies.

(A) The cytoplasmic tails of α and β subunits were labeled with FRET donor and acceptor, respectively. The separation of cytoplasmic tails is assessed by the reduction of FRET. (B) The integrin headpiece and cell membrane/integrin tailpiece were labeled with FRET donor and acceptor, respectively. The extension/unbent of integrin ectodomain is assessed by the reduction of FRET. (C) The cytoplasmic tails of α or β subunits were labeled with both FRET donor and acceptor. The clustering of integrin molecules is assessed by the increase of FRET. (D–E) The interaction of integrins and their ligands (D, both in cis and in trans) or cytoplasmic regulators (E, interaction or force measurement) can be assessed by FRET.

cytoplasmic domains (Kim *et al.*, 2003). A similar strategy has been applied to study α M β 2 integrin activation (α M-mCFP, β 2-mYFP) as well (Fu *et al.*, 2006; Lefort *et al.*, 2009). The first dual-fluorescent protein KI mice – α L β 2 FRET (α L-YFP/ β 2-CFP) mice and α M β 2 FRET (α L-YFP/ β 2-CFP) mice – have been successfully constructed. By using two-photon intravital ratiometric analysis of (CFP/YFP) in neutrophils from these mice, determination of differential regulation of integrin α L β 2 and α M β 2 during neutrophil extravasation became realized (Hyun *et al.*, 2019).

FRET can also be used to identify conformational changes in the integrin ectodomain domains. One method is to label the integrin headpiece and cell membrane/integrin tailpiece with FRET donor and acceptor, respectively, to measure the extension/unbending of integrins (Fig. 3B). In some studies, the LDV-FITC probe binding to the α 4-integrin headgroup and octadecyl rhodamine B incorporated into the plasma membrane were used as the donor/acceptor

pair for FRET assays. Several publications have proved the feasibility of detecting the extension of integrin α 4 β 1 (Chigaev *et al.*, 2003a; Chigaev *et al.*, 2008; Sambrano *et al.*, 2018). Integrin α I**b** β 3 at the surface of blood platelets plays a primary role in hemostasis. FRET using fluorescently labeled Fab fragments of monoclonal antibodies targeting the β A/I-like domain of β 3 subunit (donor, Alexa Fluor 488 conjugated P97 Fab) and the calf-2 domain of α I**b** subunit (acceptor, Cy3-M3 Fab or Cy3-M10 Fab) can determine the distance between these two domains at rest (about 6 nm) or activation (about 17 nm) states. Researchers found that activated α I**b** β 3 in living platelets exhibits a conformation less extended than proposed by the switchblade model (Coutinho *et al.*, 2007). In another study, a FITC-conjugated monoclonal antibody against integrin α M headpiece and octadecyl rhodamine B incorporated into the plasma membrane were used as the donor/acceptor pair for FRET assays to measure the extension of integrin α M β 2 (Lefort *et*

al., 2009). Two distinct allosteric antagonists (BIRT 377 and XVA-143) targeting the α LI domain and β 2 subunit I-like domain were used as donors. FRET conducted on live cells using a real-time flow cytometry approach was used to measure the distance between these two donors and a novel lipid acceptor PKH 26. Researchers found that triggering of the pathway used for T-cell activation (phorbol ester and thapsigargin) induced rapid extension of the integrin α L β 2 (Chigaev et al., 2015).

Instead of attaching donor and acceptor respectively to α and β subunits, studying integrin micro-clustering requires attachment of both the donor and acceptor to either the α or β subunit within one heterodimeric integrin (Fig. 3C). In this case, integrin micro-clustering will lead to FRET. In a study focused on *Drosophila* α PS2C β PS integrin, mVenus and mCherry were fused to cytoplasmic and transmembrane domains of integrin β subunits. Mutations in α subunit cytoplasmic domain (GFFNR to GFANA) or β subunit (V409D), which showed higher affinity for ligands, showed ~2-3-fold higher FRET values compared to that of wild type (Smith et al., 2007). In another study, K562 cells were transiently transfected with α L-mCFP, α L-mYFP, and wild-type β 2, generating approximately equal amounts of α L-mCFP/2 and α L-mYFP/2 cells. The binding of ICAM-1 oligomers resulted in significant micro-clustering. In contrast, monomeric ICAM-1 did not induce integrin α L β 2 clustering (Kim et al., 2004). Using the same methodology, researchers found the disruption of the α L β 2 transmembrane domain by mutation of a key interface residue Thr-686 in the β 2 transmembrane domain promoted binding of α L β 2 with ICAMs and facilitated α L microcluster formation (Vararattanavech et al., 2009).

FRET can also be used to assess interactions of the integrin headpiece with its ligands (Fig. 3D) and integrin cytoplasmic domains with the cytoskeleton and various signaling molecules (Fig. 3E) during integrin inside-out and outside-in signaling. In our previous study, we used FRET to detect the in-cis interaction of E⁻H⁺ β 2 integrins and ICAM-1 (Fan et al., 2016). HA58-FITC, which binds ICAM-1 domain 1 and blocks its interaction with integrin α L β 2, but not integrin α M β 2, was used as the FRET donor. Antibody mAb24-DyLight 550 binding β 2 integrin H⁺ headpiece was used as the acceptor. When integrin α M β 2 bound ICAM-1 in cis, the two antibodies were close enough to have FRET. When this interaction was blocked by mAb R6.5, which binds to integrin α M β 2-binding domain 3 of ICAM-1, or replacing the acceptor by KIM127- DyLight 550 (binding to the knees of E⁺ β 2 integrins), FRET did not occur. These results indicate that E⁻H⁺ integrin α M β 2 binds ICAM-1 in cis (Fan et al., 2016). In another study, antibodies against Fc γ RIIA (Alexa Fluor 488) and integrin α M β 2 (Alexa Fluor 568) were used as donor and acceptor, respectively, to demonstrate the cis interaction of integrin α M β 2 and Fc γ RIIA by FLIM-FRET (Saggu et al., 2018). High-throughput dynamic three-color single molecule-FRET tracking was conceived. Orthogonal labeling of RGD and PHSRN motifs within fibronectin serve as FRET donor (Alexa Fluor 555) and acceptor (Alexa Fluor 594) at residues 1381 and 1500, respectively. FRET signatures are distinctive for the folded and unfolded state. The

extracellular domain of α v β 3 was labeled with Alexa Fluor 647. By monitoring the intensity of all three dyes, the impact of fibronectin conformation and dynamics on α v β 3 integrin-binding can be determined. A more stable fibronectin- α v β 3 complex was observed when fibronectin exhibited a more folded conformation (Kastantin et al., 2017). Interaction of PKC α with β 1 integrin was detected by FLIM-FRET performed in MCF7 cells, in which GFP-PKC α fusion protein was used as the donor, and integrin β 1 antibody conjugated with Cy3.5 was used as the acceptor (Ng et al., 1999). Using FLIM-FRET, GFP-conjugated β 1 integrin of mouse embryonic fibroblasts was found to interact with mRFP conjugates of the talin rod domain and α -actinin but not the talin head domain or paxillin (Parsons et al., 2008). Schwartz and colleagues have constructed a FRET-based tension sensor methodology, which consists of monomeric teal fluorescent protein (mTFP1) and monomeric Venus (mVenus) joined by a 40 amino-acid elastic linker (Faulon Marruecos et al., 2016). The elastic linker can elongate upon tensile force in the range of 0–6 pN. Incorporation of this reporter into the β 2 subunit of integrin α L β 2 enabled researchers to find that actin polymerization and extracellular ligand-binding are in a positive feedback loop (Nordenfelt et al., 2016). FRET was used to assess the association of β 1-integrin and ErbB2, which is an important integrator of transmembrane signaling by the EGFR family, on tumor cells. (Mocanu et al., 2005).

Conclusions

Overall, optical imaging of integrin molecules helps us understand the regulation of integrin expression, localization, clustering, conformational changes, and functions. Although there are various antibodies targeting integrin to visualize integrins with different conformations, most of these antibodies are specific for human integrin molecules. This limits the use of these antibodies for studying integrins in physiologically-relevant *in vivo* systems, such as mouse disease models, as well as in loss-of-function assays of integrin regulators because it is impossible to do genetic editing in humans. It has been reported that introducing human β 2 integrins restores the infectious deficiency in β 2 integrin knockout mice (Wilson et al., 1993). Thus, replacing the mouse integrin gene with human integrin cDNA might be a way to expand the use of existing integrin antibodies.

As we discussed, super-resolution microscopy is a powerful tool for studying integrins. However, their uses in integrin studies are mostly restricted to phenomenon reports and morphology studies. Thus, finding a way to dig into the molecular details of integrin regulation and function using super-resolution microscopy needs more attention. For example, super-resolution imaging can better assess the clustering of integrin molecules. Assessing the localization of important integrin modulators, such as talin, kindlin, RIAM, etc., by super-resolution microscopy will help understand their roles in regulating integrin activation.

FRET is a powerful tool to study dynamic changes in integrin conformation, but most FRET assays of integrins

are restricted in cell lines. Only two integrin FRET mouse strains (α L β 2 and α M β 2) were developed. Thus, the development of more integrin FRET mouse strains is needed to visualize integrin conformation changes *in vivo*. Those mice could also be used in studying molecular mechanisms of integrin regulation and functions or in different disease models.

Although many techniques were developed to visualize integrin molecules as we reviewed above, whether the fluorescence labeling affects integrin function needs to be demonstrated in the specific studies, especially for activating specific integrin antibodies and fluorescent protein tags. For example, KIM127 was reported to stimulate leukocyte aggregation (Robinson *et al.*, 1992), and mAb24 may lock the H⁺ conformation of β 2 integrins (Smith *et al.*, 2005). Thus, when using them in imaging, whether they affect the specific function interested in your study becomes critical. When we use them in studying integrin activation during neutrophil rolling and arrest, we tested that they do not affect ligand binding of β 2 integrins and neutrophil arrest (Fan *et al.*, 2016). This is the same case for fluorescent protein tags. In the iPALM study of β 2 integrin (Moore *et al.*, 2018), a mEos3.2 tag was inserted in the β -propeller domain of the α L-subunit of integrin α L β 2. They measure the axial movement of the mEos3.2 tag to report E⁺ of integrin α L β 2. They have tested that the fluorescence protein insertion in this site does not affect cell adhesion and ICAM-1 binding (Bonasio *et al.*, 2007). In another study, a CFP-YFP tension sensor was inserted into the β 2 integrin cytoplasmic tail to measure the force bearing of β 2 integrins during cell migration using FRET (Nordenfelt *et al.*, 2016). They have demonstrated that the insertion they used does not affect cell migration compared to cells transfected with wild-type β 2 integrins.

Acknowledgement: We acknowledge Dr. Christopher “Kit” Bonin and Dr. Geneva Hargis from UConn Health School of Medicine for their help in the scientific writing and editing of this manuscript.

Author Contribution: Review conception and design: Z.F.; Manuscript draft: C.C.; Manuscript revision and editing: Z. F., H.S., L.H.; Figure and table preparation: Z.F., C.C.; All authors reviewed the results and approved the final version of the manuscript.

Funding Statement: This work was supported by funding from the National Institutes of Health, USA (NIH, R01HL145454), and a startup fund from UConn Health.

Conflicts of Interest: The authors declare that they have no conflicts of interest to report regarding the present study.

References

- Abbe HE (1881). VII.-On the estimation of aperture in the microscope. *Journal of the Royal Microscopical Society* **1**: 388–423. DOI 10.1111/j.1365-2818.1881.tb05909.x.
- Adair BD, Alonso JL, Van Agthoven J, Hayes V, Ahn HS, Yu IS, Lin SW, Xiong JP, Poncz M, Arnaout MA (2020). Structure-guided design of pure orthosteric inhibitors of α IIB β 3 that prevent thrombosis but preserve hemostasis. *Nature Communications* **11**: 398. DOI 10.1038/s41467-019-13928-2.
- Alivisatos AP, Gu W, Larabell C (2005). Quantum dots as cellular probes. *Annual Review of Biomedical Engineering* **7**: 55–76. DOI 10.1146/annurev.bioeng.7.060804.100432.
- Andrew DP, Berlin C, Honda S, Yoshino T, Hamann A, Holzmann B, Kilshaw PJ, Butcher EC (1994). Distinct but overlapping epitopes are involved in α 4 β 7-mediated adhesion to vascular cell adhesion molecule-1, mucosal addressin-1, fibronectin, and lymphocyte aggregation. *Journal of Immunology* **153**: 3847–3861.
- Antonov AS, Antonova GN, Munn DH, Mivechi N, Lucas R, Catravas JD, Verin AD (2011). α V β 3 integrin regulates macrophage inflammatory responses via PI3 kinase/Akt-dependent NF- κ B activation. *Journal of Cellular Physiology* **226**: 469–476. DOI 10.1002/jcp.22356.
- Argenzio E, Margadant C, Leyton-Puig D, Janssen H, Jalink K, Sonnenberg A, Moolenaar WH (2014). CLIC4 regulates cell adhesion and β 1 integrin trafficking. *Journal of Cell Science* **127**: 5189–5203. DOI 10.1242/jcs.150623.
- Arnaout MA (2002). Integrin structure: New twists and turns in dynamic cell adhesion. *Immunological Reviews* **186**: 125–140. DOI 10.1034/j.1600-065X.2002.18612.x.
- Arnaout MA (2016). Biology and structure of leukocyte β 2 integrins and their role in inflammation. *F1000Research* **5**: F1000 Faculty Rev-2433.
- Arnaout MA, Goodman SL, Xiong JP (2007). Structure and mechanics of integrin-based cell adhesion. *Current Opinion in Cell Biology* **19**: 495–507. DOI 10.1016/j.ccb.2007.08.002.
- Arnaout MA, Mahalingam B, Xiong JP (2005). Integrin structure, allostery, and bidirectional signaling. *Annual Review of Cell and Developmental Biology* **21**: 381–410. DOI 10.1146/annurev.cellbio.21.090704.151217.
- Arokiasamy S, King R, Boulaghrasse H, Poston RN, Nourshargh S, Wang W, Voisin MB (2019). Heparanase-dependent remodeling of initial lymphatic glycocalyx regulates tissue-fluid drainage during acute inflammation *in vivo*. *Frontiers in Immunology* **10**: 2316. DOI 10.3389/fimmu.2019.02316.
- Artoni A, Li J, Mitchell B, Ruan J, Takagi J, Springer TA, French DL, Collier BS (2004). Integrin β 3 regions controlling binding of murine mAb 7E3: Implications for the mechanism of integrin α IIB β 3 activation. *Proceedings of the National Academy of Sciences of the United States of America* **101**: 13114–13120. DOI 10.1073/pnas.0404201101.
- Askari JA, Tynan CJ, Webb SE, Martin-Fernandez ML, Ballestrem C, Humphries MJ (2010). Focal adhesions are sites of integrin extension. *Journal of Cell Biology* **188**: 891–903. DOI 10.1083/jcb.200907174.
- Axelrod D (1981). Cell-substrate contacts illuminated by total internal reflection fluorescence. *Journal of Cell Biology* **89**: 141–145. DOI 10.1083/jcb.89.1.141.
- Axelrod D (2001). Total internal reflection fluorescence microscopy in cell biology. *Traffic* **2**: 764–774. DOI 10.1034/j.1600-0854.2001.211104.x.
- Bagi Z, Couch Y, Broskova Z, Perez-Balderas F, Yeo T, Davis S, Fischer R, Sibson NR, Davis BG, Anthony DC (2019). Extracellular vesicle integrins act as a nexus for platelet adhesion in cerebral microvessels. *Scientific Reports* **9**: 15847. DOI 10.1038/s41598-019-52127-3.
- Bajar BT, Wang ES, Lam AJ, Kim BB, Jacobs CL, Howe ES, Davidson MW, Lin MZ, Chu J (2016). Improving brightness and photostability of green and red fluorescent proteins for live

- cell imaging and FRET reporting. *Scientific Reports* **6**: 20889. DOI 10.1038/srep20889.
- Balint S, Verdeny Vilanova I, Sandoval Alvarez A, Lakadamyali M (2013). Correlative live-cell and superresolution microscopy reveals cargo transport dynamics at microtubule intersections. *Proceedings of the National Academy of Sciences of the United States of America* **110**: 3375–3380. DOI 10.1073/pnas.1219206110.
- Barczyk M, Carracedo S, Gullberg D (2010). Integrins. *Cell and Tissue Research* **339**: 269–280. DOI 10.1007/s00441-009-0834-6.
- Battram AM, Durrant TN, Agbani EO, Heesom KJ, Paul DS, Piatt R, Poole AW, Cullen PJ, Bergmeier W, Moore SF, Hers I (2017). The Phosphatidylinositol 3,4,5-trisphosphate (PI(3,4,5)P₃) binder Rasa3 regulates Phosphoinositide 3-kinase (PI3K)-dependent Integrin α IIb β 3 Outside-in Signaling. *Journal of Biological Chemistry* **292**: 1691–1704. DOI 10.1074/jbc.M116.746867.
- Beals CR, Edwards AC, Gottschalk RJ, Kuijpers TW, Staunton DE (2001). CD18 activation epitopes induced by leukocyte activation. *Journal of Immunology* **167**: 6113–6122. DOI 10.4049/jimmunol.167.11.6113.
- Benninger RK, Piston DW (2013). Two-photon excitation microscopy for the study of living cells and tissues. *Current Protocols in Cell Biology* **59**: 4–11. DOI 10.1002/0471143030.cb0411s59.
- Berlin C, Berg EL, Briskin MJ, Andrew DP, Kilshaw PJ, Holzmann B, Weissman IL, Hamann A, Butcher EC (1993). α 4 β 7 integrin mediates lymphocyte binding to the mucosal vascular addressin MAdCAM-1. *Cell* **74**: 185–195. DOI 10.1016/0092-8674(93)90305-A.
- Bernadskaya YY, Brahmabhatt S, Gline SE, Wang W, Christiaen L (2019). Discoidin-domain receptor coordinates cell-matrix adhesion and collective polarity in migratory cardiopharyngeal progenitors. *Nature Communications* **10**: 57. DOI 10.1038/s41467-018-07976-3.
- Betzig E, Patterson GH, Sougrat R, Lindwasser OW, Olenych S, Bonifacino JS, Davidson MW, Lippincott-Schwartz J, Hess HF (2006). Imaging intracellular fluorescent proteins at nanometer resolution. *Science* **313**: 1642–1645. DOI 10.1126/science.1127344.
- Bode W, Engh R, Musil D, Thiele U, Huber R, Karshikov A, Brzin J, Kos J, Turk V (1988). The 2.0 Å X-ray crystal structure of chicken egg white cystatin and its possible mode of interaction with cysteine proteinases. *EMBO Journal* **7**: 2593–2599. DOI 10.1002/j.1460-2075.1988.tb03109.x.
- Bonasio R, Carman CV, Kim E, Sage PT, Love KR, Mempel TR, Springer TA, Von Andrian UH (2007). Specific and covalent labeling of a membrane protein with organic fluorochromes and quantum dots. *Proceedings of the National Academy of Sciences of the United States of America* **104**: 14753–14758. DOI 10.1073/pnas.0705201104.
- Bork P, Doerks T, Springer TA, Snel B (1999). Domains in plexins: Links to integrins and transcription factors. *Trends in Biochemical Sciences* **24**: 261–263. DOI 10.1016/S0968-0004(99)01416-4.
- Bouso P, Robey EA (2004). Dynamic behavior of T cells and thymocytes in lymphoid organs as revealed by two-photon microscopy. *Immunity* **21**: 349–355. DOI 10.1016/j.immuni.2004.08.005.
- Bridges LC, Sheppard D, Bowditch RD (2005). ADAM disintegrin-like domain recognition by the lymphocyte integrins α 4 β 1 and α 4 β 7. *Biochemical Journal* **387**: 101–108. DOI 10.1042/BJ20041444.
- Bui T, Rennhack J, Mok S, Ling C, Perez M, Roccamo J, Andrechek ER, Moraes C, Muller WJ (2019). Functional redundancy between β 1 and β 3 integrin in activating the IR/Akt/mTORC1 signaling axis to promote ErbB2-driven breast cancer. *Cell Reports* **29**: 589–602.e6. DOI 10.1016/j.celrep.2019.09.004.
- Burrows L, Clark K, Mould AP, Humphries MJ (1999). Fine mapping of inhibitory anti- α 5 monoclonal antibody epitopes that differentially affect integrin-ligand binding. *Biochemical Journal* **344**: 527–533.
- Byron A, Humphries JD, Askari JA, Craig SE, Mould AP, Humphries MJ (2009). Anti-integrin monoclonal antibodies. *Journal of Cell Science* **122**: 4009–4011. DOI 10.1242/jcs.056770.
- Campbell ID, Humphries MJ (2011). Integrin structure, activation, and interactions. *Cold Spring Harbor Perspectives in Biology* **3**: a004994. DOI 10.1101/cshperspect.a004994.
- Capece T, Walling BL, Lim K, Kim KD, Bae S, Chung HL, Topham DJ, Kim M (2017). A novel intracellular pool of LFA-1 is critical for asymmetric CD8⁺ T cell activation and differentiation. *Journal of Cell Biology* **216**: 3817–3829. DOI 10.1083/jcb.201609072.
- Cappenberg A, Margraf A, Thomas K, Bardel B, Mccree DA, Van Marck V, Mellmann A, Lowell CA, Zarbock A (2019). L-selectin shedding affects bacterial clearance in the lung: A new regulatory pathway for integrin outside-in signaling. *Blood* **134**: 1445–1457. DOI 10.1182/blood.2019000685.
- Carman CV (2012). Overview: Imaging in the study of integrins. *Methods in Molecular Biology* **757**: 159–189.
- Carreno R, Brown WS, Li D, Hernandez JA, Wang Y, Kim TK, Craft JW Jr., Komanduri KV, Radvanyi LG, Hwu P, Molldrem JJ, Legge GB, McIntyre BW, Ma Q (2010). 2E8 binds to the high affinity I-domain in a metal ion-dependent manner: A second generation monoclonal antibody selectively targeting activated LFA-1. *Journal of Biological Chemistry* **285**: 32860–32868. DOI 10.1074/jbc.M110.111591.
- Martins Cavaco AC, Rezaei M, Caliendo MF, Lima AM, Stehling M, Dhayat SA, Haier J, Brakebusch C, Eble JA (2018). The interaction between laminin-332 and α 3 β 1 integrin determines differentiation and maintenance of CAFs, and supports invasion of pancreatic duct adenocarcinoma cells. *Cancers* **11**: 14. DOI 10.3390/cancers11010014.
- Clark AY, Martin KE, Garcia JR, Johnson CT, Theriault HS, Han WM, Zhou DW, Botchwey EA, Garcia AJ (2020). Integrin-specific hydrogels modulate transplanted human bone marrow-derived mesenchymal stem cell survival, engraftment, and reparative activities. *Nature Communications* **11**: 114. DOI 10.1038/s41467-019-14000-9.
- Clark K, Pankov R, Travis MA, Askari JA, Mould AP, Craig SE, Newham P, Yamada KM, Humphries MJ (2005). A specific α 5 α 1-integrin conformation promotes directional integrin translocation and fibronectin matrix formation. *Journal of Cell Science* **118**: 291–300. DOI 10.1242/jcs.01623.
- Cluzel C, Saltel F, Lussi J, Paulhe F, Imhof BA, Wehrle-Haller B (2005). The mechanisms and dynamics of α 3 β 1 integrin clustering in living cells. *Journal of Cell Biology* **171**: 383–392. DOI 10.1083/jcb.200503017.
- Cohen R, Holowka DA, Baird BA (2015). Real-time imaging of Ca²⁺ mobilization and degranulation in mast cells. *Methods in Molecular Biology* **1220**: 347–363.
- Coutinho A, Garcia C, Gonzalez-Rodriguez J, Lillo MP (2007). Conformational changes in human integrin α IIb β 3 after platelet activation, monitored by FRET. *Biophysical Chemistry* **130**: 76–87. DOI 10.1016/j.bpc.2007.07.007.

- Chalfie M, Tu Y, Euskirchen G, Ward WW, Prasher DC (1994). Green fluorescent protein as a marker for gene expression. *Science* **263**: 802–805. DOI 10.1126/science.8303295.
- Chandele A, Sewatanon J, Gunisetty S, Singla M, Onlamoon N, Akondy RS, Kissick HT, Nayak K, Reddy ES, Kalam H, Kumar D, Verma A, Panda H, Wang S, Angkasekwinai N, Pattanapanyasat K, Chokephaibulkit K, Medigeshi GR, Lodha R, Kabra S, Ahmed R, Murali-Krishna K (2016). Characterization of human CD8 T cell responses in dengue virus-infected patients from India. *Journal of Virology* **90**: 11259–11278. DOI 10.1128/JVI.01424-16.
- Changede R, Cai H, Wind SJ, Sheetz MP (2019). Integrin nanoclusters can bridge thin matrix fibres to form cell-matrix adhesions. *Nature Materials* **18**: 1366–1375. DOI 10.1038/s41563-019-0460-y.
- Chao WT, Kunz J (2009). Focal adhesion disassembly requires clathrin-dependent endocytosis of integrins. *FEBS Letters* **583**: 1337–1343. DOI 10.1016/j.febslet.2009.03.037.
- Chen F, Tillberg PW, Boyden ES (2015). Optical imaging. *Expansion microscopy. Science* **347**: 543–548.
- Chen X, Xie C, Nishida N, Li Z, Walz T, Springer TA (2010). Requirement of open headpiece conformation for activation of leukocyte integrin $\alpha\beta 2$. *Proceedings of the National Academy of Sciences of the United States of America* **107**: 14727–14732. DOI 10.1073/pnas.1008663107.
- Chen Y, Ju LA, Zhou F, Liao J, Xue L, Su QP, Jin D, Yuan Y, Lu H, Jackson SP, Zhu C (2019). An integrin $\alpha\text{IIb}\beta 3$ intermediate affinity state mediates biomechanical platelet aggregation. *Nature Materials* **18**: 760–769. DOI 10.1038/s41563-019-0323-6.
- Cheng M, Li J, Negri A, Collier BS (2013). Swing-out of the $\beta 3$ hybrid domain is required for $\alpha\text{IIb}\beta 3$ priming and normal cytoskeletal reorganization, but not adhesion to immobilized fibrinogen. *PLoS One* **8**: e81609. DOI 10.1371/journal.pone.0081609.
- Chigaev A, Blenc AM, Braaten JV, Kumaraswamy N, Kepley CL, Andrews RP, Oliver JM, Edwards BS, Prossnitz ER, Larson RS, Sklar LA (2001). Real time analysis of the affinity regulation of $\alpha 4$ -integrin. The physiologically activated receptor is intermediate in affinity between resting and Mn^{2+} or antibody activation. *Journal of Biological Chemistry* **276**: 48670–48678. DOI 10.1074/jbc.M103194200.
- Chigaev A, Buranda T, Dwyer DC, Prossnitz ER, Sklar LA (2003a). FRET detection of cellular $\alpha 4$ -integrin conformational activation. *Biophysical Journal* **85**: 3951–3962. DOI 10.1016/S0006-3495(03)74809-7.
- Chigaev A, Smagley Y, Haynes MK, Ursu O, Bologa CG, Halip L, Oprea T, Waller A, Carter MB, Zhang Y, Wang W, Buranda T, Sklar LA (2015). FRET detection of lymphocyte function-associated antigen-1 conformational extension. *Molecular Biology of the Cell* **26**: 43–54. DOI 10.1091/mbc.e14-06-1050.
- Chigaev A, Smagley Y, Zhang Y, Waller A, Haynes MK, Amit O, Wang W, Larson RS, Sklar LA (2011a). Real-time analysis of the inside-out regulation of lymphocyte function-associated antigen-1 revealed similarities to and differences from very late antigen-4. *Journal of Biological Chemistry* **286**: 20375–20386. DOI 10.1074/jbc.M110.206185.
- Chigaev A, Waller A, Amit O, Sklar LA (2008). Galphas-coupled receptor signaling actively down-regulates $\alpha 4\beta 1$ -integrin affinity: A possible mechanism for cell de-adhesion. *BMC Immunology* **9**: 26. DOI 10.1186/1471-2172-9-26.
- Chigaev A, Wu Y, Williams DB, Smagley Y, Sklar LA (2011b). Discovery of very late antigen-4 (VLA-4, $\alpha 4\beta 1$ integrin) allosteric antagonists. *Journal of Biological Chemistry* **286**: 5455–5463. DOI 10.1074/jbc.M110.162636.
- Chigaev A, Zwartz G, Graves SW, Dwyer DC, Tsuji H, Foutz TD, Edwards BS, Prossnitz ER, Larson RS, Sklar LA (2003b). $\alpha 4\beta 1$ integrin affinity changes govern cell adhesion. *Journal of Biological Chemistry* **278**: 38174–38182. DOI 10.1074/jbc.M210472200.
- Chigaev A, Zwartz GJ, Buranda T, Edwards BS, Prossnitz ER, Sklar LA (2004). Conformational regulation of $\alpha 4 \beta 1$ -integrin affinity by reducing agents. “Inside-out” signaling is independent of and additive to reduction-regulated integrin activation. *Journal of Biological Chemistry* **279**: 32435–32443. DOI 10.1074/jbc.M404387200.
- Chu CC, Pinney JJ, Whitehead HE, Rivera-Escalera F, Vandermeid KR, Zent CS, Elliott MR (2020). High-resolution quantification of discrete phagocytic events by live cell time-lapse high-content microscopy imaging. *Journal of Cell Science* **133**: jcs237883. DOI 10.1242/jcs.237883.
- Damsky CH, Librach C, Lim KH, Fitzgerald ML, McMaster MT, Janatpour M, Zhou Y, Logan SK, Fisher SJ (1994). Integrin switching regulates normal trophoblast invasion. *Development* **120**: 3657–3666.
- Deppermann C, Kratofil RM, Peiseler M, David BA, Zindel J, Castanheira F, Van Der Wal F, Carestia A, Jenne CN, Marth JD, Kubers P (2020). Macrophage galactose lectin is critical for Kupffer cells to clear aged platelets. *Journal of Experimental Medicine* **217**: e20190723. DOI 10.1084/jem.20190723.
- Deschout H, Lukes T, Sharipov A, Szlag D, Feletti L, Vandenberg W, Dedecker P, Hofkens J, Leutenegger M, Lasser T, Radenovic A (2016). Complementarity of PALM and SOFI for super-resolution live-cell imaging of focal adhesions. *Nature Communications* **7**: 13693. DOI 10.1038/ncomms13693.
- Deschout H, Platzman I, Sage D, Feletti L, Spatz JP, Radenovic A (2017). Investigating focal adhesion substructures by localization microscopy. *Biophysical Journal* **113**: 2508–2518. DOI 10.1016/j.bpj.2017.09.032.
- Di Blasio L, Gagliardi PA, Puliafito A, Sessa R, Seano G, Bussolino F, Primo L (2015). PDK1 regulates focal adhesion disassembly by modulating endocytosis of $\alpha v\beta 3$ integrin. *Journal of Cell Science* **128**: 863–877. DOI 10.1242/jcs.149294.
- Dixit N, Kim MH, Rossaint J, Yamayoshi I, Zarbock A, Simon SI (2012). Leukocyte function antigen-1, kindlin-3, and calcium flux orchestrate neutrophil recruitment during inflammation. *Journal of Immunology* **189**: 5954–5964. DOI 10.4049/jimmunol.1201638.
- Dixit N, Yamayoshi I, Nazarian A, Simon SI (2011). Migrational guidance of neutrophils is mechanotransduced via high-affinity LFA-1 and calcium flux. *Journal of Immunology* **187**: 472–481. DOI 10.4049/jimmunol.1004197.
- Dixon RE, Vivas O, Hannigan KI, Dickson EJ (2017). Ground state depletion super-resolution imaging in mammalian cells. *Journal of Visualized Experiments* **129**: e56239.
- Drake CJ, Cheresch DA, Little CD (1995). An antagonist of integrin $\alpha v \beta 3$ prevents maturation of blood vessels during embryonic neovascularization. *Journal of Cell Science* **108**: 2655–2661.
- Dransfield I, Hogg N (1989). Regulated expression of Mg^{2+} binding epitope on leukocyte integrin α subunits. *EMBO Journal* **8**: 3759–3765. DOI 10.1002/j.1460-2075.1989.tb08552.x.
- Du X, Gu M, Weisel JW, Nagaswami C, Bennett JS, Bowditch R, Ginsberg MH (1993). Long range propagation of

- conformational changes in integrin α IIb β 3. *Journal of Biological Chemistry* **268**: 23087–23092.
- Egles C, Huet HA, Dogan F, Cho S, Dong S, Smith A, Knight EB, Mclachlan KR, Garlick JA (2010). Integrin-blocking antibodies delay keratinocyte re-epithelialization in a human three-dimensional wound healing model. *PLoS One* **5**: e10528. DOI 10.1371/journal.pone.0010528.
- Eisenhardt SU, Schwarz M, Schallner N, Soosairajah J, Bassler N, Huang D, Bode C, Peter K (2007). Generation of activation-specific human anti- $\alpha_M\beta_2$ single-chain antibodies as potential diagnostic tools and therapeutic agents. *Blood* **109**: 3521–3528. DOI 10.1182/blood-2006-03-007179.
- Erusappan P, Alam J, Lu N, Zeltz C, Gullberg D (2019). Integrin α 11 cytoplasmic tail is required for FAK activation to initiate 3D cell invasion and ERK-mediated cell proliferation. *Scientific Reports* **9**: 15283. DOI 10.1038/s41598-019-51689-6.
- Eva R, Crisp S, Marland JR, Norman JC, Kanamarlapudi V, Ffrench-Constant C, Fawcett JW (2012). ARF6 directs axon transport and traffic of integrins and regulates axon growth in adult DRG neurons. *Journal of Neuroscience* **32**: 10352–10364. DOI 10.1523/JNEUROSCI.1409-12.2012.
- Evangelista V, Pamuklar Z, Piccoli A, Manarini S, Dell'elba G, Pecce R, Martelli N, Federico L, Rojas M, Berton G, Lowell CA, Totani L, Smyth SS (2007). Src family kinases mediate neutrophil adhesion to adherent platelets. *Blood* **109**: 2461–2469. DOI 10.1182/blood-2006-06-029082.
- Evans R, Flores-Borja F, Nassiri S, Miranda E, Lawler K, Grigoriadis A, Monypenny J, Gillet C, Owen J, Gordon P, Male V, Cheung A, Noor F, Barber P, Marlow R, Francesch-Domenech E, Fruhwirth G, Squadrito M, Vojnovic B, Tutt A, Festy F, De Palma M, Ng T (2019). Integrin-mediated macrophage adhesion promotes lymphovascular dissemination in breast cancer. *Cell Reports* **27**: 1967–1978. e4. DOI 10.1016/j.celrep.2019.04.076.
- Evans R, Lellouch AC, Svensson L, Mcdowall A, Hogg N (2011). The integrin LFA-1 signals through ZAP-70 to regulate expression of high-affinity LFA-1 on T lymphocytes. *Blood* **117**: 3331–3342. DOI 10.1182/blood-2010-06-289140.
- Ezratty EJ, Bertaux C, Marcantonio EE, Gundersen GG (2009). Clathrin mediates integrin endocytosis for focal adhesion disassembly in migrating cells. *Journal of Cell Biology* **187**: 733–747. DOI 10.1083/jcb.200904054.
- Fabbri M, Castellani P, Gotwals PJ, Kotelianski V, Zardi L, Zocchi MR (1996). A functional monoclonal antibody recognizing the human α 1-integrin I-domain. *Tissue Antigens* **48**: 47–51. DOI 10.1111/j.1399-0039.1996.tb02604.x.
- Fan Z, Kiosses WB, Sun H, Orecchioni M, Ghosheh Y, Zajonc DM, Arnaut MA, Gutierrez E, Groisman A, Ginsberg MH, Ley K (2019). High-affinity bent β 2-integrin molecules in arresting neutrophils face each other through binding to ICAMs in cis. *Cell Reports* **26**: 119–130. e5. DOI 10.1016/j.celrep.2018.12.038.
- Fan Z, Ley K (2015). Leukocyte arrest: Biomechanics and molecular mechanisms of β 2 integrin activation. *Biorheology* **52**: 353–377. DOI 10.3233/BIR-15085.
- Fan Z, McArdle S, Marki A, Mikulski Z, Gutierrez E, Engelhardt B, Deutsch U, Ginsberg M, Groisman A, Ley K (2016). Neutrophil recruitment limited by high-affinity bent β 2 integrin binding ligand in cis. *Nature Communications* **7**: 12658. DOI 10.1038/ncomms12658.
- Fan Z, Mikulski Z, McArdle S, Sundd P, Ley K (2020). Super-STORM: Molecular modeling to achieve single-molecule localization with STORM microscopy. *STAR Protocols* **1**: 100012. DOI 10.1016/j.xpro.2019.100012.
- Faulon Marruecos D, Kastantin M, Schwartz DK, Kaar JL (2016). Dense poly(ethylene glycol) brushes reduce adsorption and stabilize the unfolded conformation of fibronectin. *Biomacromolecules* **17**: 1017–1025. DOI 10.1021/acs.biomac.5b01657.
- Fedyk ER, Wyant T, Yang LL, Csizmadia V, Burke K, Yang H, Kadambi VJ (2012). Exclusive antagonism of the α 4 β 7 integrin by vedolizumab confirms the gut-selectivity of this pathway in primates. *Inflammatory Bowel Diseases* **18**: 2107–2119. DOI 10.1002/ibd.22940.
- Feigelson SW, Pasvolsky R, Cemerski S, Shulman Z, Grabovsky V, Ilani T, Sagiv A, Lemaitre F, Laudanna C, Shaw AS, Alon R (2010). Occupancy of lymphocyte LFA-1 by surface-immobilized ICAM-1 is critical for TCR- but not for chemokine-triggered LFA-1 conversion to an open headpiece high-affinity state. *Journal of Immunology* **185**: 7394–7404. DOI 10.4049/jimmunol.1002246.
- Folling J, Bossi M, Bock H, Medda R, Wurm CA, Hein B, Jakobs S, Eggeling C, Hell SW (2008). Fluorescence nanoscopy by ground-state depletion and single-molecule return. *Nature Methods* **5**: 943–945. DOI 10.1038/nmeth.1257.
- Freeman SA, Uderhardt S, Saric A, Collins RF, Buckley CM, Mylvaganam S, Boroumand P, Plumb J, Germain RN, Ren D, Grinstein S (2020). Lipid-gated monovalent ion fluxes regulate endocytic traffic and support immune surveillance. *Science* **367**: 301–305. DOI 10.1126/science.aaw9544.
- Frelinger AL 3rd, Du XP, Plow EF, Ginsberg MH (1991). Monoclonal antibodies to ligand-occupied conformers of integrin α IIb β 3 (glycoprotein IIb-IIIa) alter receptor affinity, specificity, and function. *Journal of Biological Chemistry* **266**: 17106–17111.
- Fu G, Yang HY, Wang C, Zhang F, You ZD, Wang GY, He C, Chen YZ, Xu ZZ (2006). Detection of constitutive heterodimerization of the integrin Mac-1 subunits by fluorescence resonance energy transfer in living cells. *Biochemical and Biophysical Research Communications* **346**: 986–991. DOI 10.1016/j.bbrc.2006.06.015.
- Fuentes P, Sese M, Guijarro PJ, Emperador M, Sanchez-Redondo S, Peinado H, Hummer S, Ramon YCS (2020). ITGB3-mediated uptake of small extracellular vesicles facilitates intercellular communication in breast cancer cells. *Nature Communications* **11**: 4261. DOI 10.1038/s41467-020-18081-9.
- Galbraith CG, Galbraith JA (2011). Super-resolution microscopy at a glance. *Journal of Cell Science* **124**: 1607–1611. DOI 10.1242/jcs.080085.
- Gao X, Yang L, Petros JA, Marshall FF, Simons JW, Nie S (2005). *In vivo* molecular and cellular imaging with quantum dots. *Current Opinion in Biotechnology* **16**: 63–72. DOI 10.1016/j.copbio.2004.11.003.
- Garmy-Susini B, Avraamides CJ, Desgrosellier JS, Schmid MC, Foubert P, Ellies LG, Lowy AM, Blair SL, Vandenberg SR, Datnow B, Wang HY, Cheresch DA, Varner J (2013). PI3Ka activates integrin α 4 β 1 to establish a metastatic niche in lymph nodes. *Proceedings of the National Academy of Sciences of the United States of America* **110**: 9042–9047. DOI 10.1073/pnas.1219603110.
- Gawden-Bone C, West MA, Morrison VL, Edgar AJ, Mcmillan SJ, Dill BD, Trost M, Prescott A, Fagerholm SC, Watts C (2014). A crucial role for β 2 integrins in podosome formation, dynamics and Toll-like-receptor-signaled disassembly in dendritic cells. *Journal of Cell Science* **127**: 4213–4224. DOI 10.1242/jcs.151167.
- Ghosh S, Saha S, Goswami D, Bilgrami S, Mayor S (2012). Dynamic imaging of homo-FRET in live cells by fluorescence anisotropy microscopy. *Methods in Enzymology* **505**: 291–327.

- Giepmans BN, Adams SR, Ellisman MH, Tsien RY (2006). The fluorescent toolbox for assessing protein location and function. *Science* **312**: 217–224. DOI 10.1126/science.1124618.
- Ginsberg MH (2014). Integrin activation. *BMB Reports* **47**: 655–659. DOI 10.5483/BMBRep.2014.47.12.241.
- Girbl T, Lenn T, Perez L, Rolas L, Barkaway A, Thiriot A, Del Fresno C, Lynam E, Hub E, Thelen M, Graham G, Alon R, Sancho D, Von Andrian UH, Voisin MB, Rot A, Nourshargh S (2018). Distinct compartmentalization of the chemokines CXCL1 and CXCL2 and the atypical receptor ACKR1 determine discrete stages of neutrophil diapedesis. *Immunity* **49**: 1062–1076.e6. DOI 10.1016/j.immuni.2018.09.018.
- Göppert-Mayer M (2009). Elementary processes with two quantum transitions. *Annalen der Physik* **18**: 466–479. DOI 10.1002/andp.200910358.
- Graf R, Rietdorf J, Zimmermann T (2005). Live cell spinning disk microscopy. *Advances in Biochemical Engineering/Biotechnology* **95**: 57–75.
- Grakoui A, Bromley SK, Sumen C, Davis MM, Shaw AS, Allen PM, Dustin ML (1999). The immunological synapse: A molecular machine controlling T cell activation. *Science* **285**: 221–227. DOI 10.1126/science.285.5425.221.
- Green CE, Schaff UY, Sarantos MR, Lum AF, Staunton DE, Simon SI (2006). Dynamic shifts in LFA-1 affinity regulate neutrophil rolling, arrest, and transmigration on inflamed endothelium. *Blood* **107**: 2101–2111. DOI 10.1182/blood-2005-06-2303.
- Gronholm M, Jahan F, Bryushkova EA, Madhavan S, Aglialoro F, Soto Hinojosa L, Uotila LM, Gahmberg CG (2016). LFA-1 integrin antibodies inhibit leukocyte $\alpha 4\beta 1$ -mediated adhesion by intracellular signaling. *Blood* **128**: 1270–1281. DOI 10.1182/blood-2016-03-705160.
- Grzeszkiewicz TM, Kirschling DJ, Chen N, Lau LF (2001). CYR61 stimulates human skin fibroblast migration through Integrin $\alpha v\beta 5$ and enhances mitogenesis through integrin $\alpha v\beta 3$, independent of its carboxyl-terminal domain. *Journal of Biological Chemistry* **276**: 21943–21950. DOI 10.1074/jbc.M100978200.
- Gustafsson MG (2000). Surpassing the lateral resolution limit by a factor of two using structured illumination microscopy. *Journal of Microscopy* **198**: 82–87. DOI 10.1046/j.1365-2818.2000.00710.x.
- Gustafsson MG (2005). Nonlinear structured-illumination microscopy: Wide-field fluorescence imaging with theoretically unlimited resolution. *Proceedings of the National Academy of Sciences of the United States of America* **102**: 13081–13086. DOI 10.1073/pnas.0406877102.
- Gustafsson MG, Shao L, Carlton PM, Wang CJ, Golubovskaya IN, Cande WZ, Agard DA, Sedat JW (2008). Three-dimensional resolution doubling in wide-field fluorescence microscopy by structured illumination. *Biophysical Journal* **94**: 4957–4970. DOI 10.1529/biophysj.107.120345.
- Haeger A, Alexander S, Vullings M, Kaiser FMP, Veelken C, Flucke U, Koehl GE, Hirschberg M, Flentje M, Hoffman RM, Geissler EK, Kissler S, Friedl P (2020). Collective cancer invasion forms an integrin-dependent radioresistant niche. *Journal of Experimental Medicine* **217**: e20181184. DOI 10.1084/jem.20181184.
- Hanna SJ, McCoy-Simandle K, Leung E, Genna A, Condeelis J, Cox D (2019). Tunneling nanotubes, a novel mode of tumor cell-macrophage communication in tumor cell invasion. *Journal of Cell Science* **132**: jcs223321. DOI 10.1242/jcs.223321.
- Hantgan RR, Stahle MC, Connor JH, Horita DA, Rocco M, McLane MA, Yakovlev S, Medved L (2006). Integrin $\alpha IIb\beta 3$: Ligand interactions are linked to binding-site remodeling. *Protein Science* **15**: 1893–1906. DOI 10.1110/ps.052049506.
- Hell SW (2003). Toward fluorescence nanoscopy. *Nature Biotechnology* **21**: 1347–1355. DOI 10.1038/nbt895.
- Hell SW (2007). Far-field optical nanoscopy. *Science* **316**: 1153–1158. DOI 10.1126/science.1137395.
- Hell SW (2009). Microscopy and its focal switch. *Nature Methods* **6**: 24–32. DOI 10.1038/nmeth.1291.
- Hell SW, Wichmann J (1994). Breaking the diffraction resolution limit by stimulated emission: Stimulated-emission-depletion fluorescence microscopy. *Optics Letters* **19**: 780–782. DOI 10.1364/OL.19.000780.
- Hendey B, Lawson M, Marcantonio EE, Maxfield FR (1996). Intracellular calcium and calcineurin regulate neutrophil motility on vitronectin through a receptor identified by antibodies to integrins αv and $\beta 3$. *Blood* **87**: 2038–2048. DOI 10.1182/blood.V87.5.2038.2038.
- Hess ST, Girirajan TP, Mason MD (2006). Ultra-high resolution imaging by fluorescence photoactivation localization microscopy. *Biophysical Journal* **91**: 4258–4272. DOI 10.1529/biophysj.106.091116.
- Hickman HD, Bennink JR, Yewdell JW (2009). Caught in the act: Intravital multiphoton microscopy of host-pathogen interactions. *Cell Host & Microbe* **5**: 13–21. DOI 10.1016/j.chom.2008.12.007.
- Hildreth JE, Gotch FM, Hildreth PD, McMichael AJ (1983). A human lymphocyte-associated antigen involved in cell-mediated lympholysis. *European Journal of Immunology* **13**: 202–208. DOI 10.1002/eji.1830130305.
- Ho WC, Heinemann C, Hangan D, Uniyal S, Morris VL, Chan BM (1997). Modulation of *in vivo* migratory function of $\alpha 2\beta 1$ integrin in mouse liver. *Molecular Biology of the Cell* **8**: 1863–1875. DOI 10.1091/mbc.8.10.1863.
- Hocde SA, Hyrien O, Waugh RE (2009). Cell adhesion molecule distribution relative to neutrophil surface topography assessed by TIRFM. *Biophysical Journal* **97**: 379–387. DOI 10.1016/j.bpj.2009.04.035.
- Hofmann M, Eggeling C, Jakobs S, Hell SW (2005). Breaking the diffraction barrier in fluorescence microscopy at low light intensities by using reversibly photoswitchable proteins. *Proceedings of the National Academy of Sciences of the United States of America* **102**: 17565–17569. DOI 10.1073/pnas.0506010102.
- Hogg N, Takacs L, Palmer DG, Selvendran Y, Allen C (1986). The p150,95 molecule is a marker of human mononuclear phagocytes: Comparison with expression of class II molecules. *European Journal of Immunology* **16**: 240–248. DOI 10.1002/eji.1830160306.
- Hon A (1882). The relation of aperture and power in the microscope. *Journal of the Royal Microscopical Society* **2**: 300–309. DOI 10.1111/j.1365-2818.1882.tb00190.x.
- Honda M, Surewaard BGJ, Watanabe M, Hedrick CC, Lee WY, Brown K, McCoy KD, Kubes P (2020). Perivascular localization of macrophages in the intestinal mucosa is regulated by Nr4a1 and the microbiome. *Nature Communications* **11**: 1329. DOI 10.1038/s41467-020-15068-4.
- Hornung A, Sbarrato T, Garcia-Seyda N, Aoun L, Luo X, Biarnes-Pelicot M, Theodoly O, Valignat MP (2020). A bistable mechanism mediated by integrins controls mechanotaxis of leukocytes. *Biophysical Journal* **118**: 565–577. DOI 10.1016/j.bpj.2019.12.013.

- Howe EN, Burnette MD, Justice ME, Schnepf PM, Hedrick V, Clancy JW, Guldner IH, Lamere AT, Li J, Aryal UK, D'souza-Schorey C, Zartman JJ, Zhang S (2020). Rab11b-mediated integrin recycling promotes brain metastatic adaptation and outgrowth. *Nature Communications* **11**: 3017. DOI 10.1038/s41467-020-16832-2.
- Hsu AY, Wang D, Liu S, Lu J, Syahirah R, Bennin DA, Huttenlocher A, Umulis DM, Wan J, Deng Q (2019). Phenotypical microRNA screen reveals a noncanonical role of CDK2 in regulating neutrophil migration. *Proceedings of the National Academy of Sciences of the United States of America* **116**: 18561–18570. DOI 10.1073/pnas.1905221116.
- Hu S, Tee YH, Kabla A, Zaidel-Bar R, Bershadsky A, Hersen P (2015). Structured illumination microscopy reveals focal adhesions are composed of linear subunits. *Cytoskeleton* **72**: 235–245. DOI 10.1002/cm.21223.
- Huang B, Wang W, Bates M, Zhuang X (2008). Three-dimensional super-resolution imaging by stochastic optical reconstruction microscopy. *Science* **319**: 810–813. DOI 10.1126/science.1153529.
- Huang J, Roth R, Heuser JE, Sadler JE (2009). Integrin $\alpha_v\beta_3$ on human endothelial cells binds von Willebrand factor strings under fluid shear stress. *Blood* **113**: 1589–1597. DOI 10.1182/blood-2008-05-158584.
- Huebsch ND, Mooney DJ (2007). Fluorescent resonance energy transfer: A tool for probing molecular cell-biomaterial interactions in three dimensions. *Biomaterials* **28**: 2424–2437. DOI 10.1016/j.biomaterials.2007.01.023.
- Huet-Calderwood C, Rivera-Molina F, Iwamoto DV, Kromann EB, Toomre D, Calderwood DA (2017). Novel ecto-tagged integrins reveal their trafficking in live cells. *Nature Communications* **8**: 570. DOI 10.1038/s41467-017-00646-w.
- Huff J (2015). The Airyscan detector from ZEISS: Confocal imaging with improved signal-to-noise ratio and super-resolution. *Nature Methods* **12**: i–ii. DOI 10.1038/nmeth.f.388.
- Huff J, Bergter A, Birkenbeil J, Kleppe I, Engelmann R, Krzic U (2017). The new 2D superresolution mode for ZEISS Airyscan. *Nature Methods* **14**: 1223. DOI 10.1038/nmeth.f.404.
- Humphries JD, Byron A, Humphries MJ (2006). Integrin ligands at a glance. *Journal of Cell Science* **119**: 3901–3903. DOI 10.1242/jcs.03098.
- Hynes RO (1992). Integrins: Versatility, modulation, and signaling in cell adhesion. *Cell* **69**: 11–25. DOI 10.1016/0092-8674(92)90115-S.
- Hynes RO (2002). Integrins: Bidirectional, allosteric signaling machines. *Cell* **110**: 673–687. DOI 10.1016/S0092-8674(02)00971-6.
- Hyun YM, Choe YH, Park SA, Kim M (2019). LFA-1 (CD11a/CD18) and Mac-1 (CD11b/CD18) distinctly regulate neutrophil extravasation through hotspots I and II. *Experimental & Molecular Medicine* **51**: 1–13. DOI 10.1038/s12276-019-0227-1.
- Hyun YM, Sumagin R, Sarangi PP, Lomakina E, Overstreet MG, Baker CM, Powell DJ, Waugh RE, Sarelius IH, Kim M (2012). Uropod elongation is a common final step in leukocyte extravasation through inflamed vessels. *Journal of Experimental Medicine* **209**: 1349–1362. DOI 10.1084/jem.20111426.
- Iwata M, Hirakiyama A, Eshima Y, Kagechika H, Kato C, Song SY (2004). Retinoic acid imprints gut-homing specificity on T cells. *Immunity* **21**: 527–538. DOI 10.1016/j.immuni.2004.08.011.
- Jamerson M, Da Rocha-Azevedo B, Cabral GA, Marciano-Cabral F (2012). Pathogenic *Naegleria fowleri* and non-pathogenic *Naegleria lovaniensis* exhibit differential adhesion to, and invasion of, extracellular matrix proteins. *Microbiology* **158**: 791–803. DOI 10.1099/mic.0.055020-0.
- Janowski R, Kozak M, Jankowska E, Grzonka Z, Grubb A, Abrahamson M, Jaskolski M (2001). Human cystatin C, an amyloidogenic protein, dimerizes through three-dimensional domain swapping. *Nature Structural Biology* **8**: 316–320. DOI 10.1038/86188.
- Jin ZH, Josserand V, Razkin J, Garanger E, Boturyn D, Favrot MC, Dumy P, Coll JL (2006). Noninvasive optical imaging of ovarian metastases using Cy5-labeled RAFT-c(-RGDfK-)-4. *Molecular Imaging* **5**: 188–197. DOI 10.2310/7290.2006.00022.
- Johnson AE (2005). Fluorescence approaches for determining protein conformations, interactions and mechanisms at membranes. *Traffic* **6**: 1078–1092. DOI 10.1111/j.1600-0854.2005.00340.x.
- Kaizuka Y, Douglass AD, Varma R, Dustin ML, Vale RD (2007). Mechanisms for segregating T cell receptor and adhesion molecules during immunological synapse formation in Jurkat T cells. *Proceedings of the National Academy of Sciences of the United States of America* **104**: 20296–20301. DOI 10.1073/pnas.0710258105.
- Kamata T, Handa M, Takakuwa S, Sato Y, Kawai Y, Ikeda Y, Aiso S (2013). Epitope mapping for monoclonal antibody reveals the activation mechanism for $\alpha V\beta 3$ integrin. *PLoS One* **8**: e66096. DOI 10.1371/journal.pone.0066096.
- Kamata T, Irie A, Tokuhira M, Takada Y (1996). Critical residues of integrin αIIb subunit for binding of $\alpha IIb\beta 3$ (glycoprotein IIb-IIIa) to fibrinogen and ligand-mimetic antibodies (PAC-1, OP-G2, and LJ-CP3). *Journal of Biological Chemistry* **271**: 18610–18615. DOI 10.1074/jbc.271.31.18610.
- Kamata T, Puzon W, Takada Y (1994). Identification of putative ligand binding sites within I domain of integrin $\alpha 2 \beta 1$ (VLA-2, CD49b/CD29). *Journal of Biological Chemistry* **269**: 9659–9663.
- Kamata T, Puzon W, Takada Y (1995). Identification of putative ligand-binding sites of the integrin $\alpha 4\beta 1$ (VLA-4, CD49d/CD29). *Biochemical Journal* **305**: 945–951. DOI 10.1042/bj3050945.
- Kamata T, Tieu KK, Tarui T, Puzon-McLaughlin W, Hogg N, Takada Y (2002). The role of the CPNKEKEC sequence in the $\beta(2)$ subunit I domain in regulation of integrin $\alpha(L)\beta(2)$ (LFA-1). *Journal of Immunology* **168**: 2296–2301. DOI 10.4049/jimmunol.168.5.2296.
- Kanchanawong P, Shtengel G, Pasapera AM, Ramko EB, Davidson MW, Hess HF, Waterman CM (2010). Nanoscale architecture of integrin-based cell adhesions. *Nature* **468**: 580–584. DOI 10.1038/nature09621.
- Kashiwagi H, Schwartz MA, Eigenthaler M, Davis KA, Ginsberg MH, Shattil SJ (1997). Affinity modulation of platelet integrin $\alpha IIb\beta 3$ by $\beta 3$ -endoneixin, a selective binding partner of the $\beta 3$ integrin cytoplasmic tail. *Journal of Cell Biology* **137**: 1433–1443. DOI 10.1083/jcb.137.6.1433.
- Kastantin M, Faulon Marruecos D, Grover N, Yu Mcloughlin S, Schwartz DK, Kaar JL (2017). Connecting protein conformation and dynamics with ligand-receptor binding using three-color forster resonance energy transfer tracking. *Journal of the American Chemical Society* **139**: 9937–9948. DOI 10.1021/jacs.7b03978.
- Katz ZB, Novotna L, Blount A, Lillemeier BF (2017). A cycle of Zap70 kinase activation and release from the TCR amplifies and disperses antigenic stimuli. *Nature Immunology* **18**: 86–95. DOI 10.1038/ni.3631.

- Katz ZB, Zhang C, Quintana A, Lillemeier BF, Hogan PG (2019). Septins organize endoplasmic reticulum-plasma membrane junctions for STIM1-ORAI1 calcium signalling. *Scientific Reports* **9**: 10839. DOI 10.1038/s41598-019-46862-w.
- Kawakami N, Sakane N, Nishizawa F, Iwao M, Fukada SI, Tsujikawa K, Kohama Y, Ikawa M, Okabe M, Yamamoto H (1999). Green fluorescent protein-transgenic mice: Immune functions and their application to studies of lymphocyte development. *Immunology Letters* **70**: 165–171. DOI 10.1016/S0165-2478(99)00152-2.
- Keizer GD, Visser W, Vliem M, Figdor CG (1988). A monoclonal antibody (NKI-L16) directed against a unique epitope on the α -chain of human leukocyte function-associated antigen 1 induces homotypic cell-cell interactions. *Journal of Immunology* **140**: 1393–1400.
- Keppeler A, Gendreizig S, Gronemeyer T, Pick H, Vogel H, Johnsson K (2003). A general method for the covalent labeling of fusion proteins with small molecules *in vivo*. *Nature Biotechnology* **21**: 86–89. DOI 10.1038/nbt765.
- Kim C, Schmidt T, Cho EG, Ye F, Ulmer TS, Ginsberg MH (2011). Basic amino-acid side chains regulate transmembrane integrin signalling. *Nature* **481**: 209–213. DOI 10.1038/nature10697.
- Kim M, Carman CV, Springer TA (2003). Bidirectional transmembrane signaling by cytoplasmic domain separation in integrins. *Science* **301**: 1720–1725. DOI 10.1126/science.1084174.
- Kim M, Carman CV, Yang W, Salas A, Springer TA (2004). The primacy of affinity over clustering in regulation of adhesiveness of the integrin $\alpha_1\beta_2$. *Journal of Cell Biology* **167**: 1241–1253. DOI 10.1083/jcb.200404160.
- Kiyoshima D, Kawakami K, Hayakawa K, Tatsumi H, Sokabe M (2011). Force- and Ca^{2+} -dependent internalization of integrins in cultured endothelial cells. *Journal of Cell Science* **124**: 3859–3870. DOI 10.1242/jcs.088559.
- Klar TA, Jakobs S, Dyba M, Egner A, Hell SW (2000). Fluorescence microscopy with diffraction resolution barrier broken by stimulated emission. *Proceedings of the National Academy of Sciences of the United States of America* **97**: 8206–8210. DOI 10.1073/pnas.97.15.8206.
- Kobat D, Horton NG, Xu C (2011). *In vivo* two-photon microscopy to 1.6-mm depth in mouse cortex. *Journal of Biomedical Optics* **16**: 106014. DOI 10.1117/1.3646209.
- Kondo N, Ueda Y, Kita T, Ozawa M, Tomiyama T, Yasuda K, Lim DS, Kinashi T (2017). NDR1-dependent regulation of kindlin-3 controls high-affinity LFA-1 binding and immune synapse organization. *Molecular and Cellular Biology* **37**: e00424-16.
- Kostelnik KB, Barker A, Schultz C, Mitchell TP, Rajeev V, White JJ, Aurrand-Lions M, Nourshargh S, Cutillas P, Nightingale TD (2019). Dynamic trafficking and turnover of JAM-C is essential for endothelial cell migration. *PLoS Biology* **17**: e3000554. DOI 10.1371/journal.pbio.3000554.
- Koyano F, Okatsu K, Kosako H, Tamura Y, Go E, Kimura M, Kimura Y, Tsuchiya H, Yoshihara H, Hirokawa T, Endo T, Fon EA, Trempe JF, Saeki Y, Tanaka K, Matsuda N (2014). Ubiquitin is phosphorylated by PINK1 to activate parkin. *Nature* **510**: 162–166. DOI 10.1038/nature13392.
- Kretschmer A, Zhang F, Somasekharan SP, Tse C, Leachman L, Gleave A, Li B, Asmaro I, Huang T, Kotula L, Sorensen PH, Gleave ME (2019). Stress-induced tunneling nanotubes support treatment adaptation in prostate cancer. *Scientific Reports* **9**: 7826. DOI 10.1038/s41598-019-44346-5.
- Kruschwitz M, Fritzsche G, Schwarting R, Micklem K, Mason DY, Falini B, Stein H (1991). Ber-ACT8: New monoclonal antibody to the mucosa lymphocyte antigen. *Journal of Clinical Pathology* **44**: 636–645. DOI 10.1136/jcp.44.8.636.
- Kumar D, Ristow LC, Shi M, Mukherjee P, Caine JA, Lee WY, Kubes P, Coburn J, Chaconas G (2015). Intravital Imaging of vascular transmigration by the Lyme spirochete: Requirement for the integrin binding residues of the *B. burgdorferi* P66 protein. *PLoS Pathogens* **11**: e1005333. DOI 10.1371/journal.ppat.1005333.
- Kunkel EJ, Dunne JL, Ley K (2000). Leukocyte arrest during cytokine-dependent inflammation *in vivo*. *Journal of Immunology* **164**: 3301–3308. DOI 10.4049/jimmunol.164.6.3301.
- Kuwano Y, Spelten O, Zhang H, Ley K, Zarbock A (2010). Rolling on E- or P-selectin induces the extended but not high-affinity conformation of LFA-1 in neutrophils. *Blood* **116**: 617–624. DOI 10.1182/blood-2010-01-266122.
- Lagarrigue F, Vikas Anekal P, Lee HS, Bachir AI, Ablack JN, Horwitz AF, Ginsberg MH (2015). A RIAM/lamellipodin–talin–integrin complex forms the tip of sticky fingers that guide cell migration. *Nature Communications* **6**: 8492. DOI 10.1038/ncomms9492.
- Lakowicz JR, Masters BR (2008). Principles of fluorescence spectroscopy, third edition. *Journal of Biomedical Optics* **13**: 029901. DOI 10.1117/1.2904580.
- Lakowicz JR, Szymanski H, Nowaczyk K, Johnson ML (1992). Fluorescence lifetime imaging of free and protein-bound NADH. *Proceedings of the National Academy of Sciences of the United States of America* **89**: 1271–1275. DOI 10.1073/pnas.89.4.1271.
- Lam AJ, St-Pierre F, Gong Y, Marshall JD, Cranfill PJ, Baird MA, Mckeown MR, Wiedenmann J, Davidson MW, Schnitzer MJ, Tsien RY, Lin MZ (2012). Improving FRET dynamic range with bright green and red fluorescent proteins. *Nature Methods* **9**: 1005–1012. DOI 10.1038/nmeth.2171.
- Lammermann T, Afonso PV, Angermann BR, Wang JM, Kastenmuller W, Parent CA, Germain RN (2013). Neutrophil swarms require LTB4 and integrins at sites of cell death *in vivo*. *Nature* **498**: 371–375. DOI 10.1038/nature12175.
- Larson RS, Corbi AL, Berman L, Springer T (1989). Primary structure of the leukocyte function-associated molecule-1 alpha subunit: An integrin with an embedded domain defining a protein superfamily. *Journal of Cell Biology* **108**: 703–712. DOI 10.1083/jcb.108.2.703.
- Lau TL, Kim C, Ginsberg MH, Ulmer TS (2009). The structure of the integrin $\alpha\text{IIb}\beta_3$ transmembrane complex explains integrin transmembrane signalling. *EMBO Journal* **28**: 1351–1361. DOI 10.1038/emboj.2009.63.
- Laukaitis CM, Webb DJ, Donais K, Horwitz AF (2001). Differential dynamics of α_5 integrin, paxillin, and α -actinin during formation and disassembly of adhesions in migrating cells. *Journal of Cell Biology* **153**: 1427–1440. DOI 10.1083/jcb.153.7.1427.
- Le Marois A, Suhling K (2017). Quantitative live cell FLIM imaging in three dimensions. *Advances in Experimental Medicine and Biology* **1035**: 31–48.
- Lee EC, Lotz MM, Steele GD Jr, Mercurio AM (1992). The integrin $\alpha_6\beta_4$ is a laminin receptor. *Journal of Cell Biology* **117**: 671–678. DOI 10.1083/jcb.117.3.671.
- Lefort CT, Hyun YM, Schultz JB, Law FY, Waugh RE, Knauf PA, Kim M (2009). Outside-in signal transmission by conformational

- changes in integrin Mac-1. *Journal of Immunology* **183**: 6460–6468. DOI 10.4049/jimmunol.0900983.
- Lefort CT, Rossaint J, Moser M, Petrich BG, Zarbock A, Monkley SJ, Critchley DR, Ginsberg MH, Fassler R, Ley K (2012). Distinct roles for talin-1 and kindlin-3 in LFA-1 extension and affinity regulation. *Blood* **119**: 4275–4282. DOI 10.1182/blood-2011-08-373118.
- Lei S, Ramesh A, Twitchell E, Wen K, Bui T, Weiss M, Yang X, Kocher J, Li G, Giri-Rachman E, Trang NV, Jiang X, Ryan EP, Yuan L (2016). High protective efficacy of probiotics and rice bran against human norovirus infection and diarrhea in gnotobiotic pigs. *Frontiers in Microbiology* **7**: 1699. DOI 10.3389/fmicb.2016.01699.
- Lenter M, Uhlig H, Hamann A, Jenö P, Imhof B, Vestweber D (1993). A monoclonal antibody against an activation epitope on mouse integrin chain $\beta 1$ blocks adhesion of lymphocytes to the endothelial integrin $\alpha 6\beta 1$. *Proceedings of the National Academy of Sciences of the United States of America* **90**: 9051–9055. DOI 10.1073/pnas.90.19.9051.
- Lerche M, Elosgui-Artola A, Kechagia JZ, Guzman C, Georgiadou M, Andreu I, Gullberg D, Roca-Cusachs P, Peuhu E, Ivaska J (2020). Integrin binding dynamics modulate ligand-specific mechanosensing in mammary gland fibroblasts. *iScience* **23**: 100907. DOI 10.1016/j.isci.2020.100907.
- Levin-Konigsberg R, Montano-Rendon F, Keren-Kaplan T, Li R, Ego B, Mylvaganam S, Diccio JE, Trimble WS, Bassik MC, Bonifacino JS, Fairn GD, Grinstein S (2019). Phagolysosome resolution requires contacts with the endoplasmic reticulum and phosphatidylinositol-4-phosphate signalling. *Nature Cell Biology* **21**: 1234–1247. DOI 10.1038/s41556-019-0394-2.
- Ley K, Baker JB, Cybulsky MI, Gimbrone MA Jr, Luscinskas FW (1993). Intravenous interleukin-8 inhibits granulocyte emigration from rabbit mesenteric venules without altering L-selectin expression or leukocyte rolling. *Journal of Immunology* **151**: 6347–6357.
- Ley K, Rivera-Nieves J, Sandborn WJ, Shattil S (2016). Integrin-based therapeutics: Biological basis, clinical use and new drugs. *Nature Reviews Drug Discovery* **15**: 173–183. DOI 10.1038/nrd.2015.10.
- Liao Z, Kasirer-Friede A, Shattil SJ (2017). Optogenetic interrogation of integrin $\alpha V\beta 3$ function in endothelial cells. *Journal of Cell Science* **130**: 3532–3541. DOI 10.1242/jcs.205203.
- Lieleg O, Lopez-Garcia M, Semmrich C, Auernheimer J, Kessler H, Bausch AR (2007). Specific integrin labeling in living cells using functionalized nanocrystals. *Small* **3**: 1560–1565. DOI 10.1002/sml.200700148.
- Lim K, Hyun YM, Lambert-Emo K, Topham DJ, Kim M (2015). Visualization of integrin Mac-1 *in vivo*. *Journal of Immunological Methods* **426**: 120–127. DOI 10.1016/j.jim.2015.08.012.
- Lin W, Fan Z, Suo Y, Deng Y, Zhang M, Wang J, Wei X, Chu Y (2015a). The bullseye synapse formed between CD4⁺ T-cell and staphylococcal enterotoxin B-pulsed dendritic cell is a suppressive synapse in T-cell response. *Immunology & Cell Biology* **93**: 99–110. DOI 10.1038/icb.2014.76.
- Lin W, Suo Y, Deng Y, Fan Z, Zheng Y, Wei X, Chu Y (2015b). Morphological change of CD4(+) T cell during contact with DC modulates T-cell activation by accumulation of F-actin in the immunology synapse. *BMC Immunology* **16**: 49. DOI 10.1186/s12865-015-0108-x.
- Lock JG, Jones MC, Askari JA, Gong X, Oddone A, Olofsson H, Goransson S, Lakadamyali M, Humphries MJ, Stromblad S (2018). Reticular adhesions are a distinct class of cell-matrix adhesions that mediate attachment during mitosis. *Nature Cell Biology* **20**: 1290–1302. DOI 10.1038/s41556-018-0220-2.
- Loftus JC, Plow EF, Frelinger AL 3rd, D'Souza SE, Dixon D, Lacy J, Sorge J, Ginsberg MH (1987). Molecular cloning and chemical synthesis of a region of platelet glycoprotein IIb involved in adhesive function. *Proceedings of the National Academy of Sciences of the United States of America* **84**: 7114–7118. DOI 10.1073/pnas.84.20.7114.
- Lomakina EB, Waugh RE (2004). Micromechanical tests of adhesion dynamics between neutrophils and immobilized ICAM-1. *Biophysical Journal* **86**: 1223–1233. DOI 10.1016/S0006-3495(04)74196-X.
- Los GV, Encell LP, Mcdougall MG, Hartzell DD, Karassina N, Zimprich C, Wood MG, Learish R, Ohana RF, Urh M, Simpson D, Mendez J, Zimmermann K, Otto P, Vidugiris G, Zhu J, Darzins A, Klaubert DH, Bulleit RF, Wood KV (2008). HaloTag: A novel protein labeling technology for cell imaging and protein analysis. *ACS Chemical Biology* **3**: 373–382. DOI 10.1021/cb800025k.
- Los GV, Wood K (2007). The HaloTag: A novel technology for cell imaging and protein analysis. *Methods in Molecular Biology* **356**: 195–208.
- Lu C, Ferzly M, Takagi J, Springer TA (2001a). Epitope mapping of antibodies to the C-terminal region of the integrin $\beta 2$ subunit reveals regions that become exposed upon receptor activation. *Journal of Immunology* **166**: 5629–5637. DOI 10.4049/jimmunol.166.9.5629.
- Lu C, Shimaoka M, Salas A, Springer TA (2004). The binding sites for competitive antagonistic, allosteric antagonistic, and agonistic antibodies to the I domain of integrin LFA-1. *Journal of Immunology* **173**: 3972–3978. DOI 10.4049/jimmunol.173.6.3972.
- Lu C, Shimaoka M, Zang Q, Takagi J, Springer TA (2001b). Locking in alternate conformations of the integrin $\alpha L\beta 2$ I domain with disulfide bonds reveals functional relationships among integrin domains. *Proceedings of the National Academy of Sciences of the United States of America* **98**: 2393–2398. DOI 10.1073/pnas.041618598.
- Lu H, Murtagh J, Schwartz EL (2006). The microtubule binding drug laulimalide inhibits vascular endothelial growth factor-induced human endothelial cell migration and is synergistic when combined with docetaxel (taxotere). *Molecular Pharmacology* **69**: 1207–1215. DOI 10.1124/mol.105.019075.
- Luo BH, Carman CV, Springer TA (2007). Structural basis of integrin regulation and signaling. *Annual Review of Immunology* **25**: 619–647. DOI 10.1146/annurev.immunol.25.022106.141618.
- Luo BH, Strokovich K, Walz T, Springer TA, Takagi J (2004). Allosteric $\beta 1$ integrin antibodies that stabilize the low affinity state by preventing the swing-out of the hybrid domain. *Journal of Biological Chemistry* **279**: 27466–27471. DOI 10.1074/jbc.M404354200.
- Luque A, Gomez M, Puzon W, Takada Y, Sanchez-Madrid F, Cabanas C (1996). Activated conformations of very late activation integrins detected by a group of antibodies (HUTS) specific for a novel regulatory region (355–425) of the common $\beta 1$ chain. *Journal of Biological Chemistry* **271**: 11067–11075. DOI 10.1074/jbc.271.19.11067.
- Ma Q, Shimaoka M, Lu C, Jing H, Carman CV, Springer TA (2002). Activation-induced conformational changes in the I domain region of lymphocyte function-associated antigen 1. *Journal of Biological Chemistry* **277**: 10638–10641. DOI 10.1074/jbc.M112417200.

- Maddox PS, Moree B, Canman JC, Salmon ED (2003). Spinning disk confocal microscope system for rapid high-resolution, multimode, fluorescence speckle microscopy and green fluorescent protein imaging in living cells. *Methods in Enzymology* **360**: 597–617.
- Mahon MJ (2011). pHluorin2: An enhanced, ratiometric, pH-sensitive green fluorescent protein. *Advances in Bioscience and Biotechnology* **2**: 132–137. DOI 10.4236/abb.2011.23021.
- Mana G, Clapero F, Panieri E, Panero V, Bottcher RT, Tseng HY, Saltarin F, Astanina E, Wolanska KI, Morgan MR, Humphries MJ, Santoro MM, Serini G, Valdembrì D (2016). PPF1A1 drives active $\alpha 5 \beta 1$ integrin recycling and controls fibronectin fibrillogenesis and vascular morphogenesis. *Nature Communications* **7**: 13546. DOI 10.1038/ncomms13546.
- Marcovecchio PM, Zhu YP, Hanna RN, Dinh HQ, Tacke R, Wu R, McArdle S, Reynolds S, Araujo DJ, Ley K, Hedrick CC (2020). Frontline Science: Kindlin-3 is essential for patrolling and phagocytosis functions of nonclassical monocytes during metastatic cancer surveillance. *Journal of Leukocyte Biology* **107**: 883–892. DOI 10.1002/JLB.4HI0420-098R.
- Margraf A, Germena G, Drexler HCA, Rossaint J, Ludwig N, Prystaj B, Mersmann S, Thomas K, Block H, Gottschlich W, Liu C, Krenn PW, Haller H, Heitplatz B, Meyer Zu Brickwedde M, Moser M, Vestweber D, Zarbock A (2020). The integrin linked kinase is required for chemokine-triggered high affinity conformation of neutrophil $\beta 2$ -integrin LFA1. *Blood* **136**: 2200–2205. DOI 10.1182/blood.2020004948.
- Marki A, Buscher K, Mikulski Z, Pries A, Ley K (2018). Rolling neutrophils form tethers and slings under physiologic conditions *in vivo*. *Journal of Leukocyte Biology* **103**: 67–70.
- Martens R, Permanyer M, Werth K, Yu K, Braun A, Halle O, Halle S, Patzer GE, Bosnjak B, Kiefer F, Janssen A, Friedrichsen M, Poetzsch J, Kohli K, Lueder Y, Gutierrez Jauregui R, Eckert N, Worbs T, Galla M, Forster R (2020). Efficient homing of T cells via afferent lymphatics requires mechanical arrest and integrin-supported chemokine guidance. *Nature Communications* **11**: 1114. DOI 10.1038/s41467-020-14921-w.
- Martin AC, Cardoso AC, Selistre-De-Araujo HS, Cominetti MR (2015). Recombinant disintegrin domain of human ADAM9 inhibits migration and invasion of DU145 prostate tumor cells. *Cell Adhesion & Migration* **9**: 293–299. DOI 10.4161/19336918.2014.994917.
- Masi A, Cicchi R, Carloni A, Pavone FS, Arcangeli A (2010). Optical methods in the study of protein-protein interactions. *Advances in Experimental Medicine and Biology* **674**: 33–42.
- Mathias P, Galleno M, Nemerow GR (1998). Interactions of soluble recombinant integrin $\alpha v \beta 5$ with human adenoviruses. *Journal of Virology* **72**: 8669–8675. DOI 10.1128/JVI.72.11.8669-8675.1998.
- Matlung HL, Babes L, Zhao XW, van Houdt M, Treffers LW, van Rees D J, Franke K, Schornagel K, Verkuijlen P, Janssen H, Halonen P, Liefstink C, Beijersbergen RL, Leusen JHW, Boelens J J, Kuhnle I, van der Werff Ten Bosch J, Seeger K, Rutella S, Pagliara D, Matozaki T, Suzuki E, Menke-van der Houven van Oordt CW, van Bruggen R, Roos D, van Lier RAW, Kuijpers TW, Kubes P, van den Berg TK (2018). Neutrophils kill antibody-opsonized cancer cells by trogoptosis. *Cell Reports* **23**: 3946–3959.e6. DOI 10.1016/j.celrep.2018.05.082.
- McArdle S, Buscher K, Ghosheh Y, Pramod AB, Miller J, Winkels H, Wolf D, Ley K (2019). Migratory and dancing macrophage subsets in atherosclerotic lesions. *Circulation Research* **125**: 1038–1051. DOI 10.1161/CIRCRESAHA.119.315175.
- McArdle S, Mikulski Z, Ley K (2016). Live cell imaging to understand monocyte, macrophage, and dendritic cell function in atherosclerosis. *Journal of Experimental Medicine* **213**: 1117–1131. DOI 10.1084/jem.20151885.
- Michalet X, Pinaud FF, Bentolila LA, Tsay JM, Doose S, Li JJ, Sundaresan G, Wu AM, Gambhir SS, Weiss S (2005). Quantum dots for live cells, *in vivo* imaging, and diagnostics. *Science* **307**: 538–544. DOI 10.1126/science.1104274.
- Mielenz D, Hapke S, Poschl E, Von Der Mark H, Von Der Mark K (2001). The integrin $\alpha 7$ cytoplasmic domain regulates cell migration, lamellipodia formation, and p130CAS/Crk coupling. *Journal of Biological Chemistry* **276**: 13417–13426. DOI 10.1074/jbc.M011481200.
- Mocanu MM, Fazekas Z, Petras M, Nagy P, Sebestyen Z, Isola J, Timar J, Park JW, Vereb G, Szollosi J (2005). Associations of ErbB2, $\beta 1$ -integrin and lipid rafts on Herceptin (Trastuzumab) resistant and sensitive tumor cell lines. *Cancer Letters* **227**: 201–212. DOI 10.1016/j.canlet.2005.01.028.
- Moore TI, Aaron J, Chew TL, Springer TA (2018). Measuring integrin conformational change on the cell surface with super-resolution microscopy. *Cell Reports* **22**: 1903–1912. DOI 10.1016/j.celrep.2018.01.062.
- Morikis VA, Chase S, Wun T, Chaikof EL, Magnani JL, Simon SI (2017). Selectin catch-bonds mechanotransduce integrin activation and neutrophil arrest on inflamed endothelium under shear flow. *Blood* **130**: 2101–2110. DOI 10.1182/blood-2017-05-783027.
- Morikis VA, Masadeh E, Simon SI (2020). Tensile force transmitted through LFA-1 bonds mechanoregulate neutrophil inflammatory response. *Journal of Leukocyte Biology* **108**: 1815–1828. DOI 10.1002/JLB.3A0520-100RR.
- Mould AP, Akiyama SK, Humphries MJ (1996). The inhibitory anti- $\beta 1$ integrin monoclonal antibody 13 recognizes an epitope that is attenuated by ligand occupancy. Evidence for allosteric inhibition of integrin function. *Journal of Biological Chemistry* **271**: 20365–20374. DOI 10.1074/jbc.271.34.20365.
- Mould AP, Barton SJ, Askari JA, Mcewan PA, Buckley PA, Craig SE, Humphries MJ (2003). Conformational changes in the integrin βA domain provide a mechanism for signal transduction via hybrid domain movement. *Journal of Biological Chemistry* **278**: 17028–17035. DOI 10.1074/jbc.M213139200.
- Mould AP, Garratt AN, Askari JA, Akiyama SK, Humphries MJ (1995). Identification of a novel anti-integrin monoclonal antibody that recognises a ligand-induced binding site epitope on the $\beta 1$ subunit. *FEBS Letters* **363**: 118–122. DOI 10.1016/0014-5793(95)00301-O.
- Mould AP, Travis MA, Barton SJ, Hamilton JA, Askari JA, Craig SE, Macdonald PR, Kammerer RA, Buckley PA, Humphries MJ (2005). Evidence that monoclonal antibodies directed against the integrin β subunit plexin/semaphorin/integrin domain stimulate function by inducing receptor extension. *Journal of Biological Chemistry* **280**: 4238–4246. DOI 10.1074/jbc.M412240200.
- Mu D, Cambier S, Fjellbirkeland L, Baron JL, Munger JS, Kawakatsu H, Sheppard D, Broaddus VC, Nishimura SL (2002). The integrin $\alpha v \beta 8$ mediates epithelial homeostasis through

- MT1-MMP-dependent activation of TGF- β 1. *Journal of Cell Biology* **157**: 493–507. DOI 10.1083/jcb.200109100.
- Mylvaganam S, Riedl M, Vega A, Collins RF, Jaqaman K, Grinstein S, Freeman SA (2020). Stabilization of endothelial receptor arrays by a polarized spectrin cytoskeleton facilitates rolling and adhesion of leukocytes. *Cell Reports* **31**: 107798. DOI 10.1016/j.celrep.2020.107798.
- Najmeh S, Cools-Lartigue J, Rayes RF, Gowing S, Vourtzoumis P, Bourdeau F, Giannias B, Berube J, Rousseau S, Ferri LE, Spicer JD (2017). Neutrophil extracellular traps sequester circulating tumor cells via β 1-integrin mediated interactions. *International Journal of Cancer* **140**: 2321–2330. DOI 10.1002/ijc.30635.
- Neupane B, Ligler FS, Wang G (2014). Review of recent developments in stimulated emission depletion microscopy: Applications on cell imaging. *Journal of Biomedical Optics* **19**: 080901. DOI 10.1117/1.JBO.19.8.080901.
- Newham P, Craig SE, Clark K, Mould AP, Humphries MJ (1998). Analysis of ligand-induced and ligand-attenuated epitopes on the leukocyte integrin α 4 β 1: VCAM-1, mucosal addressin cell adhesion molecule-1, and fibronectin induce distinct conformational changes. *Journal of Immunology* **160**: 4508–4517.
- Ng T, Shima D, Squire A, Bastiaens PI, Gschmeissner S, Humphries MJ, Parker PJ (1999). PKC α regulates β 1 integrin-dependent cell motility through association and control of integrin traffic. *EMBO Journal* **18**: 3909–3923. DOI 10.1093/emboj/18.14.3909.
- Ni H, Wilkins JA (1998). Localisation of a novel adhesion blocking epitope on the human β 1 integrin chain. *Cell Adhesion and Communication* **5**: 257–271. DOI 10.3109/15419069809040296.
- Nishimichi N, Kawashima N, Yokosaki Y (2015). Epitopes in α 8 β 1 and other RGD-binding integrins delineate classes of integrin-blocking antibodies and major binding loops in a subunits. *Scientific Reports* **5**: 13756. DOI 10.1038/srep13756.
- Njus BH, Chigaev A, Waller A, Wlodek D, Ostopovici-Halip L, Ursu O, Wang W, Oprea TI, Bologa CG, Sklar LA (2009). Conformational mAb as a tool for integrin ligand discovery. *Assay and Drug Development Technologies* **7**: 507–515. DOI 10.1089/adt.2009.0203.
- Nordenfelt P, Elliott HL, Springer TA (2016). Coordinated integrin activation by actin-dependent force during T-cell migration. *Nature Communications* **7**: 13119. DOI 10.1038/ncomms13119.
- Nordenfelt P, Moore TI, Mehta SB, Kalappurakkal JM, Swaminathan V, Koga N, Lambert TJ, Baker D, Waters JC, Oldenbourg R, Tani T, Mayor S, Waterman CM, Springer TA (2017). Direction of actin flow dictates integrin LFA-1 orientation during leukocyte migration. *Nature Communications* **8**: 2047. DOI 10.1038/s41467-017-01848-y.
- Ojha N, Rainey KH, Patterson GH (2020). Imaging of fluorescence anisotropy during photoswitching provides a simple readout for protein self-association. *Nature Communications* **11**: 21. DOI 10.1038/s41467-019-13843-6.
- Omsland M, Pise-Masison C, Fujikawa D, Galli V, Fenizia C, Parks RW, Gjertsen BT, Franchini G, Andresen V (2018). Inhibition of tunneling nanotube (TNT) formation and human T-cell leukemia virus type 1 (HTLV-1) transmission by cytarabine. *Scientific Reports* **8**: 11118. DOI 10.1038/s41598-018-29391-w.
- Orecchia A, Lacal PM, Schietroma C, Morea V, Zambruno G, Failla CM (2003). Vascular endothelial growth factor receptor-1 is deposited in the extracellular matrix by endothelial cells and is a ligand for the α 5 β 1 integrin. *Journal of Cell Science* **116**: 3479–3489. DOI 10.1242/jcs.00673.
- Osicka R, Osickova A, Hasan S, Bumba L, Cerny J, Sebo P (2015). Bordetella adenylate cyclase toxin is a unique ligand of the integrin complement receptor 3. *eLife* **4**: e10766.
- Osmani N, Follain G, Garcia Leon MJ, Lefebvre O, Busnelli I, Larnicol A, Harlepp S, Goetz JG (2019). Metastatic tumor cells exploit their adhesion repertoire to counteract shear forces during intravascular arrest. *Cell Reports* **28**: 2491–2500.e5. DOI 10.1016/j.celrep.2019.07.102.
- Ostrowski PP, Freeman SA, Fairn G, Grinstein S (2019). Dynamic podosome-like structures in nascent phagosomes are coordinated by phosphoinositides. *Developmental Cell* **50**: 397–410.e3. DOI 10.1016/j.devcel.2019.05.028.
- Owen-Woods C, Joulia R, Barkaway A, Rolas L, Ma B, Nottebaum AF, Arkill KP, Stein M, Girbl T, Golding M, Bates DO, Vestweber D, Voisin MB, Nourshargh S (2020). Local microvascular leakage promotes trafficking of activated neutrophils to remote organs. *Journal of Clinical Investigation* **130**: 2301–2318. DOI 10.1172/JCI133661.
- Oxvig C, Lu C, Springer TA (1999). Conformational changes in tertiary structure near the ligand binding site of an integrin I domain. *Proceedings of the National Academy of Sciences of the United States of America* **96**: 2215–2220. DOI 10.1073/pnas.96.5.2215.
- Oxvig C, Springer TA (1998). Experimental support for a β -propeller domain in integrin α -subunits and a calcium binding site on its lower surface. *Proceedings of the National Academy of Sciences of the United States of America* **95**: 4870–4875. DOI 10.1073/pnas.95.9.4870.
- Ozawa T, Tsuruta D, Jones JC, Ishii M, Ikeda K, Harada T, Aoyama Y, Kawada A, Kobayashi H (2010). Dynamic relationship of focal contacts and hemidesmosome protein complexes in live cells. *Journal of Investigative Dermatology* **130**: 1624–1635. DOI 10.1038/jid.2009.439.
- Pampori N, Hato T, Stupack DG, Aidoudi S, Cheresch DA, Nemerow GR, Shattil SJ (1999). Mechanisms and consequences of affinity modulation of integrin α (V) β (3) detected with a novel patch-engineered monovalent ligand. *Journal of Biological Chemistry* **274**: 21609–21616. DOI 10.1074/jbc.274.31.21609.
- Panicker SR, Yago T, Shao B, Mcever RP (2020). Neutrophils lacking ERM proteins polarize and crawl directionally but have decreased adhesion strength. *Blood Advances* **4**: 3559–3571. DOI 10.1182/bloodadvances.2020002423.
- Parsons M, Messent AJ, Humphries JD, Deakin NO, Humphries MJ (2008). Quantification of integrin receptor agonism by fluorescence lifetime imaging. *Journal of Cell Science* **121**: 265–271. DOI 10.1242/jcs.018440.
- Periasamy A (2001). Fluorescence resonance energy transfer microscopy: A mini review. *Journal of Biomedical Optics* **6**: 287–291. DOI 10.1117/1.1383063.
- Peterson JA, Nyree CE, Newman PJ, Aster RH (2003). A site involving the “hybrid” and PSI homology domains of GPIIIa (β 3-integrin subunit) is a common target for antibodies associated with quinine-induced immune thrombocytopenia. *Blood* **101**: 937–942. DOI 10.1182/blood-2002-07-2336.
- Pinaud F, Michalet X, Bentolila LA, Tsay JM, Doose S, Li JJ, Iyer G, Weiss S (2006). Advances in fluorescence imaging with quantum dot bio-probes. *Biomaterials* **27**: 1679–1687. DOI 10.1016/j.biomaterials.2005.11.018.

- Pittet MJ, Weissleder R (2011). Intravital imaging. *Cell* **147**: 983–991. DOI 10.1016/j.cell.2011.11.004.
- Pouwels J, De Franceschi N, Rantakari P, Auvinen K, Karikoski M, Mattila E, Potter C, Sundberg JP, Hogg N, Gahmberg CG, Salmi M, Ivaska J (2013). SHARPIN regulates uropod detachment in migrating lymphocytes. *Cell Reports* **5**: 619–628. DOI 10.1016/j.celrep.2013.10.011.
- Powell D, Lou M, Barros Becker F, Huttenlocher A (2018). Cxcr1 mediates recruitment of neutrophils and supports proliferation of tumor-initiating astrocytes *in vivo*. *Scientific Reports* **8**: 13285. DOI 10.1038/s41598-018-31675-0.
- Prasher DC, Eckenrode VK, Ward WW, Prendergast FG, Cormier MJ (1992). Primary structure of the *Aequorea victoria* green-fluorescent protein. *Gene* **111**: 229–233. DOI 10.1016/0378-1119(92)90691-H.
- Pujals S, Feiner-Gracia N, Delcanale P, Voets I, Albertazzi L (2019). Super-resolution microscopy as a powerful tool to study complex synthetic materials. *Nature Reviews Chemistry* **3**: 68–84. DOI 10.1038/s41570-018-0070-2.
- Puzon-Mclaughlin W, Kamata T, Takada Y (2000). Multiple discontinuous ligand-mimetic antibody binding sites define a ligand binding pocket in integrin $\alpha(\text{IIb})\beta(3)$. *Journal of Biological Chemistry* **275**: 7795–7802. DOI 10.1074/jbc.275.11.7795.
- Qi J, Zhang K, Zhang Q, Sun Y, Fu T, Li G, Chen J (2012). Identification, characterization, and epitope mapping of human monoclonal antibody J19 that specifically recognizes activated integrin $\alpha 4\beta 7$. *Journal of Biological Chemistry* **287**: 15749–15759. DOI 10.1074/jbc.M112.341263.
- Ramadass M, Johnson JL, Marki A, Zhang J, Wolf D, Kiosses WB, Pestonjamas K, Ley K, Catz SD (2019). The trafficking protein JFC1 regulates Rac1-GTP localization at the uropod controlling neutrophil chemotaxis and *in vivo* migration. *Journal of Leukocyte Biology* **105**: 1209–1224. DOI 10.1002/JLB.1VMA0818-320R.
- Rapp M, Wintergerst MWM, Kunz WG, Vetter VK, Knott MML, Lisowski D, Haubner S, Moder S, Thaler R, Eiber S, Meyer B, Rohrl N, Piseddu I, Grassmann S, Layritz P, Kuhnemuth B, Stutte S, Bourquin C, Von Andrian UH, Endres S, Anz D (2019). CCL22 controls immunity by promoting regulatory T cell communication with dendritic cells in lymph nodes. *Journal of Experimental Medicine* **216**: 1170–1181. DOI 10.1084/jem.20170277.
- Ricono JM, Huang M, Barnes LA, Lau SK, Weis SM, Schlaepfer DD, Hanks SK, Cheresch DA (2009). Specific cross-talk between epidermal growth factor receptor and integrin $\alpha v\beta 5$ promotes carcinoma cell invasion and metastasis. *Cancer Research* **69**: 1383–1391. DOI 10.1158/0008-5472.CAN-08-3612.
- Robinson MK, Andrew D, Rosen H, Brown D, Ortlepp S, Stephens P, Butcher EC (1992). Antibody against the Leu-CAM β -chain (CD18) promotes both LFA-1- and CR3-dependent adhesion events. *Journal of Immunology* **148**: 1080–1085.
- Rullo J, Becker H, Hyduk SJ, Wong JC, Digby G, Arora PD, Cano AP, Hartwig J, McCulloch CA, Cybulsky MI (2012). Actin polymerization stabilizes $\alpha 4\beta 1$ integrin anchors that mediate monocyte adhesion. *Journal of Cell Biology* **197**: 115–129. DOI 10.1083/jcb.201107140.
- Russell GJ, Parker CM, Cepek KL, Mandelbrot DA, Sood A, Mizoguchi E, Ebert EC, Brenner MB, Bhan AK (1994). Distinct structural and functional epitopes of the $\alpha \text{E}\beta 7$ integrin. *European Journal of Immunology* **24**: 2832–2841. DOI 10.1002/eji.1830241138.
- Rust MJ, Bates M, Zhuang X (2006). Sub-diffraction-limit imaging by stochastic optical reconstruction microscopy (STORM). *Nature Methods* **3**: 793–795. DOI 10.1038/nmeth929.
- Sadhu C, Hendrickson L, Dick KO, Potter TG, Staunton DE (2008). Novel tools for functional analysis of CD11c: Activation-specific, activation-independent, and activating antibodies. *Journal of Immunoassay and Immunochemistry* **29**: 42–57. DOI 10.1080/15321810701735062.
- Saggu G, Okubo K, Chen Y, Vattepu R, Tsuboi N, Rosetti F, Cullere X, Washburn N, Tahir S, Rosado AM, Holland SM, Anthony RM, Sen M, Zhu C, Mayadas TN (2018). Cis interaction between sialylated Fc γ RIIA and the α I-domain of Mac-1 limits antibody-mediated neutrophil recruitment. *Nature Communications* **9**: 5058. DOI 10.1038/s41467-018-07506-1.
- Sahgal P, Alanko J, Icha J, Paatero I, Hamidi H, Arjonen A, Pietila M, Rokka A, Ivaska J (2019). GGA2 and RAB13 promote activity-dependent $\beta 1$ -integrin recycling. *Journal of Cell Science* **132**: jcs233387. DOI 10.1242/jcs.233387.
- Samarelli AV, Ziegler T, Meves A, Fassler R, Bottcher RT (2020). Rabgap1 promotes recycling of active $\beta 1$ integrins to support effective cell migration. *Journal of Cell Science* **133**: jcs243683. DOI 10.1242/jcs.243683.
- Sambrano J, Chigaev A, Nichani KS, Smagley Y, Sklar LA, Houston JP (2018). Evaluating integrin activation with time-resolved flow cytometry. *Journal of Biomedical Optics* **23**: 1–10.
- Sands BE, Peyrin-Biroulet L, Loftus EV Jr, Danese S, Colombel JF, Toruner M, Jonaitis L, Abhyankar B, Chen J, Rogers R, Lirio RA, Bornstein JD, Schreiber S, Group VS (2019). Vedolizumab versus Adalimumab for moderate-to-severe ulcerative colitis. *New England Journal of Medicine* **381**: 1215–1226.
- Schaffner P, Dard MM (2003). Structure and function of RGD peptides involved in bone biology. *Cellular and Molecular Life Sciences CMLS* **60**: 119–132. DOI 10.1007/s000180300008.
- Schleicher U, Rollinghoff M, Gessner A (2000). A stable marker for specific T-cells: A TCR α /green fluorescent protein (GFP) fusionprotein reconstitutes a functionally active TCR complex. *Journal of Immunological Methods* **246**: 165–174. DOI 10.1016/S0022-1759(00)00298-2.
- Schoen TJ, Rosowski EE, Knox BP, Bennin D, Keller NP, Huttenlocher A (2019). Neutrophil phagocyte oxidase activity controls invasive fungal growth and inflammation in zebrafish. *Journal of Cell Science* **133**: jcs236539. DOI 10.1242/jcs.236539.
- Schroder J, Benink H, Dyba M, Los GV (2009). *In vivo* labeling method using a genetic construct for nanoscale resolution microscopy. *Biophysical Journal* **96**: L1–L3. DOI 10.1016/j.bpj.2008.09.032.
- Schumacher JA, Wright ZA, Owen ML, Bredemeier NO, Sumanas S (2020). Integrin $\alpha 5$ and Integrin $\alpha 4$ cooperate to promote endocardial differentiation and heart morphogenesis. *Developmental Biology* **465**: 46–57. DOI 10.1016/j.ydbio.2020.06.006.
- Schymeinsky J, Gerstl R, Mannigel I, Niedung K, Frommhold D, Panthel K, Heesemann J, Sixt M, Quast T, Kolanus W, Mocsai A, Wienands J, Sperandio M, Walzog B (2009). A fundamental role of mAbp1 in neutrophils: Impact on $\beta(2)$ integrin-mediated phagocytosis and adhesion *in vivo*. *Blood* **114**: 4209–4220. DOI 10.1182/blood-2009-02-206169.
- Sen M, Yuki K, Springer TA (2013). An internal ligand-bound, metastable state of a leukocyte integrin, $\alpha X\beta 2$. *Journal of Cell Biology* **203**: 629–642. DOI 10.1083/jcb.201308083.

- Shah K, Weissleder R (2005). Molecular optical imaging: Applications leading to the development of present day therapeutics. *NeuroRX* **2**: 215–225. DOI 10.1602/neurorx.2.2.215.
- Shang XZ, Issekutz AC (1998). Contribution of CD11a/CD18, CD11b/CD18, ICAM-1 (CD54) and -2 (CD102) to human monocyte migration through endothelium and connective tissue fibroblast barriers. *European Journal of Immunology* **28**: 1970–1979.
- Shao B, Yago T, Panicker SR, Zhang N, Liu Z, Mcever RP (2020). Th1 cells rolling on selectins trigger DAP12-dependent signals that activate integrin α L β 2. *Journal of Immunology* **204**: 37–48. DOI 10.4049/jimmunol.1900680.
- Shao PL, Wu SC, Lin ZY, Ho ML, Chen CH, Wang CZ (2019). Alpha-5 integrin mediates Simvastatin-induced osteogenesis of bone marrow mesenchymal stem cells. *International Journal of Molecular Sciences* **20**: 506. DOI 10.3390/ijms20030506.
- Sharonov A, Hochstrasser RM (2006). Wide-field subdiffraction imaging by accumulated binding of diffusing probes. *Proceedings of the National Academy of Sciences of the United States of America* **103**: 18911–18916. DOI 10.1073/pnas.0609643104.
- Sheng M, Hu XH, Ruan CG (2003). Inhibition of angiogenesis properties by SZ-21. *Zhongguo Shi Yan Xue Ye Xue Za Zhi* **11**: 74–80.
- Shimaoka M, Springer TA (2003). Therapeutic antagonists and conformational regulation of integrin function. *Nature Reviews Drug Discovery* **2**: 703–716. DOI 10.1038/nrd1174.
- Shtengel G, Galbraith JA, Galbraith CG, Lippincott-Schwartz J, Gillette JM, Manley S, Sougrat R, Waterman CM, Kanchanawong P, Davidson MW, Fetter RD, Hess HF (2009). Interferometric fluorescent super-resolution microscopy resolves 3D cellular ultrastructure. *Proceedings of the National Academy of Sciences of the United States of America* **106**: 3125–3130. DOI 10.1073/pnas.0813131106.
- Singh S, D'mello V, Van Bergen En Henegouwen P, Birge RB (2007). A NPxY-independent β 5 integrin activation signal regulates phagocytosis of apoptotic cells. *Biochemical and Biophysical Research Communications* **364**: 540–548. DOI 10.1016/j.bbrc.2007.10.049.
- Smith A, Carrasco YR, Stanley P, Kieffer N, Batista FD, Hogg N (2005). A talin-dependent LFA-1 focal zone is formed by rapidly migrating T lymphocytes. *Journal of Cell Biology* **170**: 141–151. DOI 10.1083/jcb.200412032.
- Smith BR, Cheng Z, De A, Koh AL, Sinclair R, Gambhir SS (2008). Real-time intravital imaging of RGD-quantum dot binding to luminal endothelium in mouse tumor neovasculature. *Nano Letters* **8**: 2599–2606. DOI 10.1021/nl080141f.
- Smith EA, Bunch TA, Brower DL (2007). General *in vivo* assay for the study of integrin cell membrane receptor microclustering. *Analytical Chemistry* **79**: 3142–3147. DOI 10.1021/ac062008i.
- Somersalo K, Anikeeva N, Sims TN, Thomas VK, Strong RK, Spies T, Lebedeva T, Sykulev Y, Dustin ML (2004). Cytotoxic T lymphocytes form an antigen-independent ring junction. *Journal of Clinical Investigation* **113**: 49–57. DOI 10.1172/JCI19337.
- Sorio C, Montresor A, Bolomini-Vittori M, Caldrea S, Rossi B, Dusi S, Angiari S, Johansson JE, Vezzalini M, Leal T, Calcaterra E, Assael BM, Melotti P, Laudanna C (2016). Mutations of cystic fibrosis transmembrane conductance regulator gene cause a monocyte-selective adhesion deficiency. *American Journal of Respiratory and Critical Care Medicine* **193**: 1123–1133. DOI 10.1164/rccm.201510-1922OC.
- Spieß M, Hernandez-Varas P, Oddone A, Olofsson H, Blom H, Waithe D, Lock JG, Lakadamyali M, Stromblad S (2018). Active and inactive β 1 integrins segregate into distinct nanoclusters in focal adhesions. *Journal of Cell Biology* **217**: 1929–1940. DOI 10.1083/jcb.201707075.
- Springer TA, Dustin ML (2012). Integrin inside-out signaling and the immunological synapse. *Current Opinion in Cell Biology* **24**: 107–115. DOI 10.1016/j.ccb.2011.10.004.
- Springer TA, Zhu J, Xiao T (2008). Structural basis for distinctive recognition of fibrinogen γ C peptide by the platelet integrin α IIb β 3. *Journal of Cell Biology* **182**: 791–800. DOI 10.1083/jcb.200801146.
- Squirrell JM, Wokosin DL, White JG, Bavister BD (1999). Long-term two-photon fluorescence imaging of mammalian embryos without compromising viability. *Nature Biotechnology* **17**: 763–767. DOI 10.1038/11698.
- Stampolidis P, Ullrich A, Iacobelli S (2015). LGALS3BP, lectin galactoside-binding soluble 3 binding protein, promotes oncogenic cellular events impeded by antibody intervention. *Oncogene* **34**: 39–52. DOI 10.1038/onc.2013.548.
- Staniszewska I, Sariyer IK, Lecht S, Brown MC, Walsh EM, Tuszynski GP, Safak M, Lazarovici P, Marcinkiewicz C (2008). Integrin α 9 β 1 is a receptor for nerve growth factor and other neurotrophins. *Journal of Cell Science* **121**: 504–513. DOI 10.1242/jcs.000232.
- Stanley P, Smith A, Mcdowall A, Nicol A, Zicha D, Hogg N (2008). Intermediate-affinity LFA-1 binds α -actinin-1 to control migration at the leading edge of the T cell. *EMBO Journal* **27**: 62–75. DOI 10.1038/sj.emboj.7601959.
- Stanley P, Tooze S, Hogg N (2012). A role for Rap2 in recycling the extended conformation of LFA-1 during T cell migration. *Biology Open* **1**: 1161–1168. DOI 10.1242/bio.20122824.
- Stephens DJ, Allan VJ (2003). Light microscopy techniques for live cell imaging. *Science* **300**: 82–86. DOI 10.1126/science.1082160.
- Straub BB, Lah DC, Schmidt H, Roth M, Gilson L, Butt H-J, Auernhammer GK (2020). Versatile high-speed confocal microscopy using a single laser beam. *Review of Scientific Instruments* **91**: 033706. DOI 10.1063/1.5122311.
- Stryer L, Haugland RP (1967). Energy transfer: A spectroscopic ruler. *Proceedings of the National Academy of Sciences of the United States of America* **58**: 719–726. DOI 10.1073/pnas.58.2.719.
- Stubb A, Guzman C, Narva E, Aaron J, Chew TL, Saari M, Miihkinen M, Jacquemet G, Ivaska J (2019). Superresolution architecture of cornerstone focal adhesions in human pluripotent stem cells. *Nature Communications* **10**: 4756. DOI 10.1038/s41467-019-12611-w.
- Su G, Hodnett M, Wu N, Atakilit A, Kosinski C, Godzich M, Huang XZ, Kim JK, Frank JA, Matthey MA, Sheppard D, Pittet JF (2007). Integrin α v β 5 regulates lung vascular permeability and pulmonary endothelial barrier function. *American Journal of Respiratory Cell and Molecular Biology* **36**: 377–386. DOI 10.1165/rcmb.2006-0238OC.
- Su Y, Xia W, Li J, Walz T, Humphries MJ, Vestweber D, Cabanas C, Lu C, Springer TA (2016). Relating conformation to function in integrin α 5 β 1. *Proceedings of the National Academy of Sciences of the United States of America* **113**: E3872–E3881. DOI 10.1073/pnas.1605074113.
- Suhling K, Hirvonen LM, Levitt JA, Chung P-H, Tregido C, Le Marois A, Rusakov DA, Zheng K, Ameer-Beg S, Poland S, Coelho S, Dimble R (2015). Fluorescence Lifetime Imaging (FLIM): Basic Concepts and Recent Applications. In: Becker W, eds.

Advanced Time-Correlated Single Photon Counting Applications. Cham: Springer International Publishing. 119–188.

- Sun H, Fan Z, Gingras AR, Lopez-Ramirez MA, Ginsberg MH, Ley K (2020a). Frontline Science: A flexible kink in the transmembrane domain impairs $\beta 2$ integrin extension and cell arrest from rolling. *Journal of Leukocyte Biology* **107**: 175–183. DOI 10.1002/JLB.1HI0219-073RR.
- Sun H, Kuk W, Rivera-Nieves J, Lopez-Ramirez MA, Eckmann L, Ginsberg MH (2020b). $\beta 7$ integrin inhibition can increase intestinal inflammation by impairing homing of CD25(hi) FoxP3(+) regulatory T cells. *Cellular and Molecular Gastroenterology and Hepatology* **9**: 369–385. DOI 10.1016/j.jcmgh.2019.10.012.
- Sun H, Lagarrigue F, Gingras AR, Fan Z, Ley K, Ginsberg MH (2018). Transmission of integrin $\beta 7$ transmembrane domain topology enables gut lymphoid tissue development. *Journal of Cell Biology* **217**: 1453–1465. DOI 10.1083/jcb.201707055.
- Sun H, Liu J, Zheng Y, Pan Y, Zhang K, Chen J (2014). Distinct chemokine signaling regulates integrin ligand specificity to dictate tissue-specific lymphocyte homing. *Developmental Cell* **30**: 61–70. DOI 10.1016/j.devcel.2014.05.002.
- Sundd P, Gutierrez E, Pospieszalska MK, Zhang H, Groisman A, Ley K (2010). Quantitative dynamic footprinting microscopy reveals mechanisms of neutrophil rolling. *Nature Methods* **7**: 821–824. DOI 10.1038/nmeth.1508.
- Sundd P, Ley K (2013). Quantitative dynamic footprinting microscopy. *Immunology and Cell Biology* **91**: 311–320. DOI 10.1038/icb.2012.84.
- Svoboda K, Block SM (1994). Biological applications of optical forces. *Annual Review of Biophysics and Biomolecular Structure* **23**: 247–285. DOI 10.1146/annurev.bb.23.060194.001335.
- Takada Y, Puzon W (1993). Identification of a regulatory region of integrin $\beta 1$ subunit using activating and inhibiting antibodies. *Journal of Biological Chemistry* **268**: 17597–17601.
- Takagi J, Petre BM, Walz T, Springer TA (2002). Global conformational rearrangements in integrin extracellular domains in outside-in and inside-out signaling. *Cell* **110**: 599–511. DOI 10.1016/S0092-8674(02)00935-2.
- Takagi J, Springer TA (2002). Integrin activation and structural rearrangement. *Immunological Reviews* **186**: 141–163. DOI 10.1034/j.1600-065X.2002.18613.x.
- Tang RH, Tng E, Law SK, Tan SM (2005). Epitope mapping of monoclonal antibody to integrin $\alpha L \beta 2$ hybrid domain suggests different requirements of affinity states for intercellular adhesion molecules (ICAM)-1 and ICAM-3 binding. *Journal of Biological Chemistry* **280**: 29208–29216. DOI 10.1074/jbc.M503239200.
- Tchaicha JH, Reyes SB, Shin J, Hossain MG, Lang FF, McCarty JH (2011). Glioblastoma angiogenesis and tumor cell invasiveness are differentially regulated by $\beta 8$ integrin. *Cancer Research* **71**: 6371–6381. DOI 10.1158/0008-5472.CAN-11-0991.
- Temprine K, York AG, Shroff H (2015). Three-dimensional photoactivated localization microscopy with genetically expressed probes. *Methods in Molecular Biology* **1251**: 231–261.
- Theer P, Hasan MT, Denk W (2003). Two-photon imaging to a depth of 1000 μm in living brains by use of a Ti: Al_2O_3 regenerative amplifier. *Optics Letters* **28**: 1022–1024. DOI 10.1364/OL.28.001022.
- Thiam HR, Wong SL, Qiu R, Kittisopikul M, Vahabikashi A, Goldman AE, Goldman RD, Wagner DD, Waterman CM (2020). NETosis proceeds by cytoskeleton and endomembrane disassembly and PAD4-mediated chromatin decondensation and nuclear envelope rupture. *Proceedings of the National Academy of Sciences of the United States of America* **117**: 7326–7337. DOI 10.1073/pnas.1909546117.
- Thompson RE, Larson DR, Webb WW (2002). Precise nanometer localization analysis for individual fluorescent probes. *Biophysical Journal* **82**: 2775–2783. DOI 10.1016/S0006-3495(02)75618-X.
- Tidswell M, Pachynski R, Wu SW, Qiu SQ, Dunham E, Cochran N, Briskin MJ, Kilshaw PJ, Lazarovits AI, Andrew DP, Butcher EC, Yednock TA, Erle DJ (1997). Structure-function analysis of the integrin $\beta 7$ subunit: Identification of domains involved in adhesion to MAdCAM-1. *Journal of Immunology* **159**: 1497–1505.
- Ting LH, Fegghi S, Taparia N, Smith AO, Karchin A, Lim E, John AS, Wang X, Rue T, White NJ, Sniadecki NJ (2019). Contractile forces in platelet aggregates under microfluidic shear gradients reflect platelet inhibition and bleeding risk. *Nature Communications* **10**: 1204. DOI 10.1038/s41467-019-09150-9.
- Tng E, Tan SM, Ranganathan S, Cheng M, Law SK (2004). The integrin $\alpha L \beta 2$ hybrid domain serves as a link for the propagation of activation signal from its stalk regions to the I-like domain. *Journal of Biological Chemistry* **279**: 54334–54339. DOI 10.1074/jbc.M407818200.
- Tolomelli A, Galletti P, Baiula M, Giacomini D (2017). Can integrin agonists have cards to play against cancer? A literature survey of small molecules integrin activators. *Cancers* **9**: 78. DOI 10.3390/cancers9070078.
- Tsien RY (1998). The green fluorescent protein. *Annual Review of Biochemistry* **67**: 509–544. DOI 10.1146/annurev.biochem.67.1.509.
- Tsunoyama TA, Watanabe Y, Goto J, Naito K, Kasai RS, Suzuki KGN, Fujiwara TK, Kusumi A (2018). Super-long single-molecule tracking reveals dynamic-anchorage-induced integrin function. *Nature Chemical Biology* **14**: 497–506. DOI 10.1038/s41589-018-0032-5.
- Tuckwell D, Calderwood DA, Green LJ, Humphries MJ (1995). Integrin $\alpha 2$ I-domain is a binding site for collagens. *Journal of Cell Science* **108**: 1629–1637.
- Tuckwell DS, Smith L, Korda M, Askari JA, Santoso S, Barnes MJ, Farndale RW, Humphries MJ (2000). Monoclonal antibodies identify residues 199–216 of the integrin $\alpha 2$ vWFA domain as a functionally important region within $\alpha 2\beta 1$. *Biochemical Journal* **350**: 485–493.
- Tung CH (2004). Fluorescent peptide probes for *in vivo* diagnostic imaging. *Biopolymers* **76**: 391–403. DOI 10.1002/bip.20139.
- Turner NJ, Murphy MO, Kielty CM, Shuttleworth CA, Black RA, Humphries MJ, Walker MG, Canfield AE (2006). Alpha2 (VIII) collagen substrata enhance endothelial cell retention under acute shear stress flow via an $\alpha 2\beta 1$ integrin-dependent mechanism: An *in vitro* and *in vivo* study. *Circulation* **114**: 820–829. DOI 10.1161/CIRCULATIONAHA.106.635292.
- Tweedy L, Thomason PA, Paschke PI, Martin K, Machesky LM, Zagnoni M, Insall RH (2020). Seeing around corners: Cells solve mazes and respond at a distance using attractant breakdown. *Science* **369**: eaay9792. DOI 10.1126/science.aay9792.
- Tzima E, Del Pozo MA, Shattil SJ, Chien S, Schwartz MA (2001). Activation of integrins in endothelial cells by fluid shear stress mediates Rho-dependent cytoskeletal alignment. *EMBO Journal* **20**: 4639–4647. DOI 10.1093/emboj/20.17.4639.

- Uderhardt S, Martins AJ, Tsang JS, Lammermann T, Germain RN (2019). Resident macrophages cloak tissue microlesions to prevent neutrophil-driven inflammatory damage. *Cell* **177**: 541–555.e17. DOI 10.1016/j.cell.2019.02.028.
- Ueki Y, Saito K, Iioka H, Sakamoto I, Kanda Y, Sakaguchi M, Horii A, Kondo E (2020). PLOD2 is essential to functional activation of integrin $\beta 1$ for invasion/metastasis in head and neck squamous cell carcinomas. *iScience* **23**: 100850. DOI 10.1016/j.isci.2020.100850.
- Valencia-Gallardo C, Bou-Nader C, Aguilar-Salvador DI, Carayol N, Quenech'du N, Pecqueur L, Park H, Fontecave M, IZARD T, Tran Van Nhieu G (2019). *Shigella* IpaA binding to talin stimulates filopodial capture and cell adhesion. *Cell Reports* **26**: 921–932.e6. DOI 10.1016/j.celrep.2018.12.091.
- Van De Wiel-Van Kemenade E, Van Kooyk Y, De Boer AJ, Huijbens RJ, Weder P, Van De Kastele W, Melief CJ, Figdor CG (1992). Adhesion of T and B lymphocytes to extracellular matrix and endothelial cells can be regulated through the β subunit of VLA. *Journal of Cell Biology* **117**: 461–470. DOI 10.1083/jcb.117.2.461.
- Van Der Vieren M, Crowe DT, Hoekstra D, Vazeux R, Hoffman PA, Grayson MH, Bochner BS, Gallatin WM, Staunton DE (1999). The leukocyte integrin $\alpha D \beta 2$ binds VCAM-1: Evidence for a binding interface between I domain and VCAM-1. *Journal of Immunology* **163**: 1984–1990.
- Van Golen RF, Stevens KM, Colarusso P, Jaeschke H, Heger M (2015). Platelet aggregation but not activation and degranulation during the acute post-ischemic reperfusion phase in livers with no underlying disease. *Journal of Clinical and Translational Research* **1**: 107–115.
- Vararattanavech A, Lin X, Torres J, Tan SM (2009). Disruption of the integrin $\alpha L \beta 2$ transmembrane domain interface by $\beta 2$ Thr-686 mutation activates $\alpha L \beta 2$ and promotes micro-clustering of the αL subunits. *Journal of Biological Chemistry* **284**: 3239–3249. DOI 10.1074/jbc.M802782200.
- Vats R, Brzoska T, Bennowitz MF, Jimenez MA, Pradhan-Sundt T, Tutuncuoglu E, Jonassaint J, Gutierrez E, Watkins SC, Shiva S, Scott MJ, Morelli AE, Neal MD, Kato GJ, Gladwin MT, Sundt P (2020). Platelet extracellular vesicles drive inflammasome-IL-1 β -dependent lung injury in sickle cell disease. *American Journal of Respiratory and Critical Care Medicine* **201**: 33–46. DOI 10.1164/rccm.201807-1370OC.
- Vlahakis NE, Young BA, Atakilit A, Sheppard D (2005). The lymphangiogenic vascular endothelial growth factors VEGF-C and -D are ligands for the integrin $\alpha 9 \beta 1$. *Journal of Biological Chemistry* **280**: 4544–4552. DOI 10.1074/jbc.M412816200.
- Walpole GFW, Plumb JD, Chung D, Tang B, Boulay B, Osborne DG, Piotrowski JT, Catz SD, Billadeau DD, Grinstein S, Jaumouille V (2020). Inactivation of Rho GTPases by *Burkholderia cenocepacia* induces a WASH-mediated actin polymerization that delays phagosome maturation. *Cell Reports* **31**: 107721. DOI 10.1016/j.celrep.2020.107721.
- Wang E, Babbey CM, Dunn KW (2005). Performance comparison between the high-speed Yokogawa spinning disc confocal system and single-point scanning confocal systems. *Journal of Microscopy* **218**: 148–159. DOI 10.1111/j.1365-2818.2005.01473.x.
- Wang W, Ke S, Wu Q, Charnsangavej C, Gurfinkel M, Gelovani JG, Abbruzzese JL, Sevcik-Muraca EM, Li C (2004). Near-infrared optical imaging of integrin $\alpha \beta 3$ in human tumor xenografts. *Molecular Imaging* **3**: 343–351. DOI 10.1162/1535350042973481.
- Wang Y, Chien S (2007). Analysis of integrin signaling by fluorescence resonance energy transfer. *Methods in Enzymology* **426**: 177–201.
- Ward WW, Cody CW, Hart RC, Cormier MJ (1980). Spectrophotometric identity of the energy transfer chromophores in *Renilla* and *Aequorea* green-fluorescent proteins. *Photochemistry and Photobiology* **31**: 611–615. DOI 10.1111/j.1751-1097.1980.tb03755.x.
- Waters JC (2007). Live-cell fluorescence imaging. *Methods in Cell Biology* **81**: 115–140.
- Waxmonsky NC, Conner SD (2013). $\alpha 5 \beta 3$ -integrin-mediated adhesion is regulated through an AAK1L- and EHD3-dependent rapid-recycling pathway. *Journal of Cell Science* **126**: 3593–3601. DOI 10.1242/jcs.122465.
- Weckbach LT, Grabmaier U, Uhl A, Gess S, Boehm F, Zehrer A, Pick R, Salvermoser M, Czermak T, Pircher J, Sorrelle N, Migliorini M, Strickland DK, Klingel K, Brinkmann V, Abu Abed U, Eriksson U, Massberg S, Brunner S, Walzog B (2019). Midkine drives cardiac inflammation by promoting neutrophil trafficking and NETosis in myocarditis. *Journal of Experimental Medicine* **216**: 350–368. DOI 10.1084/jem.20181102.
- Weide T, Modlinger A, Kessler H (2007). Spatial screening for the identification of the bioactive conformation of integrin ligands. In: Peters T, eds. *Bioactive Conformation I*. Berlin Heidelberg, Berlin, Heidelberg: Springer. 1–50. DOI 10.1007/128_052.
- Weinreb PH, Simon KJ, Rayhorn P, Yang WJ, Leone DR, Dolinski BM, Pearse BR, Yokota Y, Kawakatsu H, Atakilit A, Sheppard D, Violette SM (2004). Function-blocking integrin $\alpha \beta 6$ monoclonal antibodies: Distinct ligand-mimetic and nonligand-mimetic classes. *Journal of Biological Chemistry* **279**: 17875–17887. DOI 10.1074/jbc.M312103200.
- Weitzman JB, Pasqualini R, Takada Y, Hemler ME (1993). The function and distinctive regulation of the integrin VLA-3 in cell adhesion, spreading, and homotypic cell aggregation. *Journal of Biological Chemistry* **268**: 8651–8657.
- Wen L, Fan Z, Mikulski Z, Ley K (2020a). Imaging of the immune system – towards a subcellular and molecular understanding. *Journal of Cell Science* **133**: jcs234922. DOI 10.1242/jcs.234922.
- Wen L, Marki A, Roy P, McArdle S, Sun H, Fan Z, Gingras AR, Ginsberg MH, Ley K (2020b). Kindlin-3 recruitment to the plasma membrane precedes high affinity $\beta 2$ integrin and neutrophil arrest from rolling. *Blood, Epub Ahead of Print*. DOI 10.1182/blood.2019003446.
- Werr J, Xie X, Hedqvist P, Ruoslahti E, Lindbom L (1998). $\beta 1$ integrins are critically involved in neutrophil locomotion in extravascular tissue *In vivo*. *Journal of Experimental Medicine* **187**: 2091–2096. DOI 10.1084/jem.187.12.2091.
- Wilson RW, Yorifuji T, Lorenzo I, Smith W, Anderson DC, Belmont JW, Beaudet AL (1993). Expression of human CD18 in murine granulocytes and improved efficiency for infection of deficient human lymphoblasts. *Human Gene Therapy* **4**: 25–34. DOI 10.1089/hum.1993.4.1-25.
- Wolf D, Anto-Michel N, Blankenbach H, Wiedemann A, Buscher K, Hohmann JD, Lim B, Bauml M, Marki A, Mauler M, Duerschmied D, Fan Z, Winkels H, Sidler D, Diehl P, Zajonc DM, Hilgendorf I, Stachon P, Marchini T, Willecke F, Schell M, Sommer B, Von Zur Muhlen C, Reinohl J, Gerhardt T, Plow EF, Yakubenko V, Libby P, Bode C, Ley K, Peter K, Zirlik A (2018). A ligand-specific blockade of the integrin Mac-1 selectively targets pathologic inflammation while maintaining protective host-defense. *Nature Communications* **9**: 525. DOI 10.1038/s41467-018-02896-8.

- Woods VL Jr., Schreck PJ, Gesink DS, Pacheco HO, Amiel D, Akeson WH, Lotz M (1994). Integrin expression by human articular chondrocytes. *Arthritis & Rheumatology* **37**: 537–544. DOI 10.1002/art.1780370414.
- Wright SD, Rao PE, Van Voorhis WC, Craigmyle LS, Iida K, Talle MA, Westberg EF, Goldstein G, Silverstein SC (1983). Identification of the C3bi receptor of human monocytes and macrophages by using monoclonal antibodies. *Proceedings of the National Academy of Sciences of the United States of America* **80**: 5699–5703. DOI 10.1073/pnas.80.18.5699.
- Xanthis I, Souilhol C, Serbanovic-Canic J, Roddie H, Kalli AC, Fragiadaki M, Wong R, Shah DR, Askari JA, Canham L, Akhtar N, Feng S, Ridger V, Waltho J, Pinteaux E, Humphries MJ, Bryan MT, Evans PC (2019). $\beta 1$ integrin is a sensor of blood flow direction. *Journal of Cell Science* **132**: jcs229542. DOI 10.1242/jcs.229542.
- Xiao T, Takagi J, Collier BS, Wang JH, Springer TA (2004). Structural basis for allostery in integrins and binding to fibrinogen-mimetic therapeutics. *Nature* **432**: 59–67. DOI 10.1038/nature02976.
- Xiao W, Ma W, Wei S, Li Q, Liu R, Carney RP, Yang K, Lee J, Nyugen A, Yoneda KY, Lam KS, Li T (2019). High-affinity peptide ligand LXY30 for targeting $\alpha 3\beta 1$ integrin in non-small cell lung cancer. *Journal of Hematology & Oncology* **12**: 56. DOI 10.1186/s13045-019-0740-7.
- Xie H, Cao T, Franco-Obregon A, Rosa V (2019). Graphene-induced osteogenic differentiation is mediated by the integrin/FAK axis. *International Journal of Molecular Sciences* **20**: 574. DOI 10.3390/ijms20030574.
- Xiong JP, Stehle T, Diefenbach B, Zhang R, Dunker R, Scott DL, Joachimiak A, Goodman SL, Arnaout MA (2001). Crystal structure of the extracellular segment of integrin alpha Vbeta3. *Science* **294**: 339–345. DOI 10.1126/science.1064535.
- Yago T, Petrich BG, Zhang N, Liu Z, Shao B, Ginsberg MH, Mcever RP (2015). Blocking neutrophil integrin activation prevents ischemia–reperfusion injury. *Journal of Experimental Medicine* **212**: 1267–1281. DOI 10.1084/jem.20142358.
- Yago T, Zhang N, Zhao L, Abrams CS, Mcever RP (2018). Selectins and chemokines use shared and distinct signals to activate $\beta 2$ integrins in neutrophils. *Blood Advances* **2**: 731–744. DOI 10.1182/bloodadvances.2017015602.
- Yamano K, Queliconi BB, Koyano F, Saeki Y, Hirokawa T, Tanaka K, Matsuda N (2015). Site-specific interaction mapping of phosphorylated ubiquitin to uncover Parkin activation. *Journal of Biological Chemistry* **290**: 25199–25211. DOI 10.1074/jbc.M115.671446.
- Ye Y, Chen X (2011). Integrin targeting for tumor optical imaging. *Theranostics* **1**: 102–126. DOI 10.7150/thno/v01p0102.
- Zang Q, Lu C, Huang C, Takagi J, Springer TA (2000). The top of the inserted-like domain of the integrin lymphocyte function-associated antigen-1 β subunit contacts the α subunit β -propeller domain near β -sheet 3. *Journal of Biological Chemistry* **275**: 22202–22212. DOI 10.1074/jbc.M002883200.
- Zhang C, Liu J, Jiang X, Haydar N, Zhang C, Shan H, Zhu J (2013). Modulation of integrin activation and signaling by $\alpha 1/\alpha 1'$ -helix unbending at the junction. *Journal of Cell Science* **126**: 5735–5747. DOI 10.1242/jcs.137828.
- Zhang XP, Puzon-Mclaughlin W, Irie A, Kovach N, Prokopishyn NL, Laferte S, Takeuchi K, Tsuji T, Takada Y (1999). Alpha 3 β 1 adhesion to laminin-5 and invasin: Critical and differential role of integrin residues clustered at the boundary between α 3 N-terminal repeats 2 and 3. *Biochemistry* **38**: 14424–14431. DOI 10.1021/bi990323b.
- Zhang Y, Hayenga HN, Sarantos MR, Simon SI, Neelamegham S (2008). Differential regulation of neutrophil CD18 integrin function by di- and tri-valent cations: Manganese vs. gadolinium. *Annals of Biomedical Engineering* **36**: 647–660. DOI 10.1007/s10439-008-9446-7.
- Zhao L, Zhai J, Zhang X, Gao X, Fang X, Li J (2016). Computational design of peptide-Au cluster probe for sensitive detection of $\alpha (IIb)\beta 3$ integrin. *Nanoscale* **8**: 4203–4208. DOI 10.1039/C5NR09175F.
- Zhao Z, Gruszczynska-Biegala J, Chevront T, Yi H, Von Der Mark H, Von Der Mark K, Kaufman SJ, Zolkiewska A (2004). Interaction of the disintegrin and cysteine-rich domains of ADAM12 with integrin $\alpha 7\beta 1$. *Experimental Cell Research* **298**: 28–37. DOI 10.1016/j.yexcr.2004.04.005.
- Zheng Y, Ji S, Czerwinski A, Valenzuela F, Pennington M, Liu S (2014). FITC-conjugated cyclic RGD peptides as fluorescent probes for staining integrin $\alpha v\beta 3/\alpha v\beta 5$ in tumor tissues. *Bioconjugate Chemistry* **25**: 1925–1941. DOI 10.1021/bc500452y.
- Zhou W, Hsu AY, Wang Y, Syahirah R, Wang T, Jeffries J, Wang X, Mohammad H, Seleem MN, Umulis D, Deng Q (2020). Mitofusin 2 regulates neutrophil adhesive migration and the actin cytoskeleton. *Journal of Cell Science* **133**: jcs248880. DOI 10.1242/jcs.248880.
- Zingone F, Barberio B, Compostella F, Girardin G, D'inca R, Marinelli C, Marsilio I, Lorenzon G, Savarino EV (2020). Good efficacy and safety of vedolizumab in Crohn's disease and ulcerative colitis in a real-world scenario. *Therapeutic Advances in Gastroenterology* **13**: 1756284820936536. DOI 10.1177/1756284820936536.
- Zucchetti AE, Bataille L, Carpier JM, Dogniaux S, San Roman-Jouve M, Maurin M, Stuck MW, Rios RM, Baldari CT, Pazour GJ, Hivroz C (2019). Tethering of vesicles to the Golgi by GMAP210 controls LAT delivery to the immune synapse. *Nature Communications* **10**: 2864. DOI 10.1038/s41467-019-10891-w.